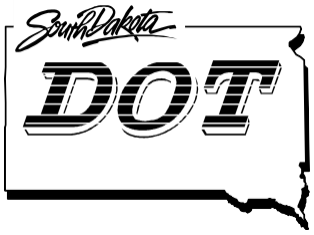

U.S. Department
of Transportation
Federal Highway Administration

SD2013-10-F

Connecting South Dakota and the Nation

South Dakota
Department of Transportation Office of Research

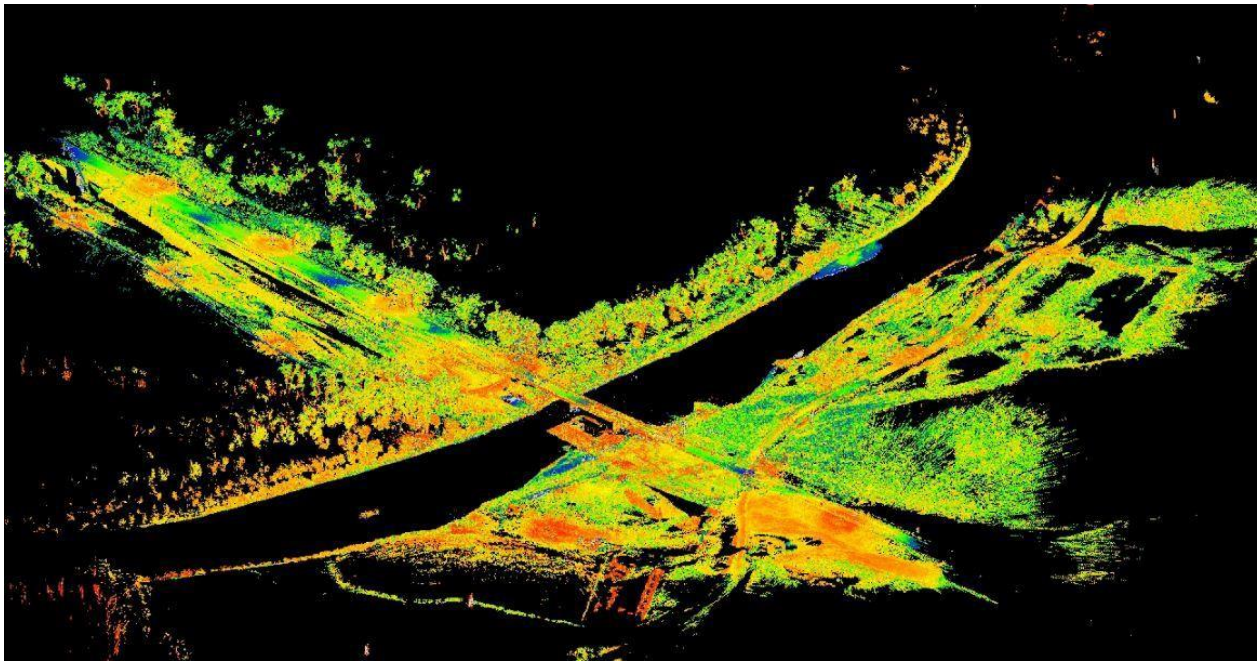

Applications of LiDAR for SDDOT

Study SD2013-10

Final Report

Prepared by

University of Nebraska-Lincoln

Lincoln, NE 68588

November 2019

DISCLAIMER

The contents of this report, funded in part through grant(s) from the Federal Highway Administration, reflect the views of the authors who are responsible for the facts and accuracy of the data presented herein. The contents do not necessarily reflect the official views or policies of the South Dakota Department of Transportation, the State Transportation Commission, or the Federal Highway Administration. This report does not constitute a standard, specification, or regulation.

The South Dakota Department of Transportation provides services without regard to race, color, gender, religion, national origin, age or disability, according to the provisions contained in SDCL 20-13, Title VI of the Civil Rights Act of 1964, the Rehabilitation Act of 1973, as amended, the Americans With Disabilities Act of 1990 and Executive Order 12898, Federal Actions to Address Environmental Justice in Minority Populations and Low-Income Populations, 1994. Any person who has questions concerning this policy or who believes he or she has been discriminated against should contact the Department's Civil Rights Office at 605.773.3540.

ACKNOWLEDGEMENTS

This work was performed under the direction of the SD2013-10 Technical Panel:

Mark Fox .....Watertown Area
Thomas Herman .....Road Design
Aaron Litka .....Research
Ken Marks ..... TIM
Jon Nelson .....Road Design
Daris Ormesher .....Research
Steve Palmer ..... Rapid City Area
Colton Stahl..... Air, Rail, and Transit
Todd Thompson .....Bridge Design
Randy Vesely ..... Winner Area
Dustin Witt .....Project Development

TECHNICAL REPORT STANDARD TITLE PAGE

1. Report No. SD2013-10-F	2. Government Accession No.	3. Recipient's Catalog No.	
4. Title and Subtitle Applications of LiDAR for SDDOT		5. Report Date 11/05/2019 6. Performing Organization Code	
7. Author(s) Yijun Liao, Mohammad Ebrahim Mohammadi, Ph.D., Daniel P. Watson, Richard L. Wood, Ph.D., Chung R. Song, Ph.D., Yong-Rak Kim, Ph.D.		8. Performing Organization Report No.	
9. Performing Organization Name and Address Department of Civil Engineering University of Nebraska-Lincoln 220 Vine Street Whittier Research Center 362K Lincoln, NE 68588		10. Work Unit No. HRY310 11. Contract or Grant No. 311261	
12. Sponsoring Agency Name and Address South Dakota Department of Transportation Office of Research 700 East Broadway Avenue Pierre, SD 57501-2586		13. Type of Report and Period Covered Final Report Jan 2017 – Nov 2019 14. Sponsoring Agency Code	
15. Supplementary Notes An executive summary is published separately as SD2013-10-X			
16. Abstract Light Detection and Ranging (LiDAR) is a valuable data collection method that is increasingly being utilized within transportation agencies to replace traditional geospatial data collection methods for infrastructure with increased accuracy and better cost- and time-efficiency. This study will identify current and potential uses for LiDAR at SDDOT, including: (1) a preliminary survey for road design; (2) clearance surveys of bridges and tunnels; and (3) a roadway geometry survey for safety analysis. LiDAR data can be acquired using three broad platforms: (1) ground-based; (2) mobile; and (3) aerial. For each potential use, the three LiDAR platforms will have their requirements described, and their costs and benefits analyzed. Based on the analysis, a set of comprehensive LiDAR Surveying and Mapping Specifications for SDDOT will be created. The specifications will outline the acceptable LiDAR platforms and minimum requirements for specific applications. The minimum requirements will be used to recommend an implementation strategy and procedure for the use of LiDAR at SDDOT for the identified and proposed applications. Also included in the project, is an example of field data collection using two commonly used surveying platforms and a detailed description of the preprocessing and postprocessing for a selected construction site at Presho, SD. The goal of the demo is to show the various steps described in the document in practice.			
17. Keywords Point clouds, lidar, drones, UAS, geospatial data		18. Distribution Statement No restrictions. This document is available to the public from the sponsoring agency.	
19. Security Classification (of this report) Unclassified	20. Security Classification (of this page) Unclassified	21. No. of Pages 88	22. Price

TABLE OF CONTENTS

Table of Contents

TABLE OF FIGURES

TABLE OF TABLES

TABLE OF ACRONYMS

Acronym	Definition
2D	2-Dimensional
3D	3-Dimensional
AGL	Above-Ground-Level
BIM	Building Information Modeling
C2C	Cloud-to-Cloud
CAD	Computer-Aided Design
Caltrans	California Department of Transportation
CDF	Cumulative Distribution Function
CI	Confidence Interval
CP	Check Point
CPU	Central Processing Unit
DEM	Digital Elevation Model
DOT	Department of Transportation
DMI	Distance Measurement Indicator
FAA	Federal Aviation Administration
FGDC	Federal Geographic Data Committee
FHWA	Federal Highway Administration
GBL	Ground-Based LiDAR
GCP	Ground Control Point
GSD	Ground Sampling Distance
GIS	Geographic Information System
GMM	Gaussian Mixture Model
GNSS	Global Navigation Satellite System
GPS	Global Positioning System
GPU	Graphics Processing Unit
H	High
HDD	Hard Disk Drive

HDR	High Dynamic Ranging
IMU	Inertial Measurement Unit
KYTC	Kentucky Transportation Cabinet
L	Low
LiDAR	Light Detection and Ranging
M	Medium
MSE	Mean Square Error
MLS	Mobile LiDAR System
MTLS	Mobile Terrestrial Laser Scanning
PPK	Post-Processing Kinematic
QC/QA	Quality Control, Quality Assurance
RAI	Rockfall Activity Index
RMS	Root Mean Square
RMSE	Root Mean Square Error
ROI	Region of Interest
RTK	Real-Time Kinematic
SBET	Smooth Best Estimate Trajectory
SDDOT	South Dakota Department of Transportation
SfM	Structure-from-Motion
SPC	State Plane Coordinate
SSD	Solid State Drive
SVD	Single-Value Decomposition
SVM	Support Vector Machine
TSSS	Total Station Surveying System
UAS	Unmanned Aerial System

1.0 Executive Summary

Light Detection and Ranging (LiDAR) is a valuable data collection method that is increasingly being utilized within transportation agencies to replace traditional geospatial data collection methods for infrastructure with increased accuracy and better cost- and time-efficiency in comparison to traditional methods. This study will identify current and potential uses for LiDAR at SDDOT including: (1) a preliminary survey for road design; (2) clearance surveys of bridges and tunnels; and (3) a roadway geometry survey for safety analysis. LiDAR data can be acquired using three broad platforms: (1) ground-based; (2) mobile; and (3) aerial. For each potential use, the three LiDAR platforms will have their requirements described, and their costs and benefits analyzed. Based on the analysis, a set of comprehensive LiDAR Surveying and Mapping Specifications for SDDOT will be created. The specifications will outline the acceptable LiDAR platforms and minimum requirements for specific applications. The minimum requirements will be used to recommend an implementation strategy and procedure for the use of LiDAR at SDDOT for the identified and proposed applications. Also included in the project, is an example of field data collection using two commonly used surveying platforms and a detailed description of the preprocessing and postprocessing for a selected construction site at Presho, SD. The goal of the demo is to show the various steps described in the document in practice.

2.0 Problem Description

Light Detection and Ranging (LiDAR) is a useful data collection method that is becoming increasingly popular within transportation agencies. LiDAR increases cost- and time-efficiency by producing a point cloud, a set of three-dimensional vertices in space, that can detect infrastructure damage and features with accuracy as low as sub-inch levels. LiDAR data can be acquired through deployment on three broad platforms: (1) ground-based or terrestrial in stationary mode; (2) mobile using vehicles, robots, and backpacks in a moving reference frame; and (3) aerial via traditional aircraft (fixed or rotary) and unmanned aerial systems (UAS or colloquially known as "drones"). Figure 1 illustrates examples of these platforms and techniques, which typically influence the accuracy and rate of capture. Accuracy with LiDAR point clouds can vary from approximately 12 inches to 0.6 inches from aerial and ground-based LiDAR (GBL) scanners, respectively.

(a) (b) (c)

Figure 1: Example LiDAR platforms: (a) ground-based (courtesy of Faro 2015); (b) mobile (courtesy of SSI 2016); and (c) aerial (courtesy of JPL 2012).

LiDAR is an example of active remote sensing, where data collection occurs via a laser waveform and distances are computed using the time-of-flight or phase shift of the returned beam. As a result, numerous benefits can be achieved through LiDAR use including recording more objective measurements (in lieu of manual measurements), semi-autonomous rapid data collection and processing, highly accurate results (including the vertical direction), and limited human exposure to the environment. Diminished human exposure reduces worker interactions with traffic and precarious structures that may be prone to collapse following an extreme load, such as a traffic collision at a bridge pier. Due to these advantages, the South Dakota Department of Transportation (SDDOT) has identified applications of interest including: (1) preliminary site surveys for road design; (2) vertical clearance surveys of structures (bridges and tunnels); and (3) roadway geometry and safety analysis. Other suggested applications include the measurement of slope geometry of cuts and fills for slope stability analysis and the volumetric calculations of excavations and fills.

During this project, we will identify the potential applications of LiDAR within the scope and framework of SDDOT and their specific recommended resolution and accuracy. We will then examine how this data is used when incorporated into existing or modified workflows. The geospatial point cloud data (as the

output from the LiDAR scans) is typically extensive, and the required data storage will have to be quantified. Depending on the project size and desired accuracy, storage demands greater than 1 gigabyte (GB) are not uncommon. LiDAR data collection will also be compared to conventional methods (manual measurements and surveying techniques) in terms of cost and benefit analysis. Finally, these lessons and recommendations will be used to develop *LiDAR Surveying and Mapping Specifications* for SDDOT.

3.0 Research Objectives

3.1 Identify Current and Potential Uses for LiDAR for SDDOT

The identified and potential uses for LiDAR at SDDOT include: (1) a preliminary survey for road design; (2) clearance surveys of bridges and tunnels; and (3) a roadway geometry survey for safety analysis. In addition, this project will consider other potential applications such as geometric analysis of slopes, cuts, and embankments and the quantification of excavations and fills during construction projects. Other applications can include roadway as-built surveys and highway attributes.

3.2 Describe the Requirements, Costs, and Benefits of Each Potential Use of LiDAR

LiDAR data can be collected through deployment on three broad platforms: (1) ground-based or terrestrial, (2) mobile, and (3) aerial. Ground-based is typically the lowest capital investment with highly accurate and dense point clouds. Aerial is typically the most expensive to collect with a coarse point density; however, it requires the least amount of data capture time. Mobile platforms perform between terrestrial and aerial applications with regard to capital investment, point density and accuracy, and data capture time. Selected platforms will govern the requirements for the point cloud to ensure that the cost and time benefits achieve an acceptable final product.

3.3 Develop Comprehensive LiDAR Surveying and Mapping Specifications for SDDOT

This project will create specifications that outline acceptable LiDAR platforms and minimum requirements for specific applications. These minimum requirements will specify the resolution, accuracy, and area of coverage for easy incorporation into existing SDDOT workflows. Also, the minimum requirements will help recommend an implementation strategy for the use of LiDAR at SDDOT.

3.4 Recommend an Implementation Strategy for LiDAR Applications at SDDOT

For the identified and proposed applications, this project will provide an outlined procedure for the best implementation of LiDAR within SDDOT workflows. This will include examples identifying its use with common software platforms including Bentley InRoads, MicroStation, and OpenRoads. Other supplemental software will be recommended, including Faro Scene and CloudCompare, an open-source software application.

4.0 Task Description

4.1 Meet with the Project's Technical Panel

Meet with the project's technical panel to review the project scope and work plan.

The first task included a trip to SDDOT in Pierre for the project kick-off meeting on January 4, 2017. This was attended by Richard Wood (PI), Chung Song (co-PI), and M. Ebrahim Mohammadi (former Ph.D. student of PI Wood). Yong-Rak Kim (co-PI) joined the meeting via a remote connection. During this meeting, an initial presentation was given by PI Wood on the project. At the end of this meeting, PI Wood presented an alternative method to produce point clouds from photogrammetry to inform the panel members of other remote sensing methods. What follows is a meeting summary as agreed upon by the project team members at UNL.

During this initial meeting (task 1), discussions were held on identifying current and potential uses as well as example applications for LiDAR. The discussion on potential uses focused on the following items:

1- Preliminary roadway and resurfacing surveys

2- Surveying bridge deck surfaces and as-built for design purposes

3- Survey of intersections existing conditions based on the Americans with Disabilities Act (ADA) concerns and compliance

A quick LiDAR application discussion included the geometric analysis of slopes on local roadways where the slope ratio along the roadway in one-quarter mile cross sections and the in-slope ratio were of interest. LiDAR could also be used for 2D scour analysis to examine the flow and scour areas.

As an example application, a recent LiDAR data collection and processing project was conducted near Rapid City, as disclosed by a panel member. This project produced *.las files and one-quarter mile cross sections. The project was approximately 22 miles in length and required a significant amount of file storage for the LiDAR files (*.las) (approximately 93 GB). This highlighted the large file storage demands for most LiDAR applications. PI-Wood and his student, Ebrahim, briefly discussed how an open-source compressed file type might be beneficial (*.e57). The e57 file format is developed by the ASTM E57 committee as a general purpose and open standard file for storing data produced by any platform that creates 3D data. E57 is a replacement of ad-hoc or proprietary file formats to store or exchange data and aims to reduce the access difficulty and provide flexibility in transferring data from one software to the software of different vendors (Huber 2011).

4.2 Review and Summarize Literature

Review and summarize the literature, including state DOT's specifications, pertaining to using airborne, mobile, and terrestrial LiDAR for transportation projects.

Chapter 5 provides the literature on the use of LiDAR and unmanned aerial systems (UASs) for transportation projects.

4.3 Identify Current and Potential Uses of Lidar for SDDOT

Identify Current and Potential Uses of Lidar for SDDOT.

The current and potential uses of LiDAR for SDDOT are outlined in Table 1 of Section 6.1.

4.4 Submit Technical Memorandum #1

Submit a technical memorandum and meet with the project's technical panel to present the results of tasks 1-3 (Technical Memorandum #1).

This was submitted to the technical panel, and their feedback has been incorporated into the remaining memorandums (#2 and #3).

4.5 Describe the Applications and How It Could Be Integrated

For each identified use: describe the application and how it could be integrated into current SDDOT workflows; identify needed accuracy and resolution; define requirements for hardware and software; describe data format, storage, and processing requirements; describe capital and operational costs; and characterize efficiency and safety benefits.

Specific to the applications identified in Table 1, the literature review section is combined to include how these applications can be integrated into current and future SDDOT workflows. Chapter 5 literature review also encompasses this focus. Moreover, Section 6.2 outlines the requested specifics for the targeted LiDAR applications. This is summarized in Table 2.

4.6 Submit Technical Memorandum #2

Submit a technical memorandum and meet with the project's technical panel to present the results of task 5 (Technical Memorandum #2).

This was submitted to the technical panel, and their feedback has been incorporated into the remaining memorandum (#3).

4.7 Identify A Project to Collect Lidar Data and Then Demonstrate the Process

In consultation with the technical panel, identify a project to collect LiDAR data and then demonstrate the process of data collection, data processing, and use in InRoads, MicroStation, and OpenRoads.

The example application project was the US 183 White River Bridge in south-central South Dakota. The UNL team first visited the project on the return trip on January 4, 2017, and this was later the selected site for the example data collection during the summer of 2018. At this site, a six-span steel bridge is present along with roadway and safety hardware features. The bridge structure was observed to have some notable damage including steel corrosion, concrete deck cracking and water penetration (at edges), and concrete pier damage (substructure). An online search identified that in a 2013 inspection

this bridge had a sufficiency rating of 42, where the deck, superstructure, and substructure were rated as fair, poor, and serious. A few example photos are provided in Figure 2. This site was confirmed during Memorandum #2 as the example application project (for task 7). The data collection and processing of this is detailed in Chapter 7. Processing was conducted in InRoads, Microstation, and OpenRoads at the request of the technical panel.

(a) overview image (upstream)

(b) deterioration and degradation detail

Figure 2: US 183 White River Bridge in northern Lyman County.

4.8 Prepare Lidar Surveying and Mapping Specifications

Prepare LiDAR Surveying and Mapping Specifications for SDDOT, including data storage, data quality, software, and hardware specifications.

Chapter 8 details the draft point cloud (including LiDAR and UAS-derived data) surveying and mapping specifications. This includes feedback provided by the technical panel included in memorandum #3.

4.9 Submit Technical Memorandum #3

Submit a technical memorandum and meet with the project's technical panel to present the results of tasks 7-8 (Technical Memorandum #3).

This was submitted to the technical panel, and their feedback has been incorporated into the final report. This included the restructuring of the report for clarity as well as the additional requested task of using Bentley OpenRoads. These comments were implemented into the draft final report.

4.10 Recommend an Implementation Strategy

Recommend an implementation strategy for the department to use LiDAR, including recommendations for the purchase of equipment or contracting LiDAR services.

Section 8.9 details the implementation strategy as recommended by the research team.

4.11 Prepare the Final Report

In conformance with Guidelines for Performing Research for the SDDOT, prepare a final report summarizing the research methodology, findings, conclusions, and recommendations.

The final report was prepared as requested and delivered to SDDOT for their review. The final report includes new sections relating to the implementation strategy (task 10), conclusions, and recommendations.

4.12 Make an Executive Presentation

Make an executive presentation to the South Dakota Department of Transportation Research Review Board at the conclusion of the project.

This will be scheduled and delivered in accordance with the SDDOT Research Review Board practice.

5.0 Literature Review

5.1 Overview and Introduction

As an emerging technology, light detection and ranging (LiDAR or sometimes stylized as lidar) platforms usage has grown rapidly in recent years in all fields of engineering. Scanners can be deployed as GBL, MLS, and aerial/airborne platforms. Within this section, the authors investigated LiDAR technology applications and implementations in asset management, roadway, structural, geotechnical, workflows and procedures, and agency reports. It can be concluded that LiDAR technology reduces the surveying time and potential risks, while increasing the efficiency for surveying tasks.

5.2 Guidelines Developed by State and Federal Agencies

The Colorado Department of Transportation published a survey manual in 2015 for the combined use of LiDAR, photogrammetry, and other remote sensing platforms for field surveys on hard road surfaces obtained from an airborne platform. It outlines the specifications for field survey processes. In this report, LiDAR, electronic, digital, or other data obtained from an airborne platform are utilized for the surveying. This report provides a guideline for the use of LiDAR geospatial data. After this report was published, guidelines were released by the Federal Highway Administration in 2016 to introduce LiDAR technology. The guidelines include new practices for roadway asset management and provide background information about program planning, LiDAR data acquisition, and future potential uses of the collected data to maintain the transportation system. Within this report, LiDAR surveys data is recommended to be used for applying to asset management, specifically roadway, by state transportation agencies. According to this guideline, LiDAR data collection is a rapid, efficient, optimized, and accurate approach for permanent data recording due to its efficiency in data acquisition and the productive properties that can be derived from the data.

California Department of Transportation (Caltrans 2016) published a survey manual on policies, procedures, and general information for land surveys. Within this manual, Chapters 6 and 7 describe the Global Positioning System (GPS) and Total Station Survey System (TSSS) surveys and provide details on executing each method. Furthermore, this working report discusses two GPS surveying methods and three surveying techniques using GPS: static GPS, fast-static GPS, and kinematic GPS, introduced in Chapter 6. Chapter 7 details the vertical and horizontal total station data collection methods as well as the other common applications (e.g., project control, land net location control, GIS surveys, engineering survey collected topographical data, etc.) for TSSS. In addition, Chapter 15 focuses on LiDAR technology and identifies potential applications of this technology. Example applications include deformation and monitoring, pavement analysis, asset inventory/management, earthwork (e.g., stockpiles, borrow pits, and landslides), documentation guidelines, and project deliverables. However, the document is still being updated. The last update was in 2016, where incomplete sections include the overview, background, introduction, and survey records.

A very recent survey manual was published in 2017 by the SDDOT. It represents the state standards, departmental rules, and practices for land and/or highway surveying and operations. The surveying method outlines the use of a total station for project control and application of total station and static and Real-Time Kinematic (RTK) GPS system, which is a technique that obtains precise point positioning from satellite systems (e.g., GPS, GLONASS, Galileo, etc.) known as global navigation satellite system or

GNSS, for land-tie survey in rural, suburban, and urban areas. Additionally, the application of ground control for photogrammetry surveys is explained within the SDDOT surveying manual in Chapter 5, as most applicable for LiDAR surveys. The survey accuracy of photogrammetric mapping and ground point measurements are dependent on the ground control field survey procedure. Furthermore, the manual describes guidelines relating to the collection of planimetric and digital model data as well as surveying for specific applications including: road and highway analysis, drainage condition, subsurface utility investigation, bridge deck inspection, and topography. Furthermore, preliminary data processing methods and survey construction are also outlined within five survey categories including: control, preliminary construction, construction, post-construction, and encroachment. This survey manual serves as a useful tool for standardizing surveying operation in transportation activities. However, it is an incomplete survey manual, particularly in the implementation of newly emerging technologies such as LiDAR-based survey methods.

To perform various processes on the collected point cloud data, numerous state agencies and private organizations have developed manuals and procedures for commercially available software. For example, the Kentucky Transportation Cabinet or KYTC (2013) developed a report that outlines a step by step procedure for processing within the MicroStation platform. Additionally, this manual provides details on how to use a specific add-on package, KyLiDAR. This add-on assists in project tiles needed for specific regions. This manual and software enable users to filter, analyze, classify/label, and utilize LiDAR data to meet their desired needs. However, this report dates to 2013 and does not reflect the current capabilities of the more recently released software versions. The most recent version of the software can create BIM-ready models from LiDAR data, which allows users to integrate the LiDAR data with other data sources to perform specific tasks. More recent tasks include clash detection or the visualization of the construction process.

The FAA Advisory Circular on remote sensing technologies (AC 150/5300-17C 2011) discusses considerations and provides guidance for the use of several LiDAR platforms (e.g., GBL or MLS) for airport surveys, including: data collection describing the physical infrastructure of an airport, calibration procedures, and specific workflow requirements such as georeferencing and data processing. Furthermore, the report discusses the technical consideration in the implementation of mobile LiDAR platforms including: accuracy components (i.e., sources of errors in data collection), point density specifications, equipment correction and calibration, and common quality control methodologies. The report provides an overview of mobile LiDAR applications. However, it only addresses technical knowledge and practices up to 2013; with current advances in data collection, post-processing, and documentation should be considered.

5.3 Potential LiDAR Application and Implementation for SDDOT Workflows

LiDAR technology, as with all equipment platforms, has various applications due to its safety and efficiency. Typically, the existing surfacing conditions can be recorded safely and preserved digitally, even in some inaccessible locations during either the day or night. Safety is increased given the remote data collection of LiDAR, limiting personnel within live traffic and roadways, slopes, precarious bridge structures, etc. These point clouds can be utilized to aid in the design process (e.g., assessing the drainage of a road or slope analysis) in a relatively quick, accurate, and economical manner compared to other ground survey methods. If the equipment is used correctly, reliable and unified results can be

obtained by the user. However, adverse weather conditions and unintended occlusion are predominating limitations. Adverse weather conditions can create erroneous points due to random diverging beams. Occlusion is a limitation, where gaps or holes exist in the data. These are often caused by obstacles, both static and transient; where examples include other vehicles, people, and roadway signage. Various methods can limit occlusions, including multiple scans and aerial photographic technologies.

5.3.1 Asset Management

As an emerging technology, light detection and ranging (LiDAR or sometimes stylized as lidar) platforms usage has growth grown rapidly in recent years in all fields of engineering, in particular, transportation engineering. Scanners can be deployed as GBL, MLS, and aerial/airborne platforms. One study examined these three technologies (Vincent and Ecker 2010). In this study, the authors investigated LiDAR technology assessment by evaluating the surface, geometry features, cost, and efficiency rates. It can be concluded that LiDAR technology reduces surveying time and potential risks. The collected point cloud resource is a permanent record that can be shared multiple times, saves time, and is cost-effective. Therefore, to implement this technology, many scholars have developed and introduced new guidelines, procedures, and methods within all branches of civil engineering.

Other applications of LiDAR for road facility monitoring and management have been investigated through MLS platforms, where an example is presented herein. Zheng et al. (2017) introduced a method to extract light poles from LiDAR data collected by MLS. In their methodology, the algorithm first eliminates the ground-level vertices through an elevation filter. Afterward, nonground vertices are clustered through *k* nearest neighbors (the standard algorithm to identify the closest desired number of points to a target point, here denoted as *k*) algorithm, where each cluster is subsequently analyzed for lighting pole detection via template matching based on intensity and shape information by Gaussian mixture model (GMM). The GMM is a finite mixture probabilistic model that is created from finite Gaussian probability distributions with unknown parameters (mean and standard deviation values) (Martí Carrillo 2015). The method requires an object library for the process of template matching.

Bendaanane et al. (2015) investigated the application of GBL and MLS for urban survey and asset management via object extraction. Furthermore, the study compares the results of two lidar LiDAR platforms with the conventional method in terms of time, direct costs, and accuracy. To achieve the objective, Bendaanane et al. (2015) outlined a workflow to collect, preprocess, detect and extract objects (denoted as an advanced processing step), and compared the results of each method as shown in Figure 3.

To conduct the survey, two streets with lengths of 984 ft (300 m) were selected for data collection. The GBL platform used within this study was a Faro Focus 3D laser scanner, and the scanning settings were optimized such that each scan had a duration of only 5 minutes. This corresponds to resolution and quality variables of 1/8 and 4×, respectively, and a resultant point-to-point spacing of 0.47 to 0.8 inches (1.2 to 2.0 cm) within the range of 50 to 65 ft (15 to 20 m). As a result, a total of 15 scans were taken in 3 hours to scan the 984 ft (300 m). The collected data was initially preprocessed and registered within Scene software, and then it was georeferenced in AutoCAD using known surveyed points. In the final step, the file was exported as *.e57 to preserve RGB and intensity values.

The MLS platform selected was a RoadScanner3. The RoadScanner3 system, as shown in Figure 4, contains multiple sensors, including a laser scanner, ground penetration radar, thermal diagnostics sensors, and cameras. The system used within the study collected inertial measurement unit (IMU) and navigation data (GPS data) in addition to LiDAR data and supplemental images. The duration of data collection with the MLS platform was 45 minutes. POSPac software was used to process the trajectory data and output the planimetric positions (North and East) with RMSE of 0.4 to 0.8 inches (1 to 2 cm). This data was used to synchronize (attributing a time and a position) the point clouds and images. The synchronization was carried with RSPostProcess and RoadSIT platforms, proprietary software.

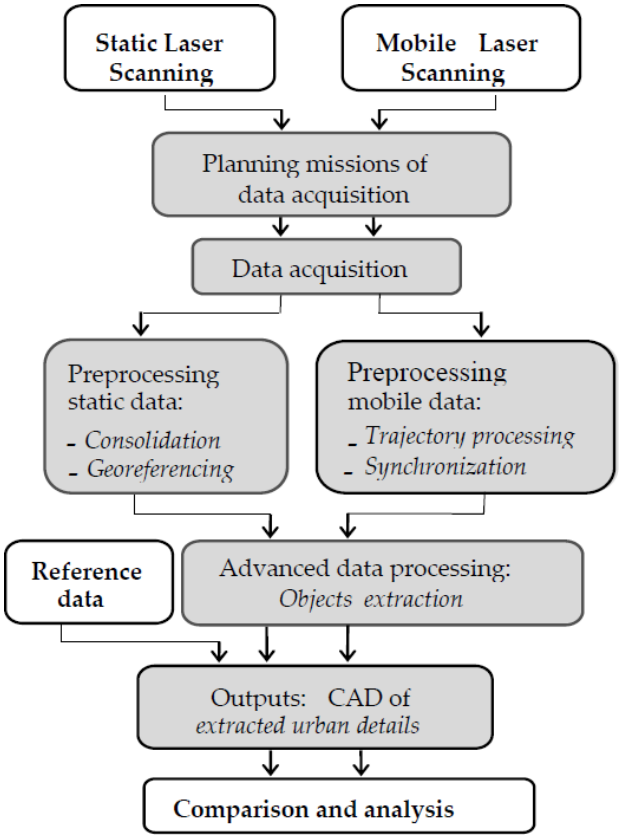

Figure 3: Flowchart of the proposed workflow to compare LiDAR platforms for urban survey and asset management (courtesy of Bendaanane et al. 2015).

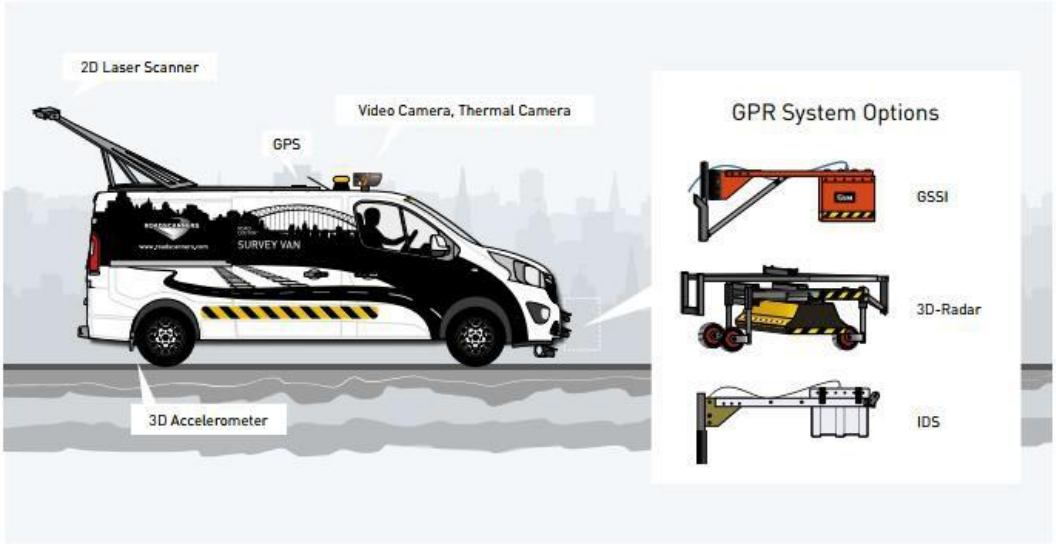

Figure 4: RoadScanner Road Doctor MLS survey van (courtesy of RoadScanners Inc. 2017).

A semi-automatic approach carried out the object extraction task within the developed method to classify the objects into three classes. This includes isolated details (e.g., trees, streetlights), characteristic lines (e.g., sidewalks), and building limits. To perform the extraction of GBL collected data, TopoDOT software was used. In addition, the AutoCAD plug-in RoadScanner3 package and TopoDOT were used independently on the MLS data for comparison. To extract the objects with TopoDOT for the GBL data, a cell library of isolated objects was created in MicroStation V8i software. Then, using the developed library, various isolated objects were selected, the appropriate labels were assigned to each object, and the objects were accurately extracted. To extract the characteristic lines (e.g., sidewalk or crosswalk edges), the approximate sidewalk edge was detected through a breakline extraction function within the TopoDOT software. Similarly, the third class of objects used a breakline extraction function within the TopoDOT software to identify the building extents. Once the building extents were identified, the buildings could be extracted manually. To extract objects from MLS data with TopoDOT, similar steps to those of GBL data were taken. The workflow for the AutoCAD plug-in software is also similar to TopoDOT software. First, a cell library is created, and then by selected the appropriate object, the software localizes the object, and a label is assigned.

Finally, Bendaanane et al. (2015) compared each method in terms of the time of data collection, processing time, the accuracy of detection and object extraction, and implementation costs. The study approximated that the conventional survey method took 18 hours (or approximately three working days) and further required 25 hours to process and prepare the deliverables. The data acquisition for GBL and MLS were 180 and 45 minutes, respectively. As for the processing time, the total time to process the point cloud data and extract object for GBL and MLS were 17 and 18 hours, respectively. This indicates that using GBL data can reduce the surveying time by 54% in comparison to those of the traditional method. Furthermore, using an MLS platform can further improve the GBL method time by 11%, for this limited length of roadway. The point cloud collected was denser for GBL in comparison to the MLS method. However, the MLS point clouds were less vulnerable to occlusion effect (due to trees, signs, etc.) and had more consistent point-to-point spacing. As for the object detection and extraction,

when both MLS and GBL data were processed within TopoDOT software, GBL data resulted in more accurate detections and object extraction. The AutoCAD plug-in RoadScanner3 software also was used to extract similar objects from the same MLS data. However, the results were not improved in comparison to those of TopoDOT software. To estimate the cost of each method, only the deployment expenses were considered. The study reported that the cost of GBL and MLS methods in comparison to the cost of the traditional method is 50% and 71% cheaper, respectively, and therefore both LiDAR platforms not only are cost-effective but are faster in data collection and processing. This implies that the equipment platforms have been procured.

Oskouie et al. (2015) developed a methodology to monitor a mechanically stabilized earth (MSE) wall horizontal joints displacement through point cloud data (Figure 5). Their proposed method did not use MicroStation nor ArcGIS software. However, the work is reproducible through these software platforms as well as CloudCompare, Cyclone, or Faro Scene (example LiDAR manufacturer scanner software). This work can be further visualized in MicroStation or ArcGIS with minimal manual processing.

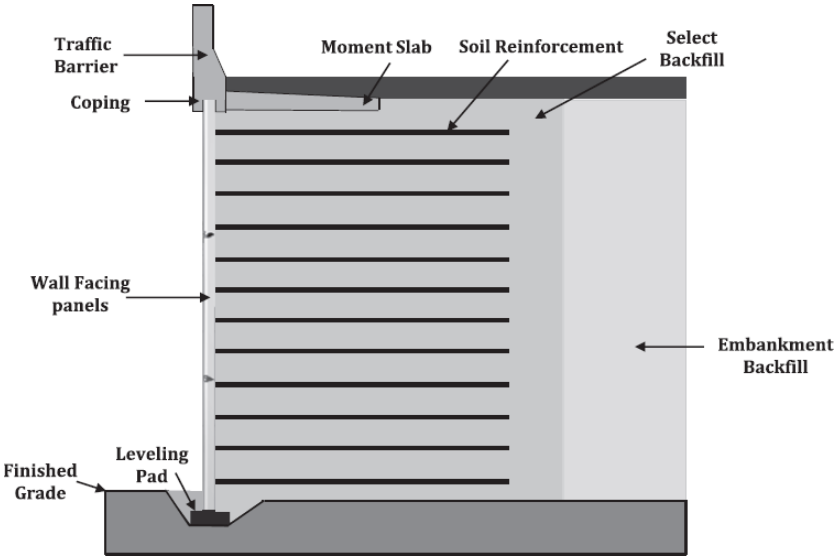

Figure 5: Cross-section of an MSE wall (courtesy of Passe 2000).

The developed methodology has four steps including noise removal, plane fitting, extracting horizontal joints of MSE walls, and measuring horizontal joint displacement through comparing a point cloud data with a baseline dataset. The noise removal step consisted of removing erroneous points within the data through statistical analyses of point-to-point spacing, which is a standard common noise removal approach in LiDAR processing software. For example, the noise removal step can be applied to the data at the time of preprocessing in Faro Scene software (Faro 2011). Oskouie et al. (2015) used the neighboring size of 50 for a point cloud with a point-to-point spacing of 0.55 inch (1.4 cm). To identify the planes in the regions of interest (ROI), Oskouie et al. (2015) used the RANSAC algorithm to find the best fit shape of the MSE walls. Similar to noise removal, this can be achieved in a variety of software including CloudCompare and Faro Scene. Once the planes are selected and exported, the horizontal joints can be easily compared for two separate point cloud datasets with one dataset serving as the

baseline to measure the change in horizontal displacements (Figure 6). The study measured the proposed method accuracy by comparing the real-world data with synthetic data (as a baseline dataset) to assess the developed method. The study concluded that the accuracy of measurement was less than 0.04 inches (1 mm).

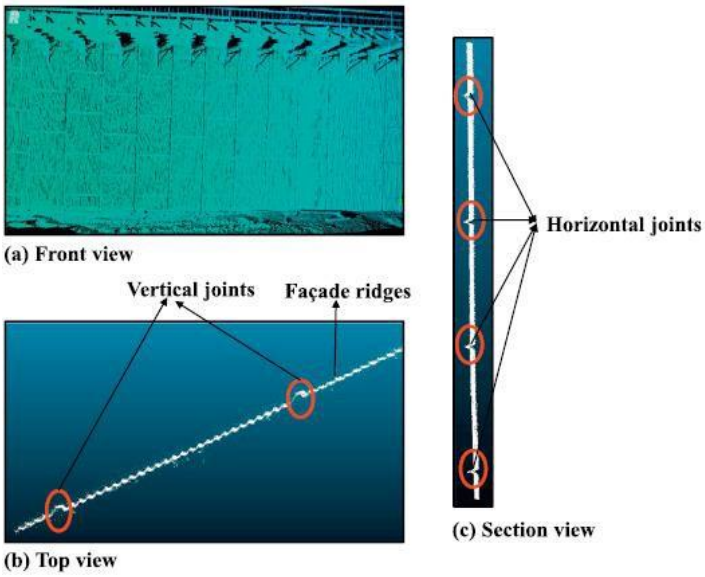

Figure 6: Point cloud view of the MSE wall with the identified joints (courtesy of Oskouie 2015).

Yang et al. (2017) introduced a method to classify road facility objects within MLS data. The proposed method initially detects the ground surface and then classifies the vertices into either ground or non-ground vertices. Afterward, the non-ground vertices are categorized into three subsequent groups based on their local dimensional features and segmented into meaningful potential object candidates. Then, the point-based, semantic-based, and object-based features along with their relative position, relative direction, and spatial distribution of these segments are computed, and consequently, each segment is further classified into various classes. Finally, these classes are recognized based on predefined objects (e.g., building, street lights, cars, guardrails, etc.) through a support vector machine (SVM) learning algorithm. The SVM is a polynomial classifier, like artificial neural networks. However, the SVMs use the approach of maximization of the margin of error and duality to classify the instances. To manually train the SVM, labeled data from various datasets and point densities were used. The proposed method worked well to document the current inventories (predefined objects of known geometries), however identifying damaged objects where the contextual feature such as relative orientation, direction, or locations are changed, is not well demonstrated. A similar approach in the use of aerial LiDAR data for the detection of highway assets was published in 2017 (He et al. 2017). The objects of interest include signs and signals, light poles, guardrails, and culverts. In this work, a field experiment was conducted with an aerial system consisting of a LiDAR scanner, inertial measurement unit, and flight navigation unit. He et al. (2017) concludes that the point cloud density resulted from the deployed aerial lidar platform provides sufficient resolution for most of the asset management

applications. In addition, the aerial platforms provide a different point of view compared to the ground-based lidar platforms. Objects that are usually occluded in ground-based derived point clouds can be detected using the aerial platforms. However, objects such as road signs that have relatively small sizes compared to larger objects like culverts may not be detected due to low point density.

Gargoum et al. (2017) use the MLS data to identify and extract highway signs. The method is divided into three main parts: intensity filtering, clustering, and geometric filtering. In the first stage, the point cloud vertices are grouped based on the vertices intensity values by selecting two lower and upper bound threshold values (identified via trial and error) until all the signs are categorized within the desired group. Afterward, the vertices are clustered based on their spatial location. Then, in the second stage, the clustering process is repeated using a density-based clustering algorithm to cluster group the vertices. In the third and final stage, the clusters created in the second stage are analyzed based on their width, height, and areas and these clusters are extracted and imported into Google Maps to verify the sign positions. Although this workflow is easy to implement, it requires significant manual operations which limits its scalability to larger datasets.

5.3.2 Roadway

Point cloud technology (including LiDAR) has been widely implemented in transportation applications during the past decades, including such topics as road facilities extraction, aggregation analysis, and highway and concrete defect detections. Compared to conventional methods, point cloud technology is an efficient, accurate technology for data collection, although point density diminishes with increasing collection distance. Recently, roadway analysis with point cloud data collected by mobile LiDAR platforms is an active topic of research in the development of methodologies to rapidly assess and update transportation infrastructure.

Olsen et al. (2013a) developed guidelines for the use of mobile LiDAR in transportation applications as part of the National Cooperative Highway Research Program Report 784. The report aims to provide effective approaches in the implementation of mobile LiDAR technology within the field of transportation. In greater detail, the report initially outlines the potential application of mobile LiDAR technology including safety (e.g., forensics/accident investigation), operations (e.g., land use, zoning, and building information modeling or BIM), maintenance (e.g., bridge inspection, landslide assessment, and drainage/flooding), project development (e.g., feature extraction for CAD modeling and virtual models to assist CAD), and project planning (e.g., environmental studies and general measurements). After reviewing the various applications of mobile LiDAR, the report covers typical data collection workflows as well as data management and mining strategies, as proposed by the American Society for Photogrammetry and Remote Sensing committee and the Federal Aviation Administration Advisory Circular on standards for using remote sensing technologies in airport surveys.

In addition to roadway and highway equipment management, LiDAR technology has been deployed to evaluate the road surface and geometry. GBL can create highly detailed and geometrically accurate point datasets, leading to its application to roadways being investigated by others. For example, Liu et al. (2017) discussed the application of the LiDAR point cloud data collected by GBL for evaluating the severity of rail-highway hump crossings with respect to road grade profile and vehicle dimensions. This method starts by updating the point cloud data of the rail-highway hump crossing coordinate system,

subsampling, and then computing the elevation map. For a given point cloud dataset and seven example vehicle dimensions, the elevation difference between each vehicle bottom and the pavement surface inputted is evaluated and checked as illustrated in Figure 7. The results of the method are analyzed to determine if the rail-highway crossing is safe for the example vehicle. The proposed method can accept any vehicle's dimensions; however, no detailed description is provided on how the original data coordinate system is established or subsampled.

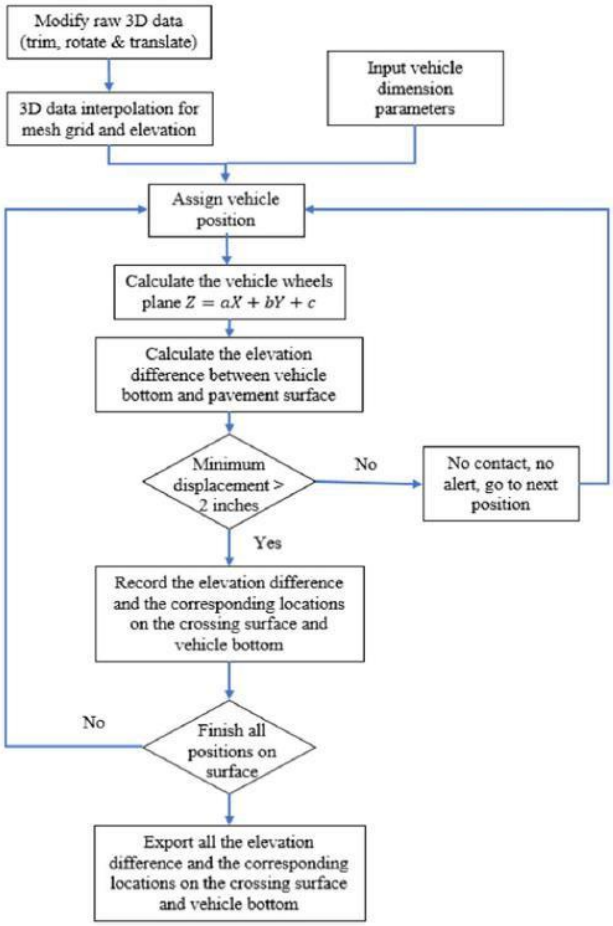

Figure 7: Analysis flowchart for the rail-highway crossing hump evaluation (courtesy of Liu et al. 2017).

GBL also can be used to assess the degradation and volumetric changes of paved roads under climatological effects. Akgul et al. (2017) studied the application of GBL for monitoring the degradation rate of pavement exposed to deformations induced by climatological changes for six months. The roadway was scanned in monthly intervals, and the data was registered and georeferenced. After the data collection, a raster road surface model (RSM) at 0.4 inches was created within ArcGIS. The changes or degradation rates were computed using subtraction of the RSM images of consecutive months. To measure the performance of the developed method, Akgul et al. (2017) compares the final results to the established method for measuring the volumetric changes via aerial derived DEM models. Akgul et al. (2017) concludes that the GBL assessment closely matched an aerial DEM model.

LiDAR point cloud technology is considered as a highly promising approach to perform a level analysis and drainage assessment of roadways (Figure 8). Gurganus et al. (2017) carried out a study on a

highway corridor to improve the drainage. The first step in the redesign process was to capture the existing surface geometry over a selected roadway by a mobile LiDAR platform. The selected roadway had a length of approximately 0.6 miles (1.0 km) long. Through collected LiDAR data, the design team assessed the roadway efficiently and safely for roadside ditch flowline, slope stability along the frontage road, and depth of cut within the pavement for installation of the underdrain. The assessment results allowed the team to create a new profile of the roadway and roadside ditch flowline to improve the drainage performance. As shown in Figure 8, the design team was able to capture the current road elevation and identify the amount of cut at each location with a high level of accuracy.

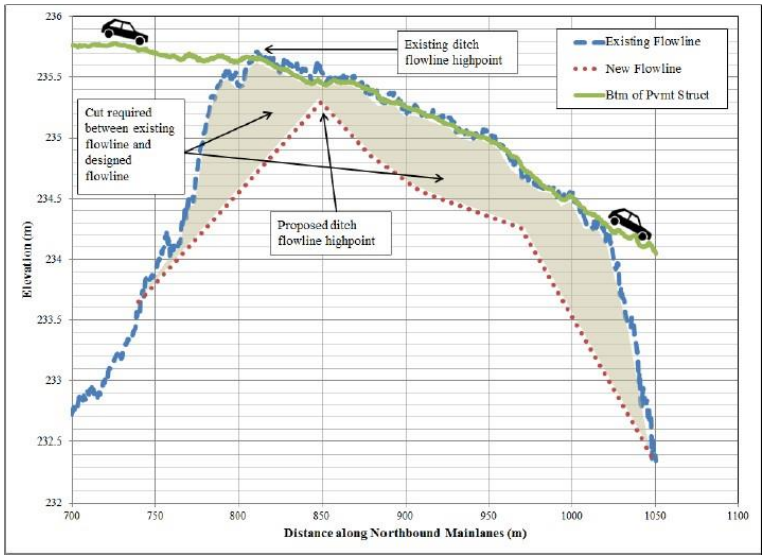

Figure 8: Existing and proposed drainage design on US 75 in north Texas (courtesy of Gurganus et al. 2017).

Iowa DOT has published a report on the comparison of MLS to a total station survey at I-35 and IA 92 interchanges (Miller et al. 2012). The survey covers one mile of I-35 and IA 92, respectively, which contained a total of four interchange ramps and bridges. The selected MLS platform used in the study had multiple LiDAR scanners, onboard IMU, GPS, cameras, and a distance measurement indicator (DMI). LiDAR data acquisition was carried out by Riegl's RiACQUIRE software, which is the common Riegl software solution for both MLS and aerial scanning data acquisition. In addition, the vehicle trajectory analyses were performed using Applanix's POSPac MMS version 5.3 software. Furthermore, Miller et al. (2012) processed the data in the forward and backward directions to generate optimal results and to resolve any potential lapses in the GPS data. Afterward, the data were further processed in Riegl's RiPROCESS software, which enabled the raw scans to be matched with a smoothed best estimate of the trajectory (SBET). Once this step is completed, Miller et al. (2012) utilize MicroStation software package TopoDOT's "Control Point to Data Analysis" function to average elevation accuracy analyses, where the RMSE accuracy was quantified as 0.013 ft (0.396 cm) overall. This RMSE accuracy value meets Iowa DOT specifications for an engineering survey. Finally, Miller et al. (2012) compared the resulted accuracy of MLS data to that of the traditional survey (via a total station) using a total of 1,823 points. To achieve

this task, the sum of the elevation difference was quantified and reported as 8.81 ft (2.68 m) for all points, with an average elevation difference squared of 0.057 inches (0.146 cm), and a root mean square error (RMSE) of 0.834 inches (2.118 cm). A summary of the differences, indicating the various tolerances for the points, is shown in Figure 9.

Tolerance	No. of Pts.	Percent				
> 0.25	3	0.16%				
0.20 to 0.25	5	0.27%	99.67%			
0.15 to 0.20	30	1.65%		99.07%		
0.10 to 0.15	168	9.22%			96.54%	
0.05 to 0.10	492	26.99%				86.51%
-0.05 to 0.05	1012	55.51%	+/- 0.25'	+/- 0.20'	+/- 0.15'	+/- 0.10'
-0.05 to -0.10	73	4.00%				86.51%
-0.10 to -0.15	15	0.82%			96.54%	
-0.15 to -0.20	16	0.88%		99.07%		
-0.20 to -0.25	6	0.33%	99.67%			
> -0.25	3	0.16%				
TOTALS	1823	100.00%				

Figure 9: Tolerance (in ft) of MLS compared to a traditional survey of 1,823 points (courtesy of Miller et al. 2012).

5.3.3 Structural

Point cloud feature extraction algorithms have other significant applications in addition to highway and railway components. Hoensheid (2012) evaluated a concrete deck surface using GBL data. Within the study, LiDAR point cloud data was used to quantify deterioration of a concrete bridge surface, where surface deterioration was classified as spalling, scaling, and cracking. During the research progress, LiDAR was found to be an accurate, economically acceptable, and efficient technology for measurements, surface damage detection, and model construction. Furthermore, the authors identified some parameters including the angle of incident, collection rate, reflectivity, and the height of the scanner as potential sources of errors. Other parameters not addressed in the study that would impact the sources of error include the distance of the scanner and scanning resolution, which are chosen by the surveyor and are a function of the available equipment and scanning settings.

In addition, LiDAR-derived point clouds can be used to identify surface defects (e.g., cracking, concrete spalling, loss of cross-section, etc.) in bridge piers, girders, or other structural members point clouds underlying geometrical features. For example, Yu et al. (2017) developed a method to detect and quantify damage percentile of such damage through extracting two classes of features based on computational geometry and statistical distribution of vertices in the 3D space. Within this study, the two classes of features were computed for each vertex of the point cloud data, and the distribution of computed feature values was evaluated to identify the location of potential surface defects within

planar and multiplanar surfaces for various levels of an eighteen-story structure. Yu et al. (2017) concluded that the results acquired by LiDAR data analysis agreed well with traditional structural health monitoring methods as well as the identified system properties and the response prediction of the calibrated finite element method model.

Harris et al. (2016) studied a series of bridge monitoring remote sensing techniques that can evaluate the bridge and the deck performance with minimal impact on the traffic. Within all methods outlined, including LiDAR and photogrammetric derived point clouds, the applications of point cloud data for bridge deck inspection are reviewed within MicroStation with TopoDOT, QuickTerrain modeler, and ArcGIS software. To perform a LiDAR survey, initially, the scans of a site of interest were collected through Leica ScanStation C10 GBL. Afterward, the various scan data were aligned and georeferenced in the Leica Cyclone Version 7.0 software, and then LAS format files were further processed in commercial software packages including MicroStation with TopoDOT, QuickTerrain modeler, and ArcGIS. Within the postprocessing step, the point clouds ROI were cropped, denoised, and prepared for analyses including surface condition assessment through measuring surface spalls, cracking, and girder section losses. Harris et al. (2016) provided a summary on point cloud results for measuring surface spalls, cracking, and girder section losses and compared the results to those computed through photogrammetry models in terms of accuracy and applicability. The study reports that the detectability accuracy of the point cloud data (collected by GBL platform) for bridge deck relatively agrees to that of identified with a close-range photogrammetry 3DOBS (Ahlborn et al. 2013). The accuracy of every photogrammetry technique is a function of equipment (i.e., the camera, focal length, etc.) and the distance of the object of interest to the camera. For this study, the collected images had a resolution of 0.07 inches (2 mm) per pixel, and the model created through the images had a resolution of 0.2 inches (5 mm) horizontal and 0.07 inches (2 mm) vertical. The quantified defect values (e.g., spalling area) from GBL data were 20% higher than compared to those computed through images. The study also reports that the accuracy of GBL data diminishes as the distance of the area of interest to scanner increases more than 65 ft (20 m) for a 50,000 point/second scanning rate setting.

Kong et al. (2013) investigated the capability of a GBL for structural health monitoring applications. To achieve this task, the study evaluated TerraSolid, TopoDOT, and Reigl RiSCAN software packages. The TerraSolid and TopoDOT software packages are add-ons that run within the Bentley software suite (e.g., MicroStation V8, PowerCivil, MicroStation CONNECT Edition, Open Roads Designer, etc.). These two packages can be utilized to create, edit contours or meshes, perform volume computations, and visualize surface models of point cloud data and finite element models. The study only outlines the initial usage of the GBL and these packages. Furthermore, their report outlines how these packages apply to LiDAR scanners within the field of structural health monitoring.

A bridge structure case study was commissioned by the Indiana Department of Transportation (DOT) to illustrate an MLS assessment process of a bridge structure (Johnson et al. 2015). Within this work, a total of four datasets with various point densities and color/intensity information were collected, and the mobile mapping registration was performed using Leica's Cyclone software. Afterward, bridge clearance values were evaluated for each dataset by an algorithm that the team developed to locate the lane strips in the point clouds accurately. Then, the results of the developed algorithm were verified by the MicroStation with TopoDOT software package. The report recommended that the point clouds are required to have a minimum point density of 2 points per in^2. This corresponds to a point-to-point spacing with a minimum of 1.4 inches (3.5 cm). Johnson et al. (2015) reported that more accurate and

reliable data could be extracted from datasets with a point density of 6 or 8 points per in^2. These point densities correspond to the point-to-point spacing of approximately 0.75 and 0.5 in (1.9 and 1.2 cm), respectively. Since the bridge clearance measurements required manual positioning or pre-defined lane positions; unfortunately, this method can result in subjective results. One take away of this work is that Cyclone software can preprocess, register, and further allows region extraction efficiently, while TopoDOT is optimized for specialized post-processing tasks and is not efficient in loading point cloud data with a large number of points. In other words, TopoDOT software package was proven to be a very convenient and accessible tool to perform specialized tasks, including feature extractions, cross-sectioning, clearance measurements, etc. TopoDOT, however, is limited based on the number of points that can be loaded into the software. The number of points that can be loaded into the software is related to workstation specifications. Within TopoDOT software, users can specify a hard limit on the total number of points that can be loaded into TopoDOT for software performance that matches the workstation specifications.

5.3.4 Geotechnical

LiDAR data acquisition can also be used in key geotechnical analyses. Applications to rockfall hazards were introduced in Dunham et al. (2017). Dunham et al. (2017) introduced a method to assess rockfall hazards via point cloud data by creating and computing a defined Rockfall Activity Index (RAI). To achieve this task, Dunham et al. (2017) initially organized the point cloud data into cells and then computed a normal vector for each cell. Through the normal vector orientation, the surface of the rock was classified into 7 categories based on their topographic style and geometric expressions. Figure 10 depicts the algorithm flowchart that was used to classify the rock surface.

In addition to rock classification, RAI is computed for every meter segment of the slope of interest using equation 1

$$RAI = \sum_{i=1}^{n} \frac{1}{2} m_i v_i^2 r_j \quad (1)$$

where *m* denotes the mass, *v* represents the velocity computed assuming free fall, and *r* is the instability rate. The method presented can be applied to point cloud data with various resolutions. The two proposed methods, RAI index and surface morphology, can identify rock-falling contributing effects in local and global scales, respectively. However, the developed method cannot utilize aerial LiDAR data (2.5-dimensional data). In this case, 2.5-dimensional data are essentially 2D images that use techniques such as graphical projections to simulate the appearance of 3D data. Acceptable data sources include GBL or photogrammetric approaches (structure-from-motion or SfM) after the vegetation is manually removed.

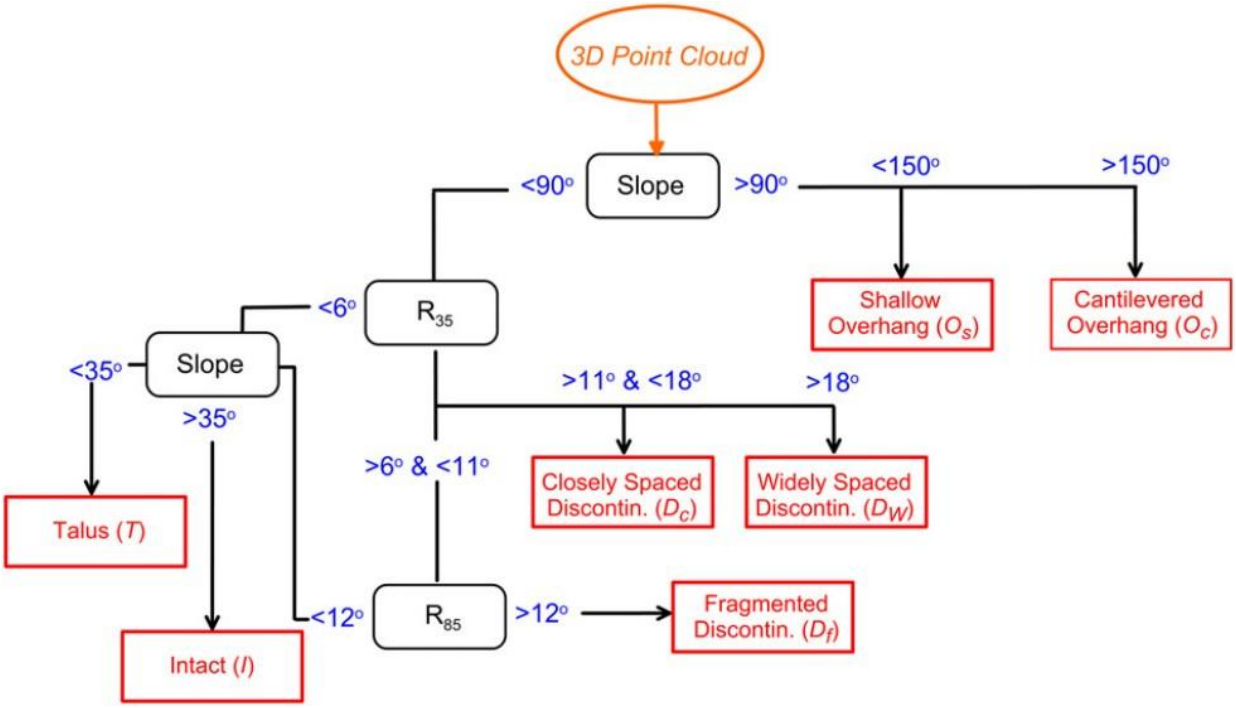

Figure 10: Rock surface morphology classification algorithm (courtesy of Dunham et al. 2017).

Eker et al. (2015) described a workflow using UAS-SfM derived point clouds and the opensource software CloudCompare's M3C2 function. This function is an example change detection algorithm to assess temporal changes of a surface (e.g., landslide assessment). The outputs of M3C2 include distance uncertainty and nonsignificant change between two datasets. Eker et al. (2015) analyzed a geotechnical slope of approximately 21,500 ft^2 (2000 m^2) wide (Figure 11). To perform the survey, the baseline data was created using approximately 400 images, and two more surveys with an interval of roughly 5 months were carried out that resulted in a total of 200 additional images (100 images per survey). To register and increase the accuracy for analysis, a total of 9 ground control points were surveyed for each site visit using Real-Time Kinematic-Global Positioning System (RTK-GPS). Eker et al. (2015) were able to estimate the volume of eroded and accumulated material. For each flight mission, the deliverables included point clouds, digital elevation models (DEMs), and orthophotos, which can be used for further analysis in GIS and point cloud processing software. As a result, the M3C2 function output a mean value of 5.2 inches (13.4 cm) and a standard deviation of 0.3 inches (7.4 mm). Therefore, the M3C2 function was proved to be an accurate and suitable change detection algorithm to quantify landslides and other similar change-detection scenarios (at the displacements at the sub-inch level). While this was performed using a UAS, this could be similarly applied to GBL and aerial LiDAR, where the latter is preferred due to fewer areas of occlusion.

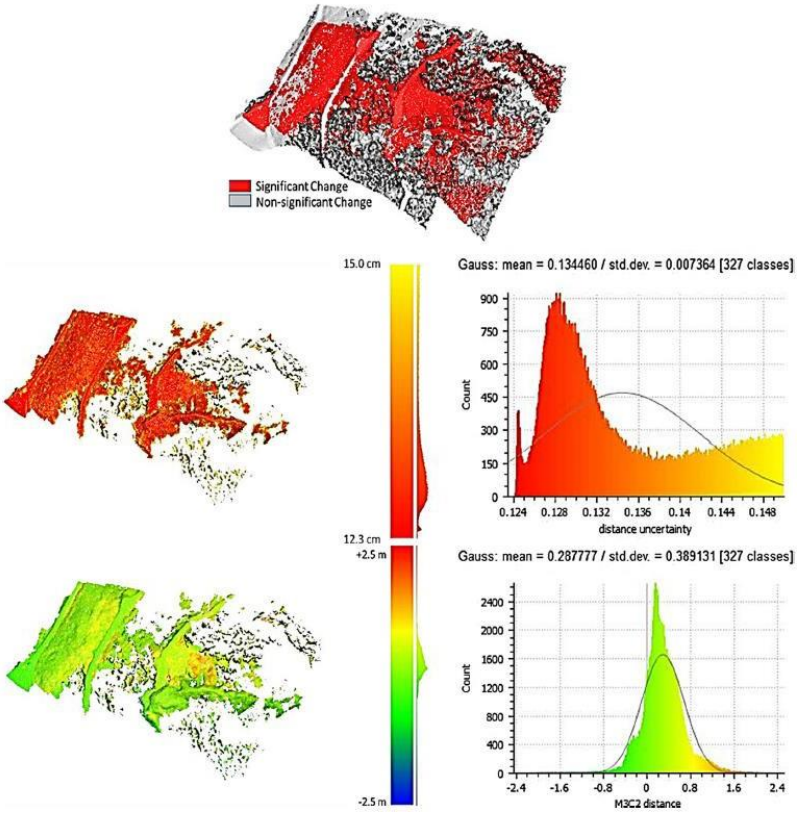

Figure 11: Cloud-to-cloud comparison of a landslide using change detection (courtesy of Eker et al. 2015).

5.3.5 Workflows and Procedures

One example of the usage of mobile LiDAR for surveying workflow and procedure is Ellis (2017). In this work, the process is briefly outlined for the point cloud CAD/GIS use including registration, calibration, and feature extraction. This example was explicitly performed for highway operation, maintenance, and/or design using data from New York City. A comparison between a mobile LiDAR point cloud and its corresponding extracted features is shown in Figure 12 and Figure 13.

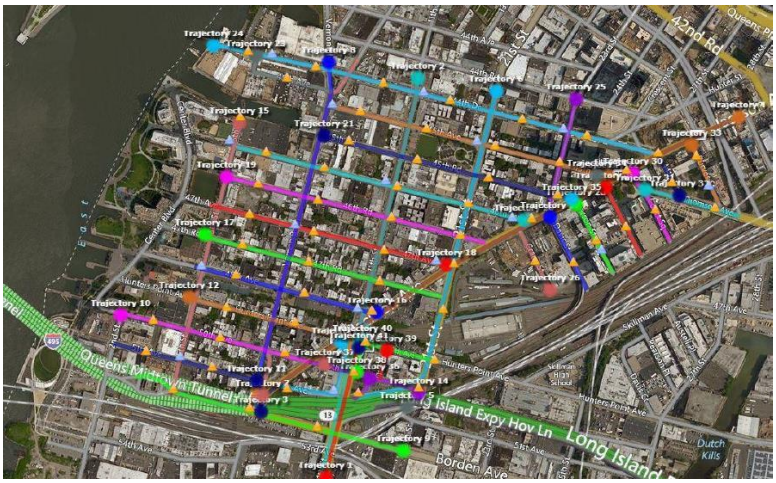

Figure 12: Mobile LiDAR point cloud and its key features (courtesy of Ellis 2017).

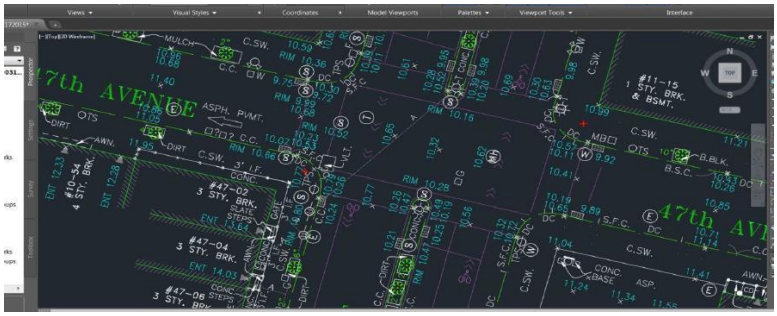

Figure 13: AutoCAD Civil 3D plan drawing created from the extracted features (courtesy of Ellis 2017).

Miyamoto (2016) developed a procedural document on how to pre- and post-process point clouds within AutoCAD Civil 3D. This report outlines a step-by-step procedure to down-sample and creates meshes within the software above. The surface mesh creation can be used within any processed point cloud datasets, including GBL, MLS, or aerial LiDAR. Such surface meshes can be developed for coastal areas, streets, and busy intersections for various uses. However, this method requires human interactions as all steps are performed in a non-automated method using AutoCAD specific operations.

Another investigator focused on MLS-derived data management and visualization within the Bentley software suite (Guo 2016). The study proposed a workflow to develop 3D design models from LiDAR data (Figure 14). The workflow includes MicroStation with GeoPAK, InRoads, and Open Roads, as these are one of the most commonly used software in design surveys, archival applications, and asset management purposes. Autodesk AutoCAD Civil 3D in conjunction with Bentley products were also used within the workflow for 3D design model as well as Leica Cyclone, 3D Reshaper, TopoDOT, Quick Terrain Modeler, and ArcGIS Pro, for LiDAR data pre-processing (e.g., point cloud registration or object extraction). Within this workflow, once point cloud data are registered and filtered (denoised), an accuracy check is performed to identify if the data meets the requirement. Afterward, the data can be imported into a post-processing or modeling software for feature extraction or designed based modeling, respectively. These products can be merged from other resources and can be delivered to

agencies, consultants, or contractors. Unfortunately, this study, while outlining a procedure, provided no guidance on accuracy or resolution requirements.

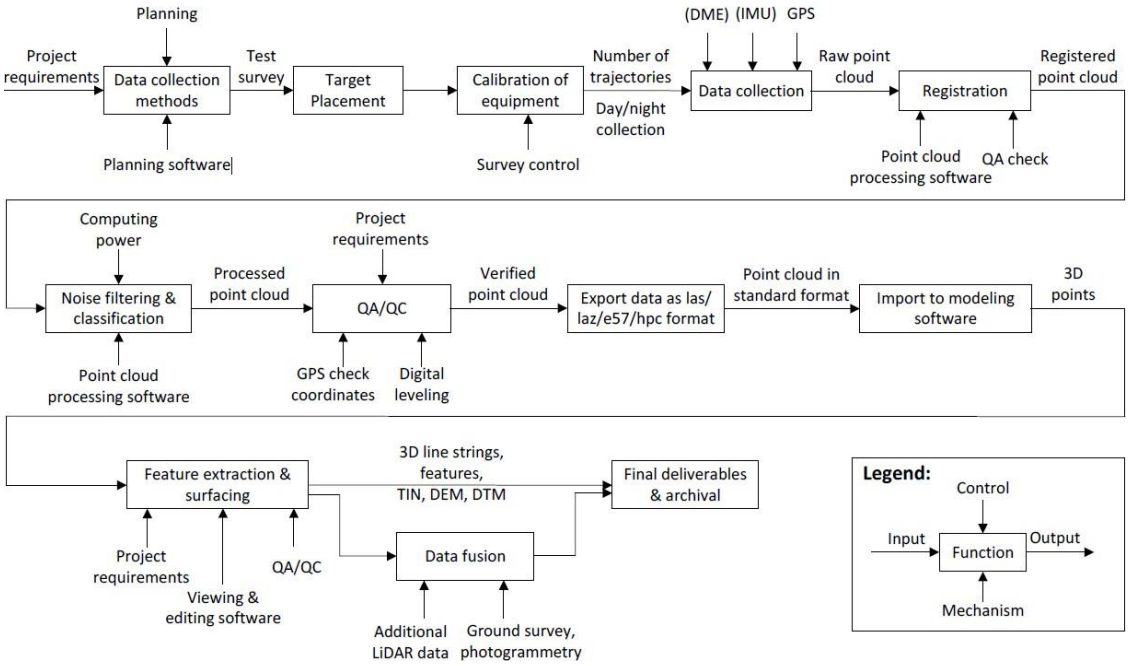

Figure 14: Finalized workflow for developing design models from LiDAR data (courtesy of Guo 2016).

The University of California at Davis and California Department of Transportation (Caltrans) performed a study on the MLS-derived data management standards and its application (Swanston et al. 2016). One of the objectives of the research was to develop software tools for automated data cataloging with easy internal sharing and public access (via a web platform). The research resulted in a solution for exploring and managing the MLS-derived data using LidarCrawl. LidarCrawl provides automatic processing with regard to the extraction of project and file metadata from MLS datasets. The solution for MLS data storage is to use NetApp to prevent data loss due to hard drive failure and increase data redundancy. As shown in Figure 15, it is a user-level application that avoids duplication of work (as the data can be shared and accessed by various sections within Caltrans). This software, while not used for feature extraction or post-processing, is one of the applications recently developed tools for automated MLS-derived data management and cataloging that is compatible with GIS tools or a web browser.

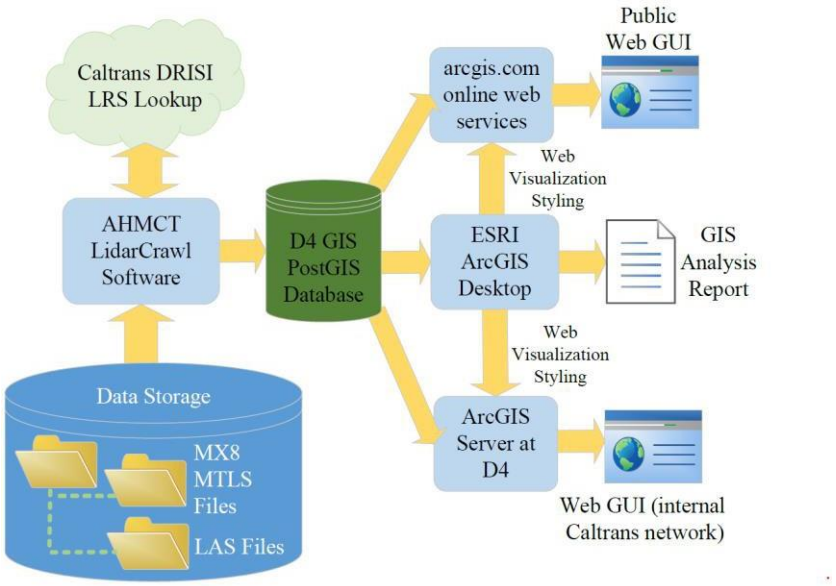

Figure 15: LidarCrawl software data flow diagram (courtesy of Swanston et al. 2016).

6.0 Current, Potential and Recommend Uses of Lidar for SDDOT

6.1 Identify Current and Potential Uses for LiDAR at SDDOT

In this task, the research team has identified several current and potential uses for LiDAR. This is presented below in Table 1. The uses were discovered during the literature review and summarized above in task 2.

Table 1: Current and potential uses for LiDAR.

No.	Area	Application	LiDAR Platforms[1]			Description
			GBL	MLS	Aerial	
1	Asset Management	Inventory Management		X		Condition assessment of signs, guardrails, barriers, poles, etc.
2	Transportation	Roadway Survey	X	X	X	Assess the condition of pavement and road surface marking
3	Transportation	Roadway Design	X	X	X	Improve design by identifying site obstructions and a better understanding of pre-construction conditions
4	Transportation	Roadway Construction	X	X	X	Project progress monitoring and document condition at the completion of the construction to ensure project specifications are met or document the plan change
5	Transportation	Hydraulic/ Drainage	X	X	X	Identify local runoff and watershed features, and assess the drainage performance of roads and highways
6	Structural	Bridge Survey	X	X	X	Identify as-built and current condition of the bridge to perform accurate measurements
7	Structural	Bridge Assessment	X			Structural condition and damage assessment to study the effects of a scourge, corrosion, cracking, damaged connection, etc.
8	Geotechnical	Slope Analysis	X		X	Slope stability and monitoring of large areas in particular
9	Geotechnical	Earthwork	X	X	X	Quantification of extraction and fill volumes
10	Geotechnical/ Structural	Tunnel Assessment	X	X	X[2]	Survey of conditions and damage assessment
11	Geotechnical/ Structural	Scour Assessment	X		X	Condition monitoring and assessment of scouring and changes in time
12	Surveying/ Environmental	Terrain Mapping	X		X	Natural terrain mapping, vegetation management, etc.

[1]Notes: Various LiDAR platforms may include ground-based lidar (GBL), mobile lidar scanning (MLS), and aerial platforms such as an airplane, helicopter, or unmanned aerial system.

[2]This type of assessment may be possible given some aerial platforms.

6.2 Applications and Recommendations of Uses for LiDAR at SDDOT

As previously identified, a summary list of applications is shown previously in Table 1. Specific to this work, these applications are detailed for recommended accuracy, resolution, and recommended platform (Table 2). Table 3 provides additional details on the processing software and data format options. Lastly, Table 4 and 5 detail the capital and operating costs, and Table 6 illustrates efficiency characteristics and safety benefits for each identified area. Note the capital and operating costs are approximated as based on a survey of consultant services conducted in the Fall of 2019. These costs demonstrate an average, but they are known to vary given the project requirements and size.

Accuracy indicates how closely the collected data represent the true condition of objects in the real world. Precision represents the degree of consistency for a group of observations. On the other hand, resolution, or spatial resolution within this document, illustrates the number of collected points per time, area, or volume. Figure 16 shows the relationship between accuracy, precision, and resolution. As illustrated, resolution defines the sampling frequency of sensors. LiDAR platforms are designed and maintained (through routine calibration process) to collect data with a high level of accuracy and precision. Therefore, the accuracy within Table 2 refers to the accuracy of aligned or registered data (e.g., denoised and registered data). This accuracy (of the registration) is independent of the resolution, which guides the desired point-to-point spacing or resultant ground sampling distance (GSD). In addition, the accuracy was provided qualitatively as it will depend on numerous factors (e.g., number of scans, post-processing methods, etc.). In this section, an accuracy denoted as "low" corresponds to applications that can be carried out with a dataset with rough or approximate alignments (i.e., an error of 10 inches) without significantly affecting the results. An accuracy of "medium" denotes modest alignment or registration (i.e., 5 inches). Finally, a "high" accuracy corresponds to a dataset with lowest alignment error (e.g., less than 0.5 inches), where a tight tolerance may be required. It is noted that the accuracy of the project deliverables will vary by project need.

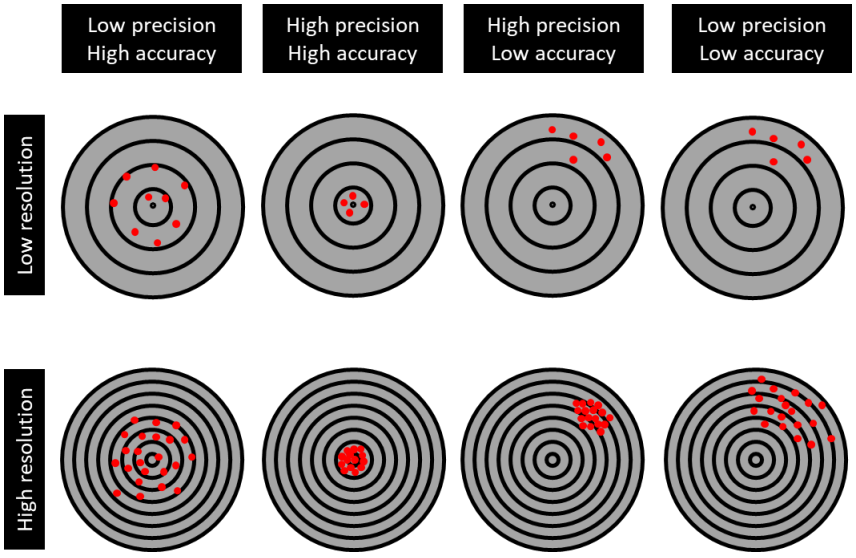

Figure 16. Visual demonstration of accuracy, precision, and resolution.

Table 2: Accuracy, resolution, and recommended platform identified various workflows.

No.	Area	Application	Accuracy[1]	Resolution[2] (in.)	Recommended Platform
1	Asset Management	Inventory Management	M	1 to 4	MLS
2	Transportation	Roadway Survey	L	0.8 to 1	MLS, GBL, Aerial
3	Transportation	Roadway Design	H, M	1 to 2	MLS, GBL, Aerial
4	Transportation	Roadway Construction	L, M	1 to 2	MLS, GBL, Aerial
5	Transportation	Hydraulic/Drainage	L, M	1 to 4	MLS, GBL, Aerial
6	Structural	Bridge Survey	M	0.5	MLS, GBL, Aerial
7	Structural	Bridge Assessment	H	0.25 to 0.5	GBL
8	Geotechnical	Slope Analysis	L	1 to 4	GBL, Aerial
9	Transportation	Earthwork	L	1 to 4	GBL, Aerial, MLS
10	Geotechnical/ Structural	Tunnel Assessment	L, M	0.5 to 1	MLS, GBL, Aerial
11	Geotechnical/ Structural	Scour Assessment	L, M	0.5 to 4	GBL, Aerial
12	Surveying/ Environmental	Terrain Mapping	M, H	>4	GBL, Aerial

[1]The accuracy within this table corresponds to the alignment or registration accuracy of two or multiple lidar datasets. The L corresponds to low (less than 10 in.), M corresponds to medium (less than 5 in.), and H refers to high (less than 0.5 in.) level of alignment accuracy.

[2]The resolution represented based on the point-to-point spacing of points within a point cloud dataset.

The collected data can be pre-processed, analyzed, and stored in unified formats with various software solutions depending on the project type, analysis required, and potential future usage. Table 3 demonstrates the potential software that can be used to perform the desired analysis. Currently, the listed software and analyses can be run with a machine that minimally runs Windows 10 – 64 bit and has a 4 to 6 core CPU, 16 GB of RAM, 4 GB GPU, and 1 TB SSD.

Table 3: Software recommended to process LiDAR for various workflows.

No.	Area	Application	Recommended Software	Data Format
1	Asset Management	Inventory Management	MicroStation with TopoDOT. AutoCAD with Siteco	LAS, E57, CSV
2	Transportation	Roadway Survey	MicroStation with TopoDOT and TerraScan, ArcGIS Pro	LAS, E57,DTM, DEM, CSV
3	Transportation	Roadway Design	MicroStation with TopoDOT and TerraStreet	LAS, E57, DTM, DEM, CSV
4	Transportation	Roadway Construction	MicroStation with TopoDOT and TerraStreet	LAS, E57, DTM, DWG, DEM
5	Transportation	Hydraulic/Drainage	MicroStation with TopoDOT and TerraSolid, ArcGIS Pro	LAS, E57, CSV
6	Structural	Bridge Survey	MicroStation with TopoDOT, ArcGIS Pro, CloudCompare	LAS, E57, CSV
7	Structural	Bridge Assessment	MicroStation with TopoDOT	LAS, E57, CSV
8	Geotechnical	Slope Analysis	MicroStation with TopoDOT and TerraSolid, ArcGIS Pro	LAS, E57, CSV
9	Transportation	Earthwork	MicroStation with TerraSolid or TopoDOT, MicroStation GeoPAK	LAS, E57, CSV
10	Geotechnical/ Structural	Tunnel Assessment	MicroStation with TopoDOT, CloudCompare	LAS, E57, CSV
11	Geotechnical/ Structural	Scour Assessment	MicroStation with GeoPAK, CloudCompare	LAS, E57, CSV
12	Surveying/ Environmental	Terrain Mapping	ArcGIS Pro, CloudCompare	LAS, E57, CSV

Table 4. The average purchase and rental cost of various platforms.

Platform	Average Purchase Cost	Average Rental Cost
GBL	$100,000	$700/ Day
MLS	$500,000	$1550/Day
Aerial	$350,000 (plus the aircraft acquisition costs)	$1950/Day

Table 5: The average operating cost and mobilization for various platforms.

Platform	Total Operating Cost	Estimated Data Collection Per Day	Description	Mobilization Cost
GBL	$700/mile	1 mile	High resolution data collection	$250 to $1250 travel day - per person
	$350/mile	2 miles	Medium to low resolution data collection	
MLS	$500/mile	16 miles	Data collection with a base GNSS setup	
	$200/mile	40 miles	Data collection in the GNSS network range	
Aerial	$200/mile	20 miles	2-mile data collection per hour	

Table 6: LiDAR recommended use integration for SDDOT Workflows – additional details.

No.	Area	Application	Efficiency[1]	Benefits
1	Asset Management	Asset Inventory	MLS: H	Safe, accurate, and rapid data collection; reduced traffic congestion
2	Transportation	Roadway Survey	MLS: H GBL: L Aerial: H	Safe, rapid, and highly accurate data collection, ease data sharing, reduced traffic congestion
3	Transportation	Roadway Design	MLS: H GBL: L Aerial: H	Increase design accuracy, ease data sharing and integration
4	Transportation	Roadway Construction	MLS: H GBL: L Aerial: H	Allow to create accurate BIM, increase inspection capabilities
5	Transportation	Hydraulic/ Drainage	MLS: H GBL: L Aerial: H	Safer and rapid condition assessment, highly accurate and reliable data
6	Structural	Bridge Survey	MLS: H GBL: L Aerial: H	Safe, accurate, and rapid data collection, reduced traffic congestion
7	Structural	Bridge Assessment	GBL: H	Enhance data accuracy and reliability, keep staff in a safe condition, allow assessment in a safe environment
8	Geotechnical	Slope Analysis	GBL: L Aerial: H	Perform a rapid and accurate data collection at a safe distance
9	Geotechnical	Earthwork	MLS: H GBL: L Aerial: H	Improve volume estimation and rapid data collection at a safe distance
10	Geotechnical/ Structural	Tunnel Assessment	MLS: H GBL: L Aerial: H	Safe, rapid, and highly accurate data collection, ease data sharing, reduced traffic congestion
11	Geotechnical/ Structural	Scour Assessment	GBL: L Aerial: H	Perform a rapid and accurate data collection at safe distance
12	Surveying/ Environmental	Terrain Mapping	GBL: L Aerial: H	Perform a rapid and accurate data collection efficiently and cost effectively

[1]The L, M, and H correspond to low, medium, and high efficiency in data collection which were determined based on time required to achieve the recommended resolution and accuracy shown in Table 2

7.0 Example Data Collection Summary

This chapter summarizes the example field data collection process. It summarizes the data collection steps, data processes, and deliverables of two different remote sensing platforms. Initially, the implemented surveying platforms used within the demonstration are introduced. Afterward, the data collection planning and strategies are discussed. In addition, data processing for each platform is described, and the result of each platform is compared to identify the final accuracies and each platform deliverables. In the final section, potential post-processing options using Bentley software are presented and discussed.

7.1 Data Collection

The site selected for the survey is the White River bridge which is a three-span steel girder structure that is located south of Presho, SD on US Route 183 (approximately at latitude of 43.704352 and longitude of -100.041172). The survey area consisted of the bridge and the surrounding regions within 1000 ft of the bridge in the cardinal directions (Figure 17). To carry out the surveying task of the selected area within a day, two different remote sensing platforms, a LiDAR scanner, and a medium-size drone with an onboard camera were employed.

Figure 17. The selected site for surveying operation.

The team collected a total of 40 LiDAR scans of the bridge and its surrounding regions using two GBL scanners. The LiDAR scanners included Faro Focus3D S-350 (Figure 18a) and Faro Focus3D X-130 (Figure 18b). Two scanners were utilized for speed and efficiency in the data collection. The Faro S-350 uses laser class 1 with a wavelength of 1,550 nm and has a maximum range of 1,150 ft. In addition, S-350 is equipped with a High Dynamic Range (HDR), a high-resolution camera (up to 160 MP) and can collect up to 976,000 points per second with a ranging error of ± 0.07 in and an angular resolution of 0.009˚. The Faro Focus3D X-130 uses an identical laser class. However, the X-130 has a maximum range of 420 ft and can create pictures with a maximum resolution of 70 MP. During the survey, each LiDAR platform collected a total of 20 scans at various locations.

(a) (b) (c)

Figure 18. Remote sensing platforms used to collect data: (a) Faro Focus3D S-350 LiDAR scanner, (b) Faro Focus3D X-130 LiDAR scanner, and (c) DJI Inspire 2 UAS platform.

7.1.1 LiDAR Data Collection

To perform the LiDAR survey, the team used a closed transverse scanning strategy. Within this strategy, a series of scan setups are planned to create a loop, where the first and last scans link together. This allows a reduction in the error propagation during the alignment process. As illustrated in Figure 19, within each region (e.g., south of the bridge), two rows of scan setups exist to facilitate a closed scanning strategy. In addition, each scan setup collects data of at least one checkerboard target, which is used within the UAS data processing. To optimize LiDAR data collection process regarding data quality for the surveying time, each scan setting was set to execute a scan with a point-to-point spacing of 0.2 inches at a distance of 30 ft, which corresponds to a total of 48 million points per scan within 15 minutes. The computer used to process the LiDAR point cloud data is equipped with 6-core CPU, 4 GB dedicated GPU, 64 GB of RAM, and SSD. In addition, the computer processed the data in 24 hours.

Figure 19. Scan setup locations for X-130 and S-350 laser scanners.

7.1.2 SfM Platform

The equipment for the aerial surveys was a DJI Inspire 2 UAS with an onboard Zenmuse X5 camera and mounted 15 mm lens. Figure 18c depicts the platform used in this survey. The selected flight paths were autonomously controlled with the Pix4dcapture application on a handheld Android-based tablet. In total, six flights were performed with an 85% overlap at an average above-ground-level (AGL) altitude of 150 ft. This produced a total of 3024 images with 0.15 square miles of the area covered, with a resultant GSD of 0.72 in. As can be observed in Figure 20, the flights covered the roadway, bridge deck, and the nearby riverbanks. Note that the image locations are shown in red circles in Figure 20. Throughout the surveyed area, 40 checkerboards were placed to serve as GCPs and checkpoints (CP) for the UAS survey. The collected images were processed for 17.5 hours using a cloud server with a Xeon 8 core CPU and dedicated GPU, and the machine used a total of 70 GB of RAM.

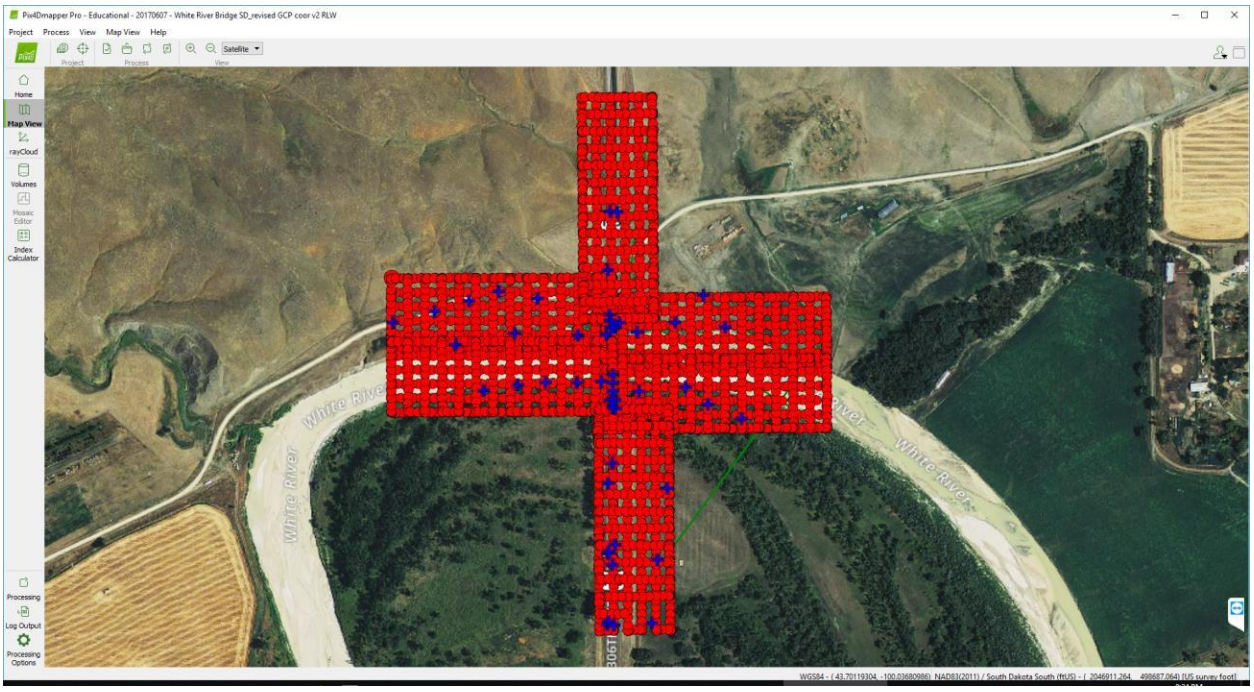

Figure 20. UAS-SfM image locations.

7.1.3 RTK Platform

To georeference the collected data and serve as GCP/CP for the UAS survey, the team collected GPS coordinates of all checkerboard targets through a Real-Time Kinematic (RTK) survey as a ground control point GCP or CP. The RTK system acquired a total of 47 points including 32 checkerboards and 15 natural feature points within the survey area. Eight of the checkerboards were disrupted during the data process due to traffic and other activities. Afterward, the collected GCP data was imported in state plate coordinates to Pix4D for the finalized point cloud generation.

7.2 Data Processing

7.2.1 LiDAR Data Processing

The team used the Faro Scene software platform to align the collected LiDAR scans. Faro Scene is proprietary software that matches the LiDAR equipment platform. Figure 21 illustrates the LiDAR and SfM data processing main steps within this case study. The LiDAR data processing steps are shown in the left branch of the flowchart. To achieve the alignment task, initially, the site was divided into five segments: northeast, northwest, bridge, southeast, and southwest. Each segment contained the scans corresponding to the designated region as well as one or more scans that had an overlap with adjacent segments (e.g., a scan that covers regions in both the northeast and northwest segments). Afterward, the point cloud of each segment was created by loading the sequential scans to the software and aligning the scans through a cloud-to-cloud optimization technique. Then, the registered segments

were aligned together, and the overall alignment accuracy was further enhanced using an additional cloud-to-cloud process (

Figure 22). The final point cloud has a total of 542 million points, with a mean alignment error of 0.0814 ft, a standard deviation of 0.0419 ft, and an RMSE of 0.0914 ft. In addition, the computed RMSE 95% confidence interval (CI) value was equal to 0.1477 ft. Figure 23 depicts the final LiDAR point cloud.

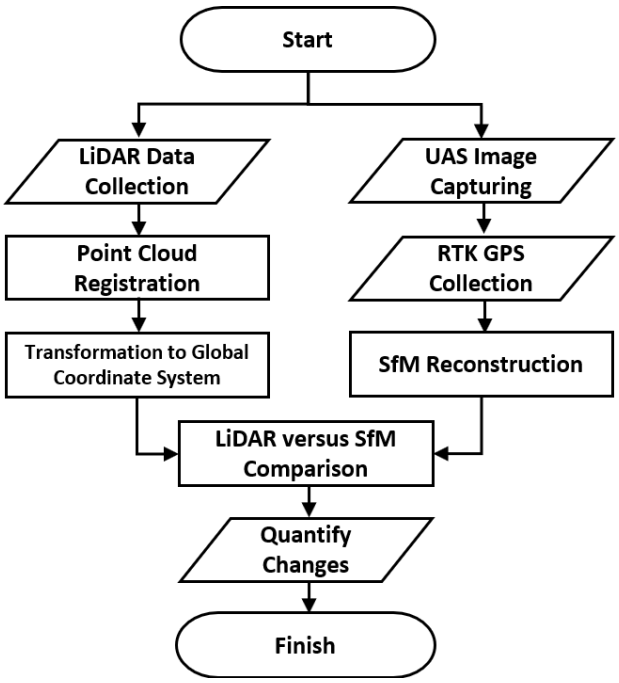

Figure 21. Flowchart of LiDAR and SfM data processing.

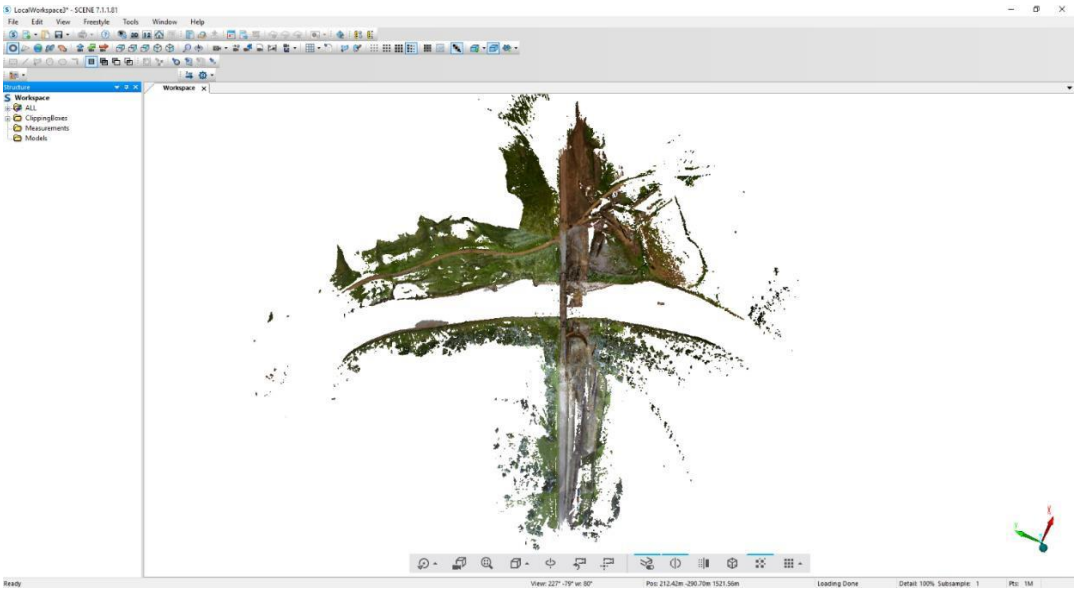

Figure 22. Point cloud processing in Faro Scene software.

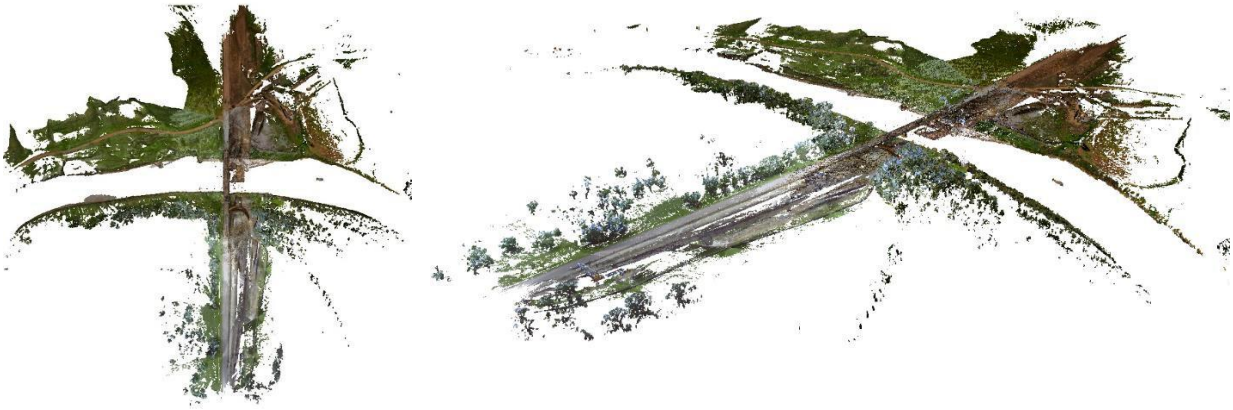

(a) (b)

Figure 23. White River bridge LiDAR point cloud: (a) top view and (b) southeast isometric view.

Once the alignment process concluded, the resultant LiDAR point cloud was transformed to state plane coordinates (SPC) based on the GPS data collected during the RTK survey. To identify the most accurate transformation, two transformation methods were explored within this study. The first method uses single-value decomposition (SVD) to compute the transformation matrix. The second transformation is performed using the Scene software. The transformation parameters within both methods are computed based on coordinates of the GCP checkerboards acquired using the RTK survey and the point cloud, respectively. Note that the RTK coordinates are considered here in this study as the reference points. To identify the GCPs that result in the most accurate transformation, initially, the two transformations were estimated based on all available GCPs. Then, the eleven GCPs that resulted in the least error values within the last step are identified and used to estimate 2 additional transformations: SVD-based and internally with the Scene software. In conclusion, the transformation results (of the four

various approaches) are compared against the georeferenced SfM derived point cloud to identify the most accurate method. This is detailed in the next sections.

7.2.2 SfM Data Processing

Pix4D is a commercial software commonly utilized for UAS Structure-from-Motion (SfM) processing, which utilizes high-resolution images to produce accurate deliverables, including point clouds, orthomosaics, digital terrain models, etc. The right branch of the flowchart shown in Figure 21 illustrates the SfM data processing steps. The example of 2D images generating a 3D point cloud at the White River bridge deck is displayed in Figure 24. A total of 42 GCPs (checkerboard and natural features) and three CPs were imported prior to point cloud processing in the Pix4D software to constrain and reduce the point cloud uncertainty. Furthermore, the processing template for data processing is selected as 3D maps, including parameters such as one-half image scale, optimal point density, and a minimum number of three matches. Figure 25 illustrates the resultant SfM point cloud generated by Pix4D software, which has a total of 204 million points. To evaluate the resultant point cloud regarding the accuracy, the resultant location of CPs was compared with respect to the RTK survey results. As shown in Table 7, the final point cloud proves to be accurate as the CPs comparison demonstrates low error values, as constrained by the accuracy of the RTK survey. The direct output from Pix4D is the point cloud in SPC. Note the output from Pix4D can be specified in other coordinate systems as SPC is one option.

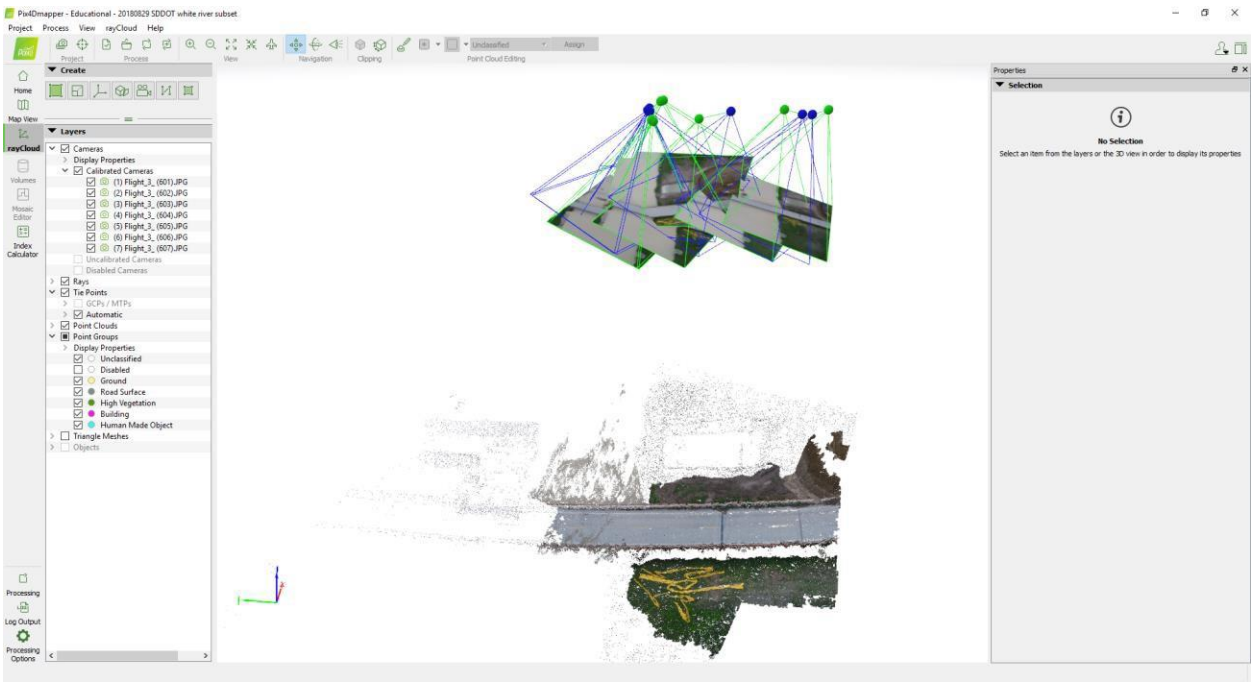

Figure 24. UAS-SfM point cloud generation in Pix4D.

(a) (b)

Figure 25. White River bridge SfM point cloud: (a) top view and (b) southeast isometric view.

Table 7: Errors at CPs.

CP ID	Error X (ft)	Error Y (ft)	Error Z (ft)
5013	0.0581	0.0329	0.0759
5015	0.0642	0.0126	0.0181
5010	0.0256	-0.0074	-0.0476
Mean	0.0493	0.0127	0.0155
Sigma	0.0169	0.0165	0.0504
RMS Error	0.0521	0.0208	0.0528

7.3 Data Comparison: LiDAR versus UAS-SfM

To identify the most accurate transformation process conducted to transfer LiDAR-derived point cloud to SPC, the resultant point cloud of each of the four transformation processes are compared to the georeferenced SfM derived point cloud in SCP. To compare the two point cloud datasets, the cloud-to-cloud (C2C) function within the CloudCompare software is used. The C2C function segmented the reference and compared point cloud data into small regions and compares the corresponding segments as measured from the reference. Figure 26 depicts the C2C results for each transformation. Within this figure, the points with a deviation value of zero to 0.3 ft are colored blue, and as the color changes and approaches dark red, the deviation increases. As illustrated in Figure 26, the LiDAR point cloud that was transformed using an SVD-based method using all available GCPs resulted in the most accurate transformation, while the transformation using the Scene software with 11 GCPs resulted in the least accurate and highest deviation results. To further study the transformation accuracy, the cumulative point count versus the deviation measured between transformed LiDAR and georeferenced SfM point clouds were constructed within a cumulative density function (CDF). The CDF is illustrated in Figure 27, where the transformation method based on SVD and all GCPs resulted in more points with smaller deviations.

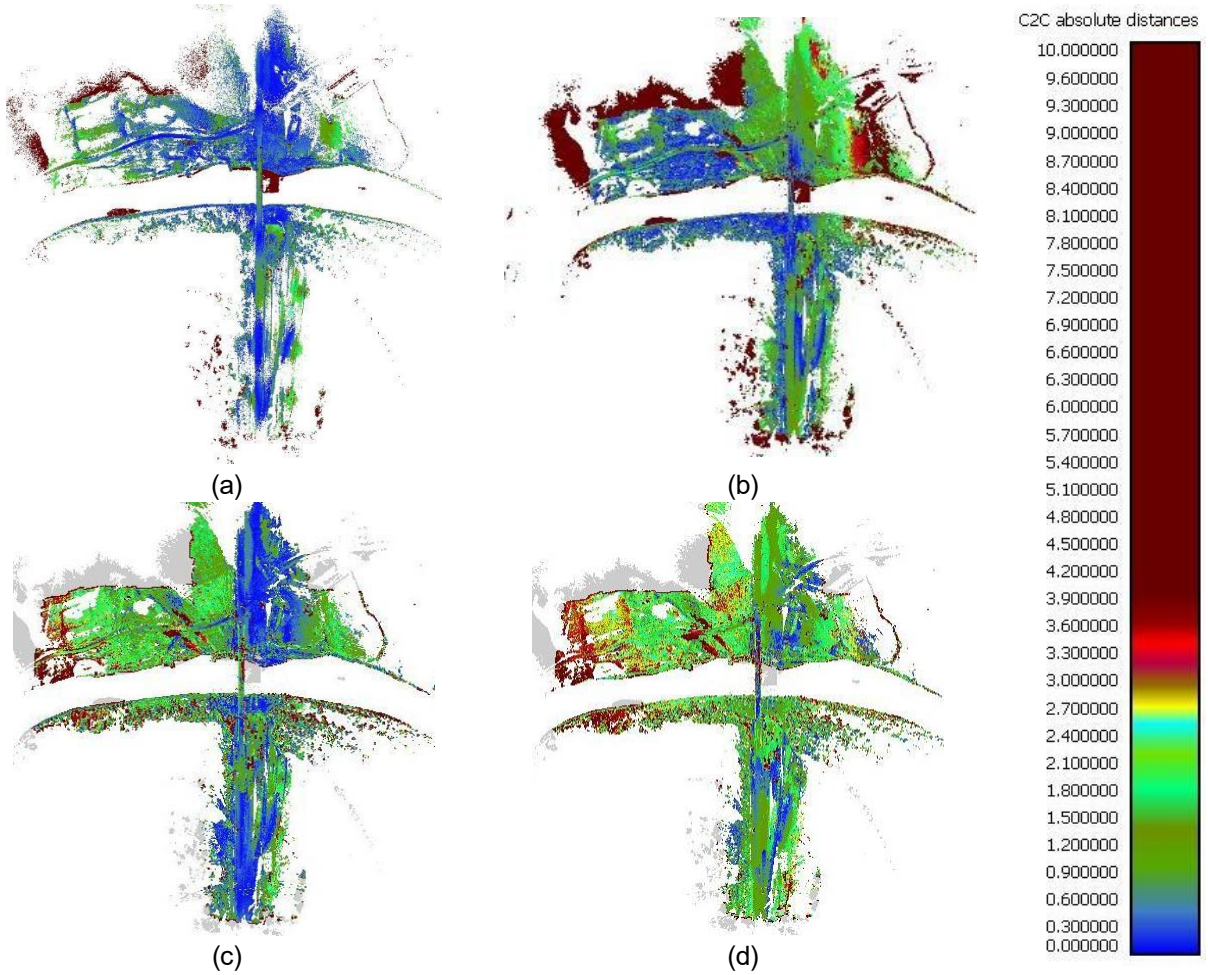

Figure 26. Color-coded point cloud for distance discrepancy between UAS-SfM point cloud and LiDAR point cloud transformed with various approaches: (a) SVD-based method using all points, (b) SVD-based method using eleven points, (c) Scene-based transformation using all points, and (d) Scene-based transformation using eleven points.

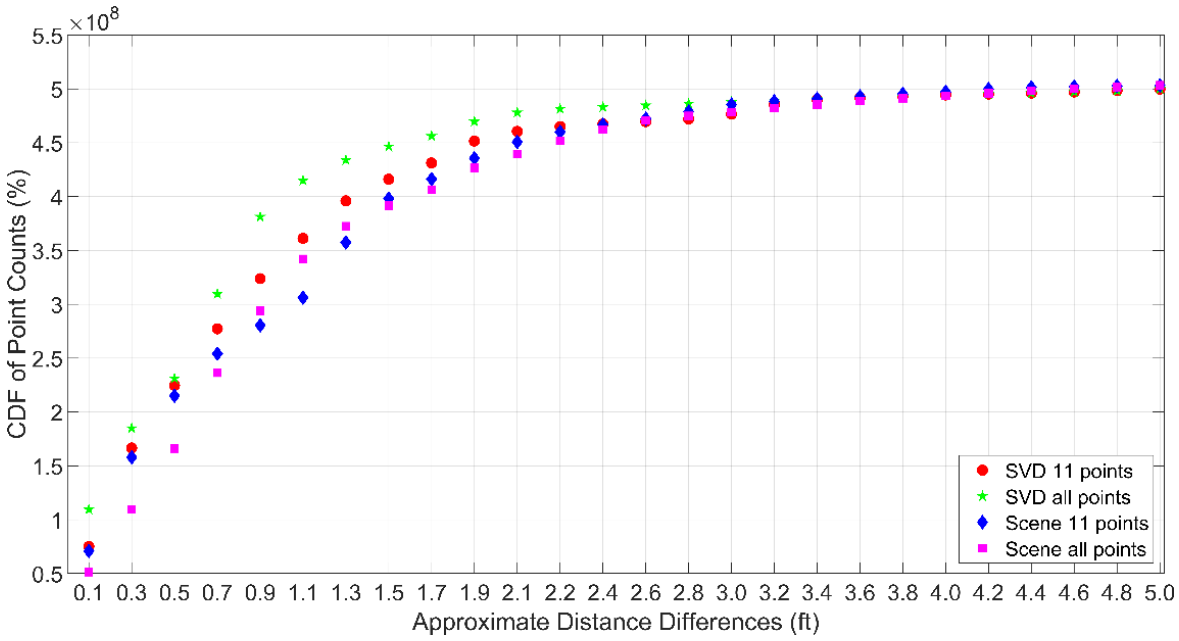

Figure 27. The cumulative distribution function of point counts histogram of the discrepancy between SfM point cloud vs. LiDAR point cloud transformed through various techniques and parameters.

In summary, Table 8 presents the GCP errors estimated for both optimally transformed LiDAR and final SfM point clouds. The optimally transformed LiDAR point cloud is the SVD-method based on all points. As illustrated, the coordinates of GCP in the final SfM point cloud demonstrates low error values in comparison to the LiDAR point cloud. Note that some GCPs were not identified within the LiDAR point cloud data due to occlusion or undesirable checkerboard movement during the survey process (i.e., vehicular-induced winds). Based on the checkpoints (or control points) for the SfM point cloud, the SfM data is compiled to meet 0.0719 feet (3D) accuracy at the 95% confidence level, which is computed using all three components in the X, Y, and Z directions. Likewise, for the LiDAR point cloud, the LiDAR data is compiled to meet 2.2061 feet 3D accuracy at the 95% confidence level. Table 9 provides the final density comparisons, demonstrating that the data has numerous points for a given cubic-foot. These values are generally much higher than required for some specific applications.

Table 8: Errors at GCPs.

GCP ID	Error X (ft)		Error Y (ft)		Error Z (ft)	
	SfM	LiDAR	SfM	LiDAR	SfM	LiDAR
2	0.023	-	-0.004	-	-0.010	-
3	0.001	2.501	0.003	-1.316	0.022	-0.139
101	-0.004	-0.077	0.009	5.206	0.054	-0.345
102	0.028	0.216	0.016	3.332	-0.014	-0.114
103	-0.270	0.296	-0.033	2.579	-0.062	0.040
104	-0.000	0.618	0.052	1.068	-0.047	-0.035
105	-0.034	0.027	-0.045	0.147	-0.066	-0.029
206	0.046	-0.078	0.033	-1.550	-0.021	-0.042
207	-0.037	-0.534	-0.073	-1.620	-0.008	0.405
234	-0.020	-1.129	0.014	-1.529	-0.078	-0.126
235	0.012	-	0.039	-	0.033	-
239	-0.061	-1.254	0.009	-1.773	-0.038	0.582
308	0.073	-0.691	0.062	-1.276	-0.017	0.181
309	0.018	-0.732	0.003	-0.634	0.084	0.162
310	0.000	-0.736	-0.001	0.820	0.022	-0.006
311	0.006	-0.970	-0.021	2.679	0.036	-0.326
314	0.004	-0.438	-0.040	-3.439	0.080	-1.370
315	0.011	-0.741	-0.062	-1.734	-0.056	0.800
316	-0.015	-0.564	0.011	-2.735	0.065	0.563
317	-0.003	-0.686	-0.003	-3.795	0.026	0.830
318	0.015	-1.788	0.087	-1.075	0.107	0.792
319	0.017	-1.805	-0.049	-0.659	-0.027	0.694
320	-0.007	-	0.002	-	0.009	-
321	0.009	-	-0.007	-	0.050	-
322	-0.007	-	-0.011	-	0.087	-
324	0.030	-0.924	-0.003	-1.697	-0.063	0.696
325	0.001	-1.059	-0.002	-1.807	-0.016	0.158
326	0.033	0.197	0.002	-1.834	-0.044	0.112
327	-0.034	-0.096	-0.040	-0.443	0.057	-1.720
328	-0.022	-2.127	0.016	-0.440	-0.010	-1.077
329	-0.024	-0.809	-0.026	-1.731	0.014	2.046
331	0.041	-1.980	-0.038	-3.033	-0.043	-1.312
332	-0.039	-	0.001	-	0.026	-
333	0.026	-	-0.001	-	-0.002	-
340	0.001	-0.877	-0.004	-1.944	0.003	0.776
5001	-0.013	-0.544	-0.005	-1.426	0.023	0.461
5002	0.016	-0.741	0.008	-1.006	-0.084	0.735
5003	-0.099	-0.888	0.064	-1.099	-0.013	0.457
5005	-0.011	-	0.003	-	-0.072	-
5006	0.024	-	0.002	-	-0.103	-
5007	0.003	-3.501	0.003	-3.429	-0.060	0.199
5008	-0.007	-2.393	-0.005	-1.438	-0.034	0.066
5009	-0.002	-1.224	-0.040	-1.584	-0.063	0.007
5012	0.047	-	0.035	-	-0.042	-
5014	-0.065	-	-0.011	-	0.021	-
5016	0.038	-	0.004	-	0.021	-
5020	0.049	-	0.038	-	0.009	-
Mean	-0.0043	-0.7509	-0.000170	-0.8887	-0.0052	0.1212
Sigma	0.0507	1.0185	0.0320	1.9544	0.0495	0.7204
RMS Error	0.0504	1.2533	0.0316	2.1207	0.0498	0.7200

Table 9: Density comparison.

Platform	NE (pts/ft^3)	SE (pts/ft^3)	SW (pts/ft^3)	NW (pts/ft^3)	Bridge deck (pts/ft^3)
LiDAR	11127	11135	6706	4823	46276
SfM	4161	4133	2825	2507	4265

7.4 MicroStation Processing

MicroStation is a Bentley commercial software that can be used in various engineering industries specific to civil engineering transportation-focused applications. Bentley software is widely implemented for modeling, analyses, and design. Bentley InRoads is a Bentley software utilized mainly for surveying, construction drawing, and design using powerful embedded automation functions (currently and anticipated to be replaced by OpenRoads in a few years). A specific section outlining similar processing in OpenRoads is presented in section 7.5. Bentley InRoads is executed within the MicroStation environment. As a result, a point cloud file can only be opened in Pointools as a .pod file format. The MicroStation file format is saved as *.dgn format. As for files generated in Bentley InRoads, surface data of point cloud is saved in .dtm format. In tools named “Point Cloud” and “Point Cloud – Advanced”, point cloud functions like navigation, display parameters, segmentation, classification, import and export, etc. can be implemented. In the demonstration below, the processes were conducted in MicroStation V8i (SELECTseries 4), InRoads (SELECTseries 2), and InRoads (SELECTseries 4).

Figure 28 presents the previous RTK survey file obtained from SDDOT, where the roadway and White River were identified. Figure 29 and Figure 30 are top views of LiDAR and SfM subsampled point clouds (at 1.0-inch spacing). Figure 31 shows the main processing steps to create breaklines and contours using MicroStation software. The roadway breaklines and countors were created within 15 and 30 minutes, respectively, using a computer that is equipped with a 6-core CPU, 32 GB of RAM, GPU with 4 GB of global memory, and SSD.

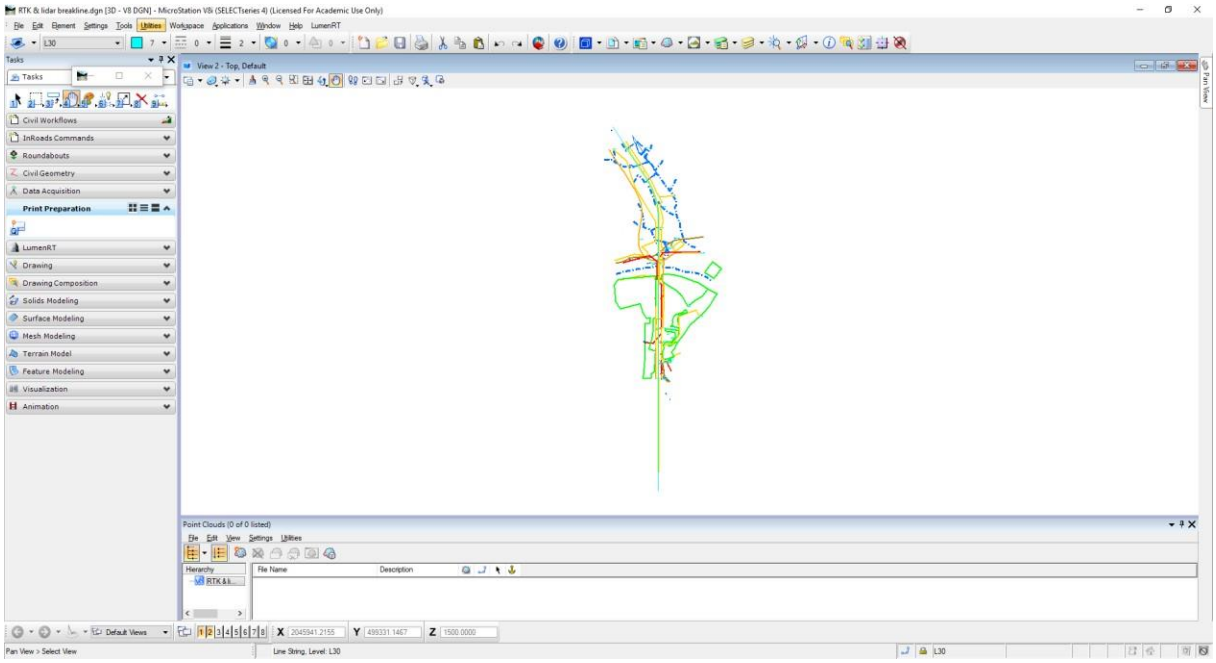

Figure 28. SDDOT RTK survey in MicroStation.

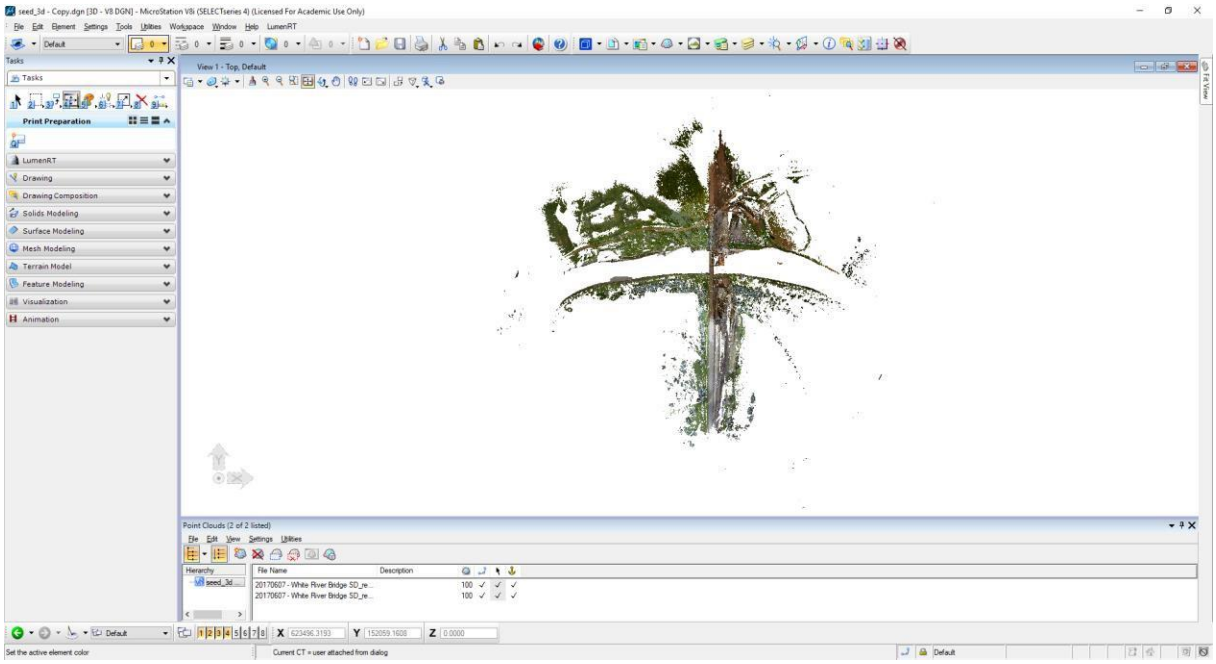

Figure 29. Collected LiDAR point cloud in MicroStation.

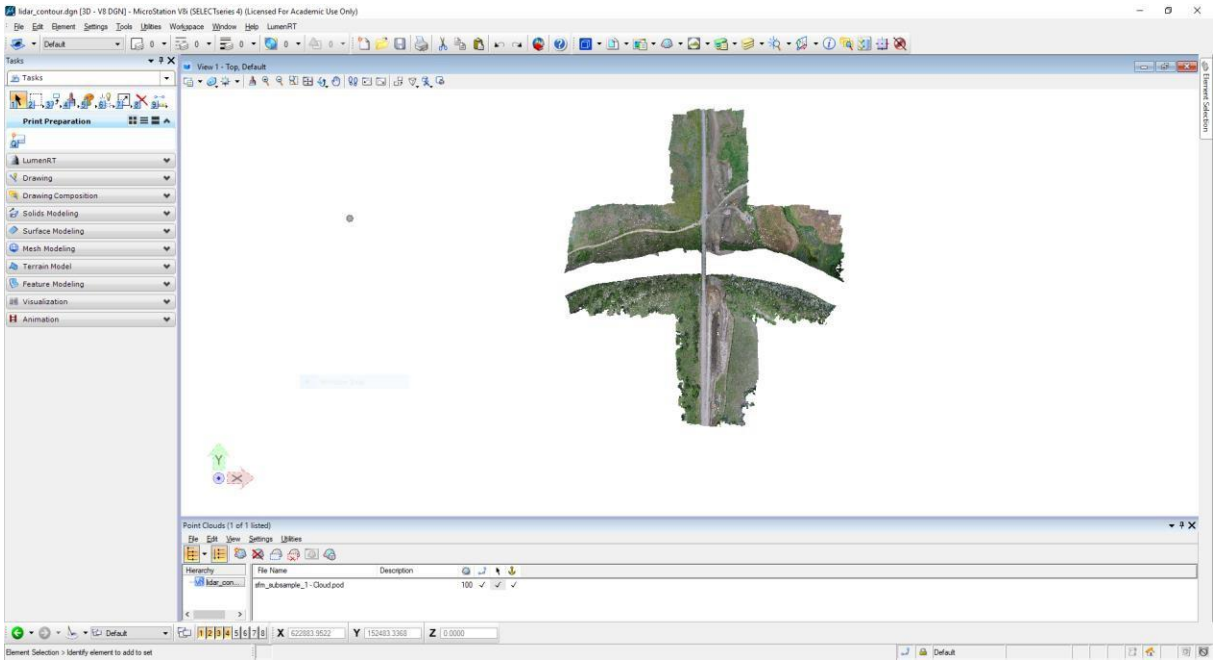

Figure 30. Collected SfM point cloud in MicroStation.

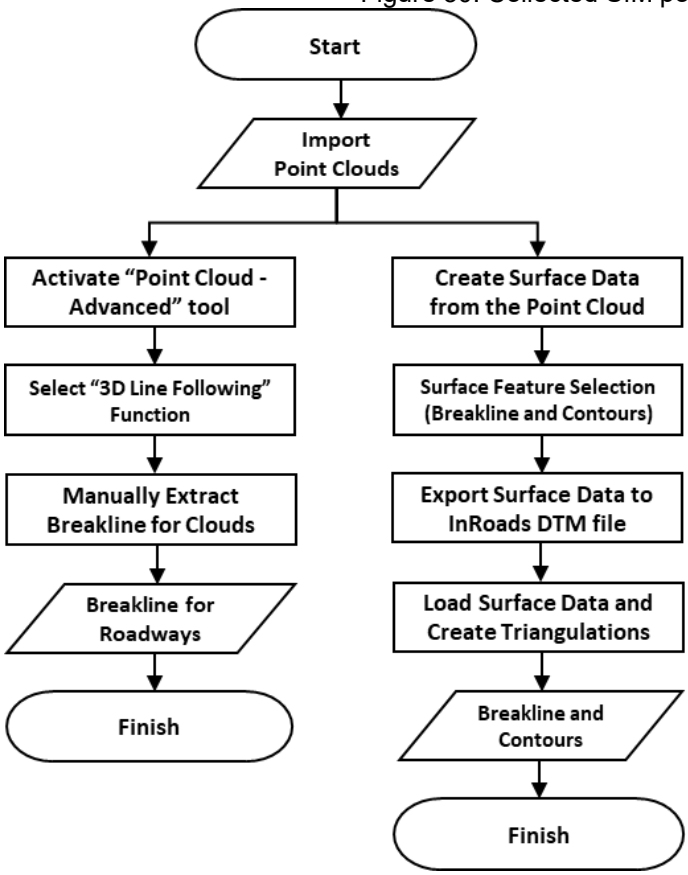

Figure 31. Flowchart of MicroStation processing.

To extract the roadway breaklines, the “3D Line Following” tool in MicroStation was utilized as illustrated in Figure 32. Note that this tool is actually located in MicroStation and not InRoads. Prior to the process, the “Point Cloud – Advanced” tool needs to be activated by the user in Tools ➔ Product Add-Ins ➔ Activate Descartes. With the 3D Line Following function, the roadway breaklines can be identified and manually extracted. Both breaklines for LiDAR and SfM point clouds were constructed and compared with previous SDDOT work in Figure 33 and Figure 34. It can be observed that the roadways overlap on point clouds and RTK file, indicating the point cloud datasets closely match the RTK provided by SDDOT. Also, Figure 35 shows the breaklines comparison between LiDAR and SfM point clouds. The roadway location and shapes are identical except for the different point cloud boundaries in the north section, which is due to a lack of data in the LiDAR point cloud.

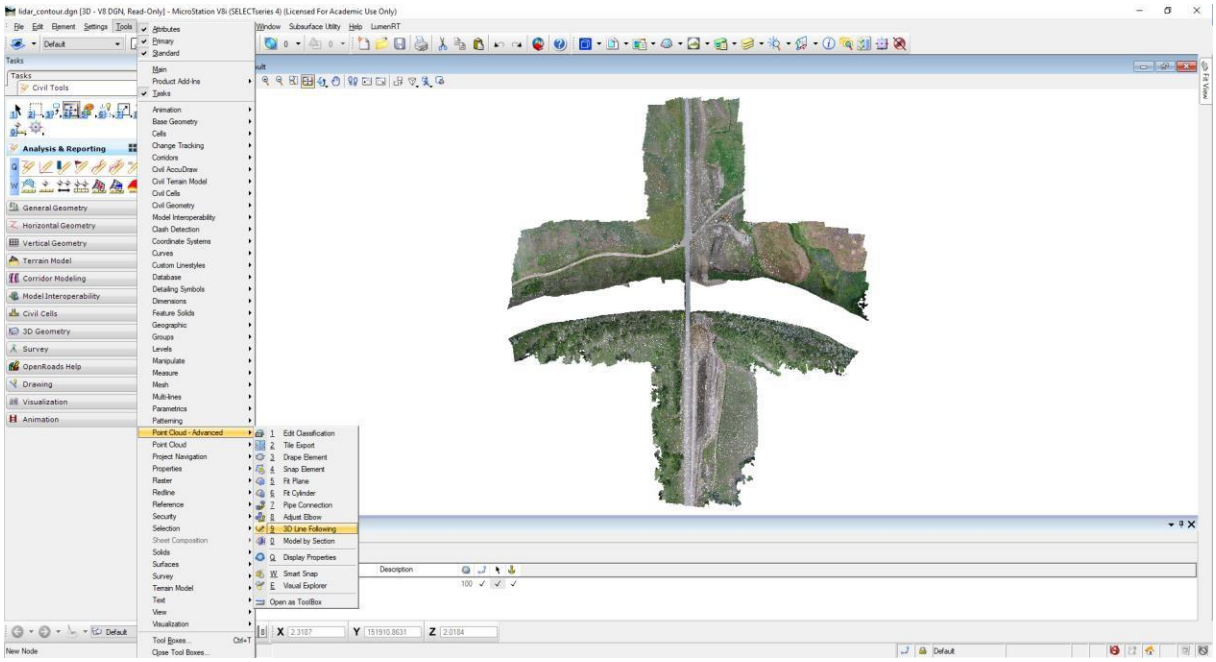

Figure 32. Construction of “3D Line Following Function” in MicroStation.

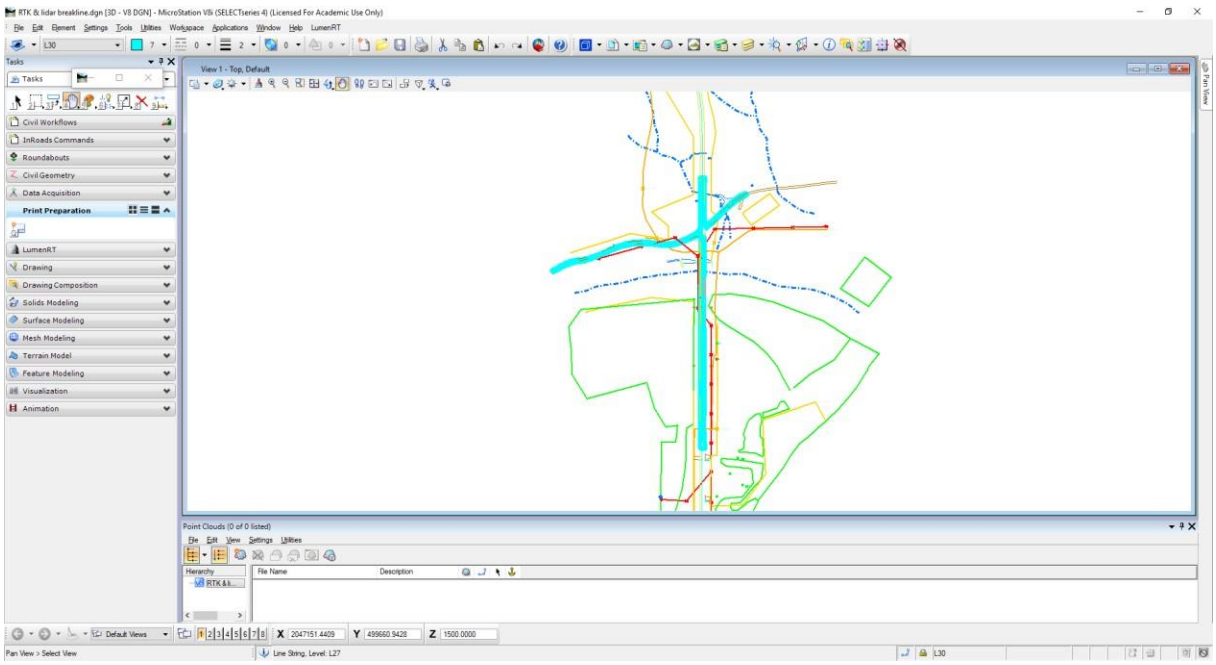

Figure 33. RTK and LiDAR breaklines construction in MicroStation.

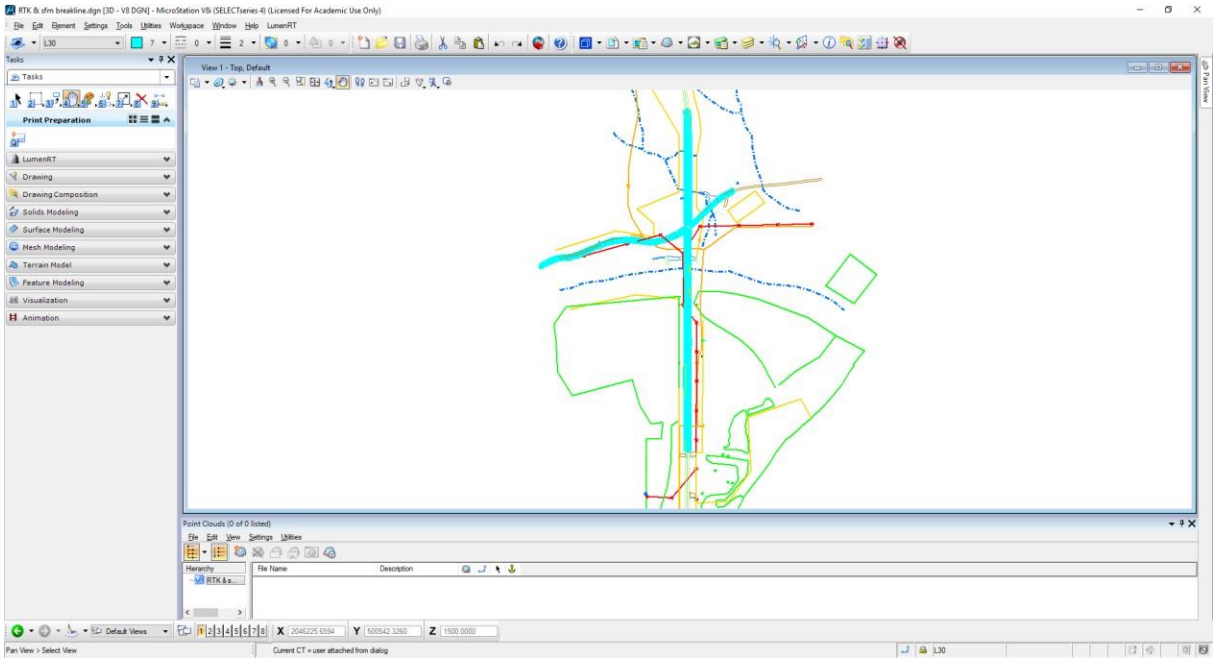

Figure 34. RTK and SfM breaklines construction in MicroStation.

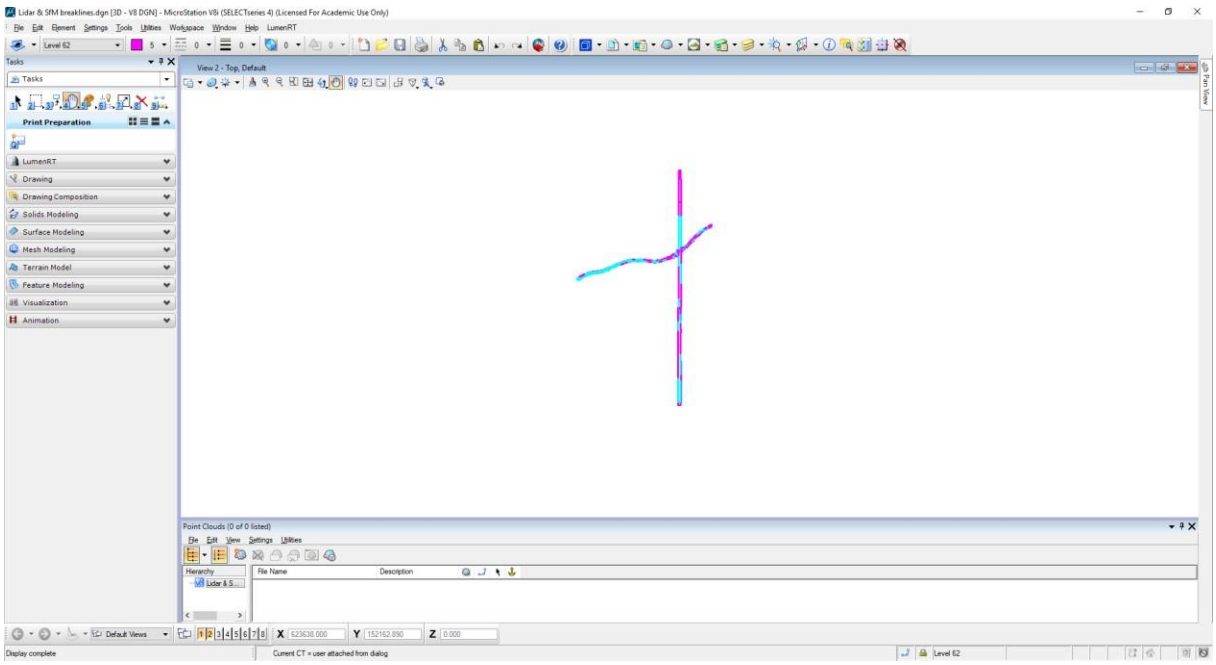

Figure 35. LiDAR and SfM breaklines construction in MicroStation.

Point cloud surface data processing is an exclusive function in InRoads (SELECTseries 2), which is used to generate point cloud contours. The steps are shown in Figure 36 (a) and (b). First, open the Data Acquisition tool and create surface data from the point cloud. Since the datasets are filtered and cleaned, select “No Filter” and accept it in the appeared window. The newly created surface is added under Data Acquisition box in Figure 36 (c). Depending on the need of surface data, desired options (breaklines and contours) are checked.

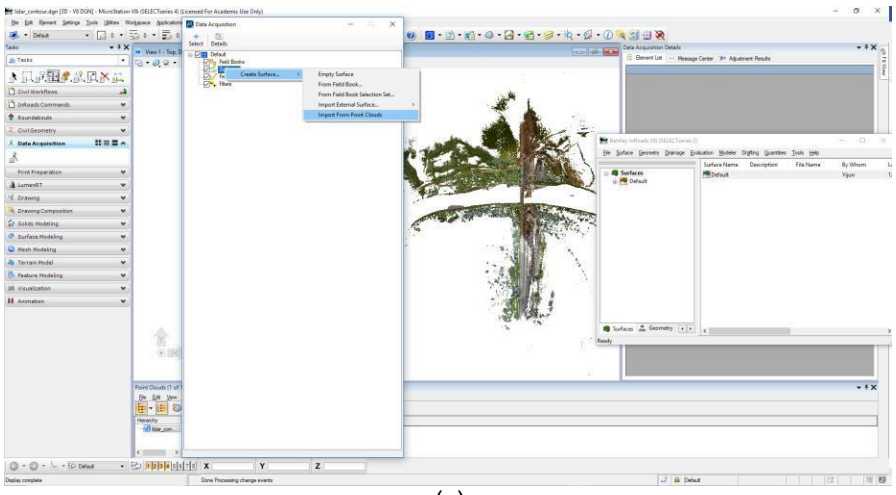

(a)

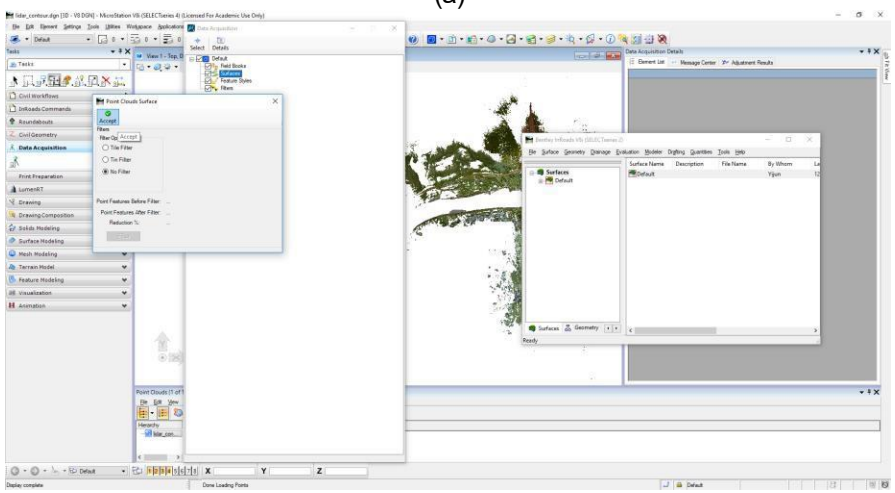

(b)

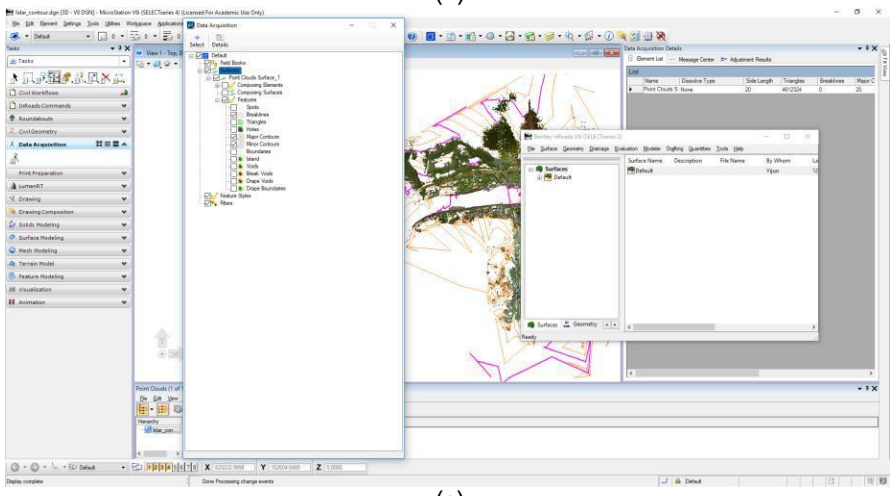

(c)

Figure 36. Steps of creating surface contour in MicroStation: (a) create a surface from the point cloud, (b) no filter for surface generation, and (c) surface features selection.

Surface data must be exported and saved within an InRoads DTM file as demonstrated in Figure 37. Before continuing to the next step, all files, as well as MicroStation and InRoads software, should be closed. The next step is to open an empty design file in InRoads, then open the created surface data in a DTM file, right-click on the surface, and triangulate as shown in Figure 38. After the triangulation processing is completed, under the surface tab within the InRoads interface as demonstrated in Figure 39, the user can view and adjust parameters of contours processing. In Figure 40, the contours were created at an interval of 5 ft for the LiDAR point cloud, which corresponds to the hilly geometry in north and less than 5 ft of elevation change in the south roadway section. Similarly, the contour interval is at 3 ft for the SfM point cloud in Figure 41. Denser contours exist on the west side of the point cloud due to vegetation. Recall the UAS-SfM corresponds to the canopy top of the site of interest, which is different from the GBL data.

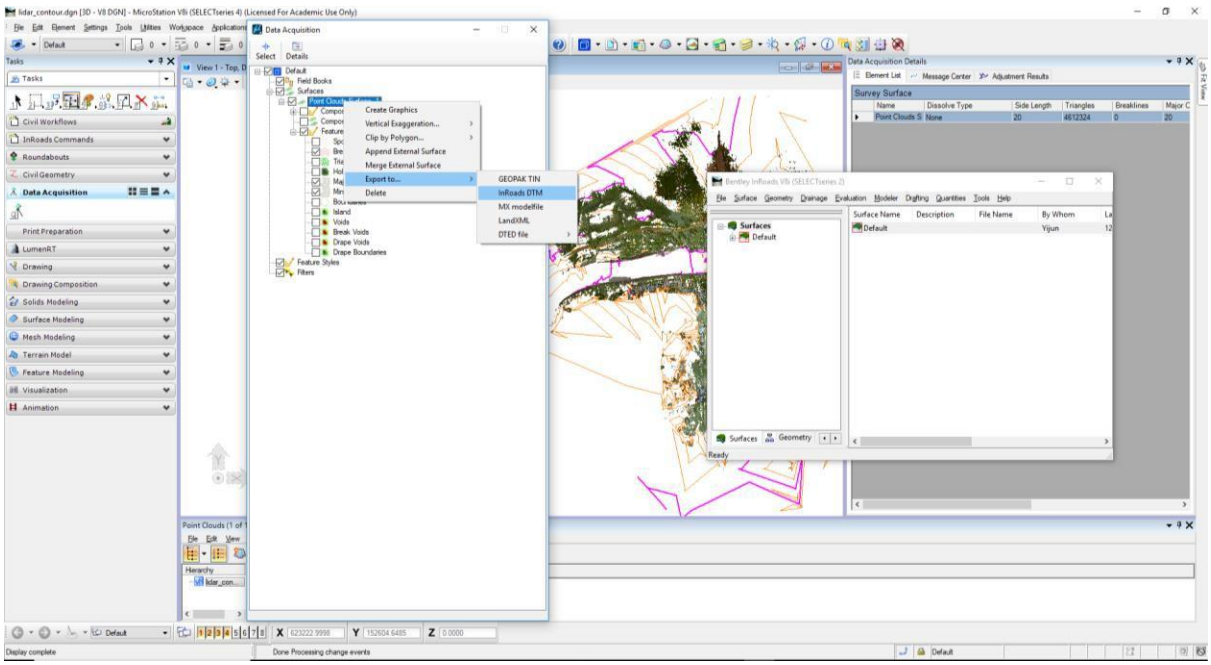

Figure 37. Export created surface to InRoads dtm file in MicroStation.

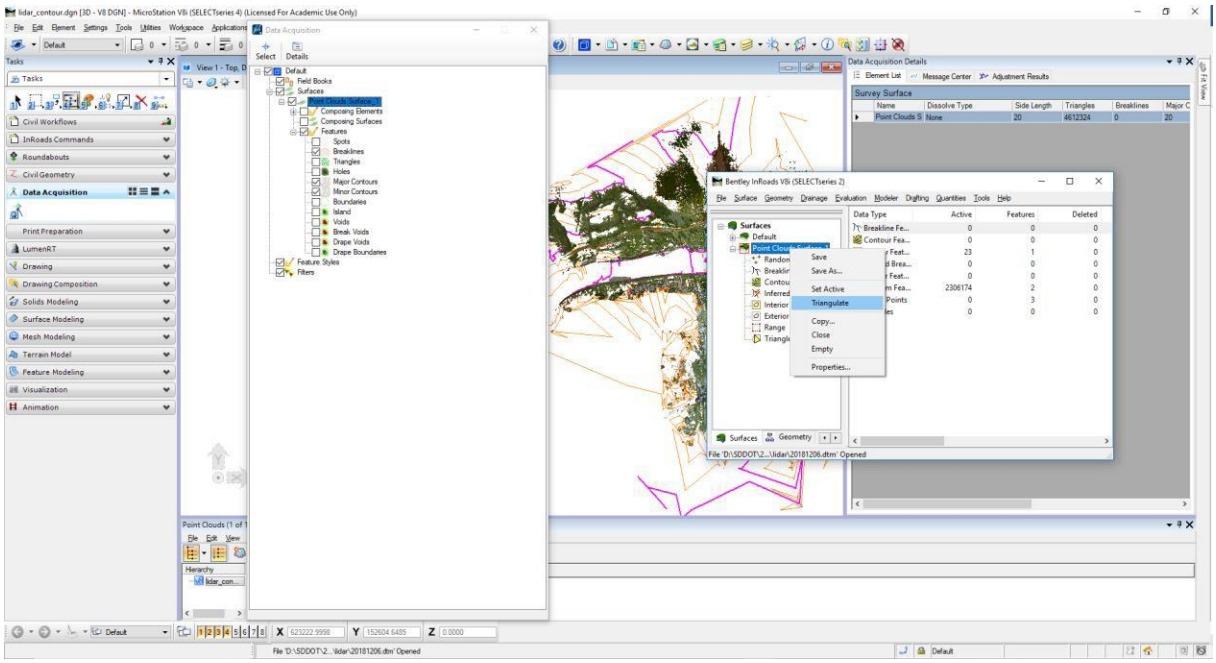

Figure 38. Loading a dtm file and performing triangulation creation in InRoads software.

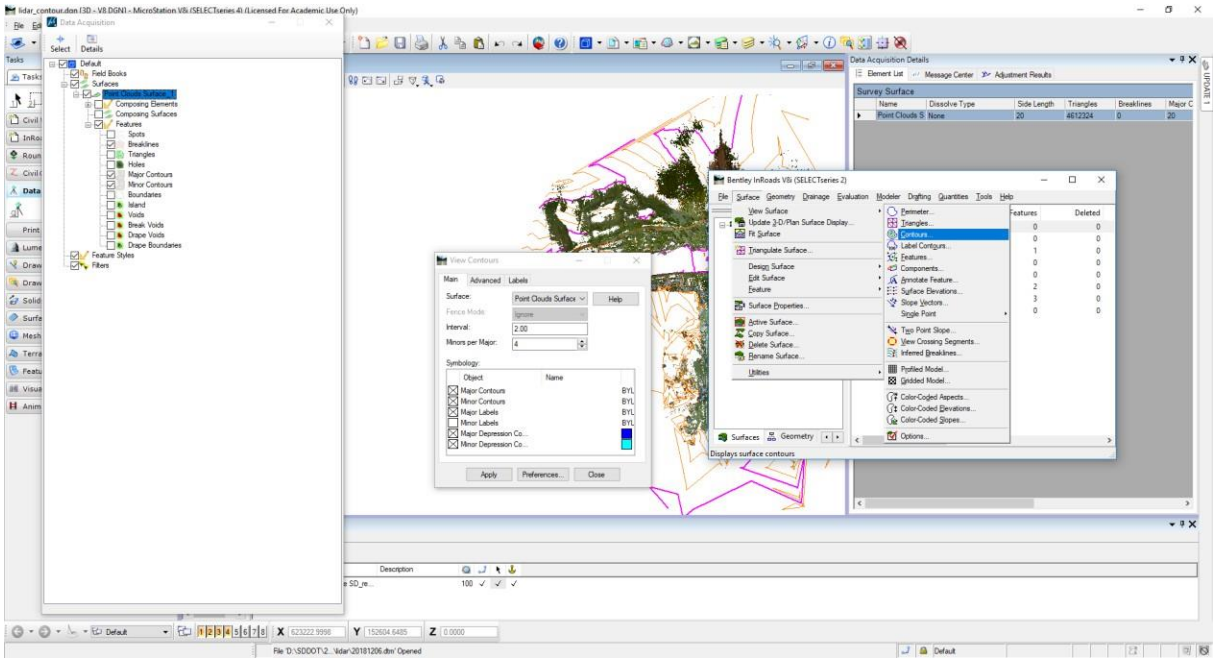

Figure 39. View and adjust parameters of contours.

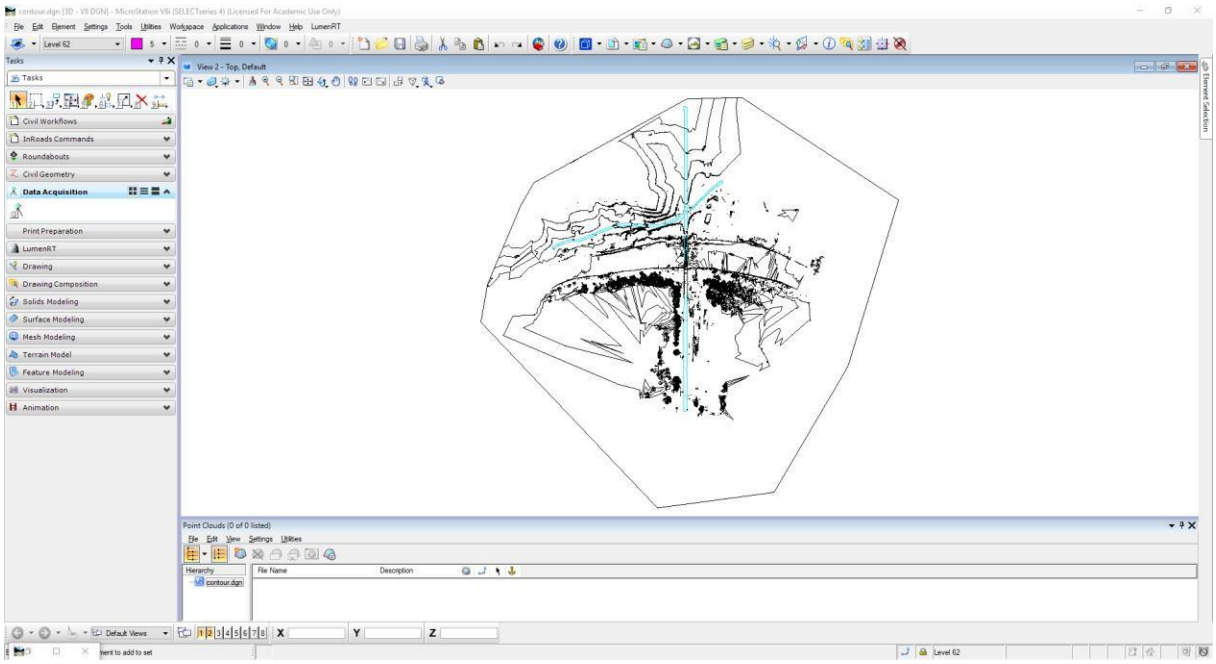

Figure 40. Created contours for the LiDAR point cloud.

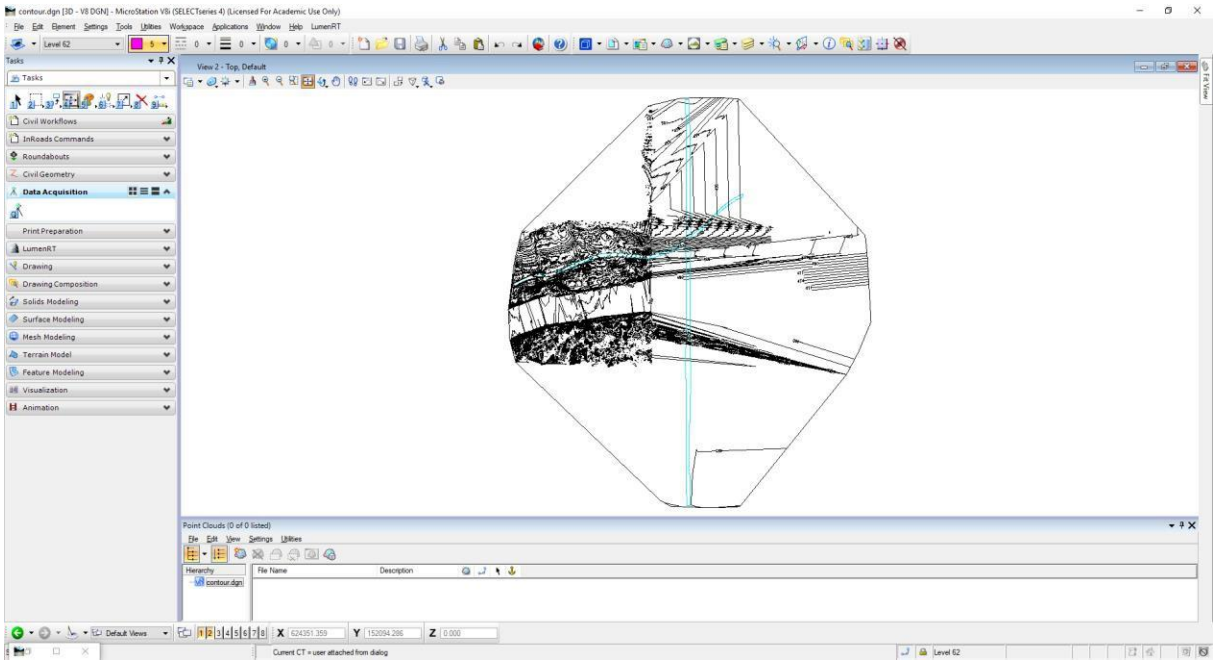

Figure 41. Created contours for the SfM point cloud.

7.5 OpenRoads Processing

OpenRoads Designer is a Bentley commercial software for civil engineering design and analyze. It is widely applied to geotechnical, surface utilities, surveying, terrain, roadway design, as well as the

combination with reality meshes, imagery, point clouds, and another dataset from real-world conditions. This is anticipated to be the replacement of all capabilities delivered via InRoads, GEOPAK, MX, and PowerCivil. In addition, OpenRoads Designer provides the latest technology and tools to efficiently and accurately establish the design model. Therefore, OpenRoads Designer is an advanced civil engineering design software for multi-discipline applications, and it is likely to replace MicroStation InRoads for various workflows in the near future.

Similar to MicroStation and InRoads, point cloud files can only be opened as a *.pod file format. The OpenRoads Designer file format is *.dgn. The process was conducted in OpenRoads Designer CONNECT Edition – 2018 Release 3, as the flowchart shown in Figure 42. When opening the software, the interface is shown in Figure 43. Reprehensive example videos are available on the left, and the news and announcements are listed on the right. To start the work session, Figure 44 illustrates to create new *.dgn files as a work session. After creating the work files, the first step is to attach the point cloud file in OpenRoads Design, as shown in Figure 45. The attached point cloud can be visualized in Figure 46. The OpenRoads software created the terrain from the point cloud dataset within 40 minutes using a computer that is equipped with a 6-core CPU, 32 GB of RAM, GPU with 4GB of global memory, and SSD.

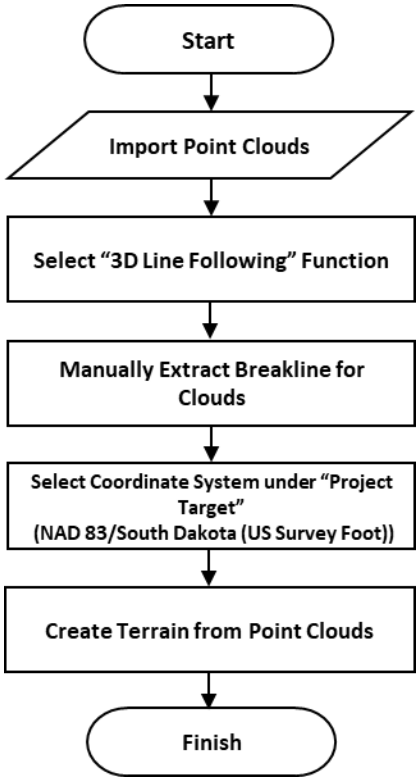

Figure 42. Flowchart of OpenRoads processing.

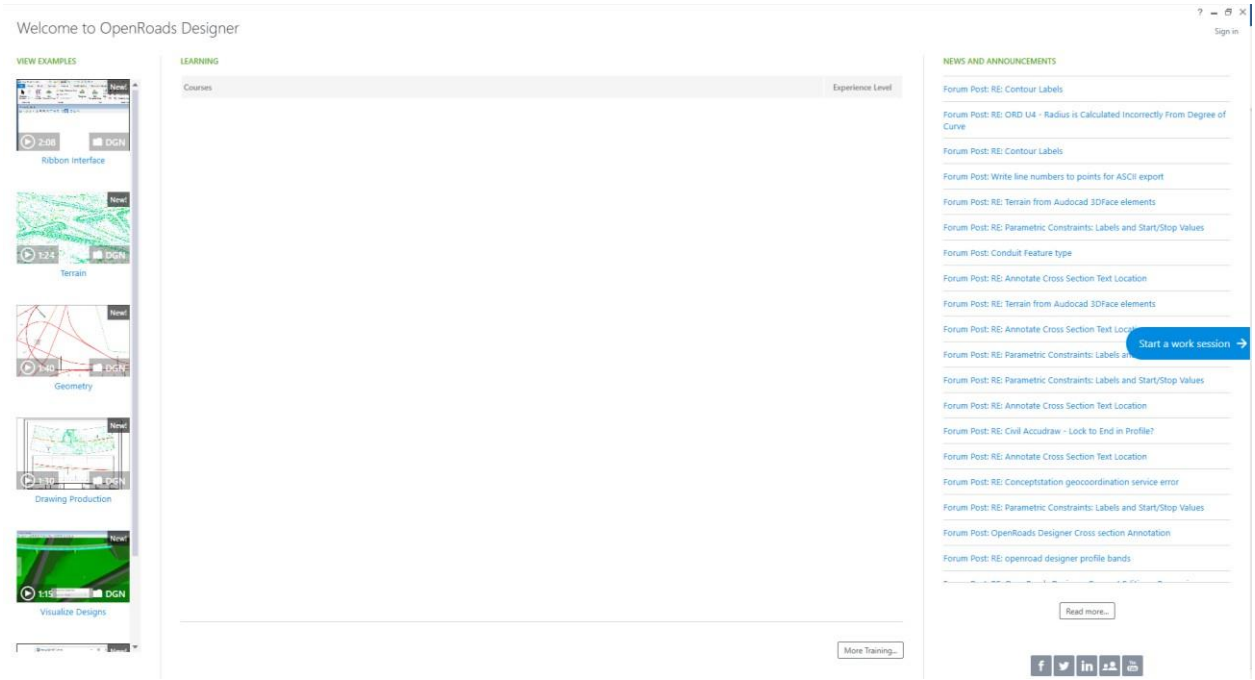

Figure 43. OpenRoads Design interface.

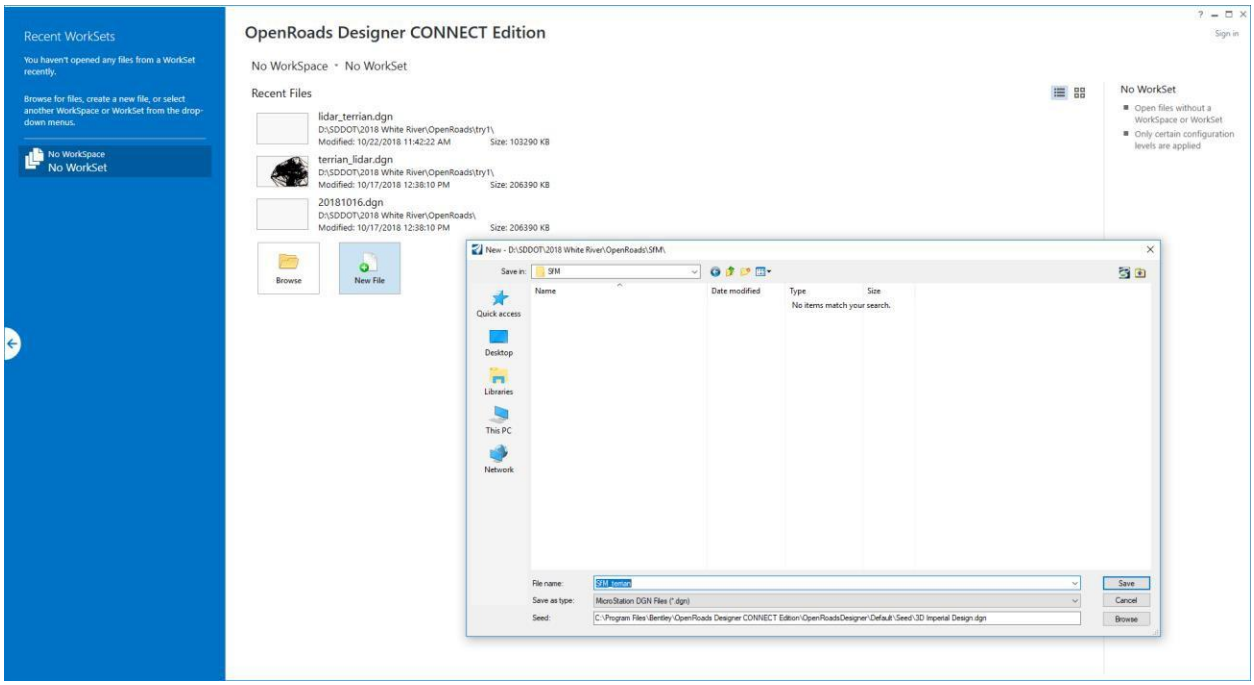

Figure 44. Create new *.dgn files in OpenRoads Design.

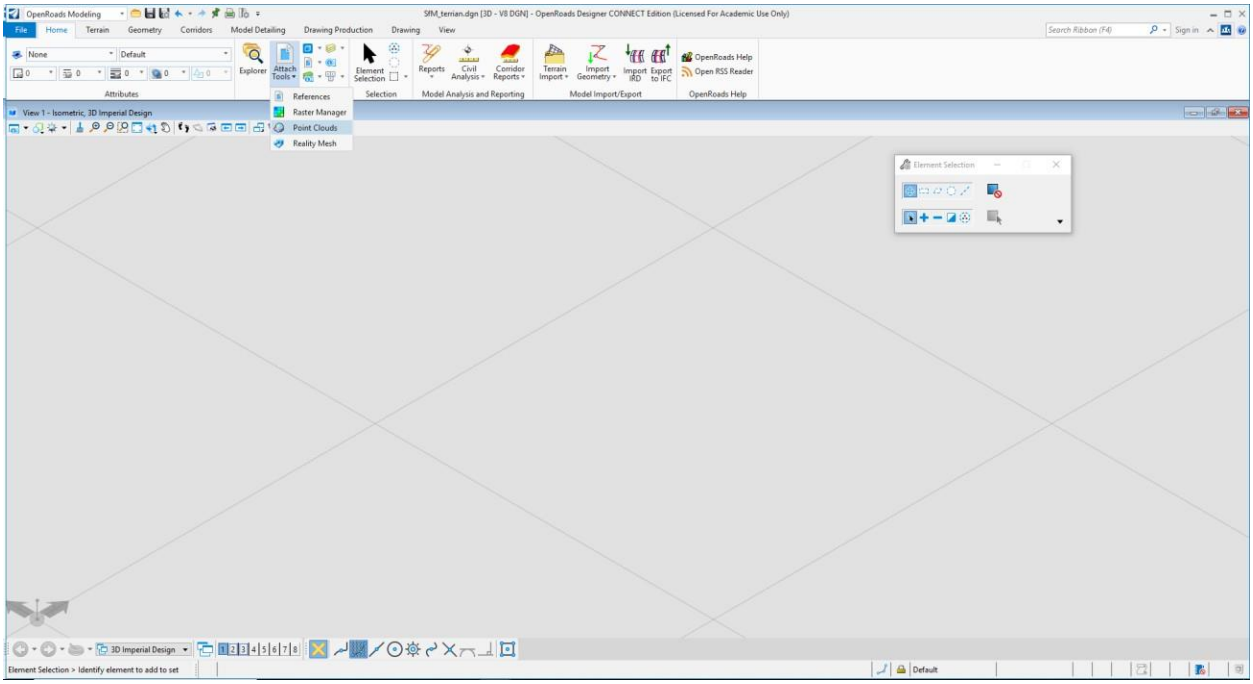

Figure 45. Attach processed point cloud in *.pod file type.

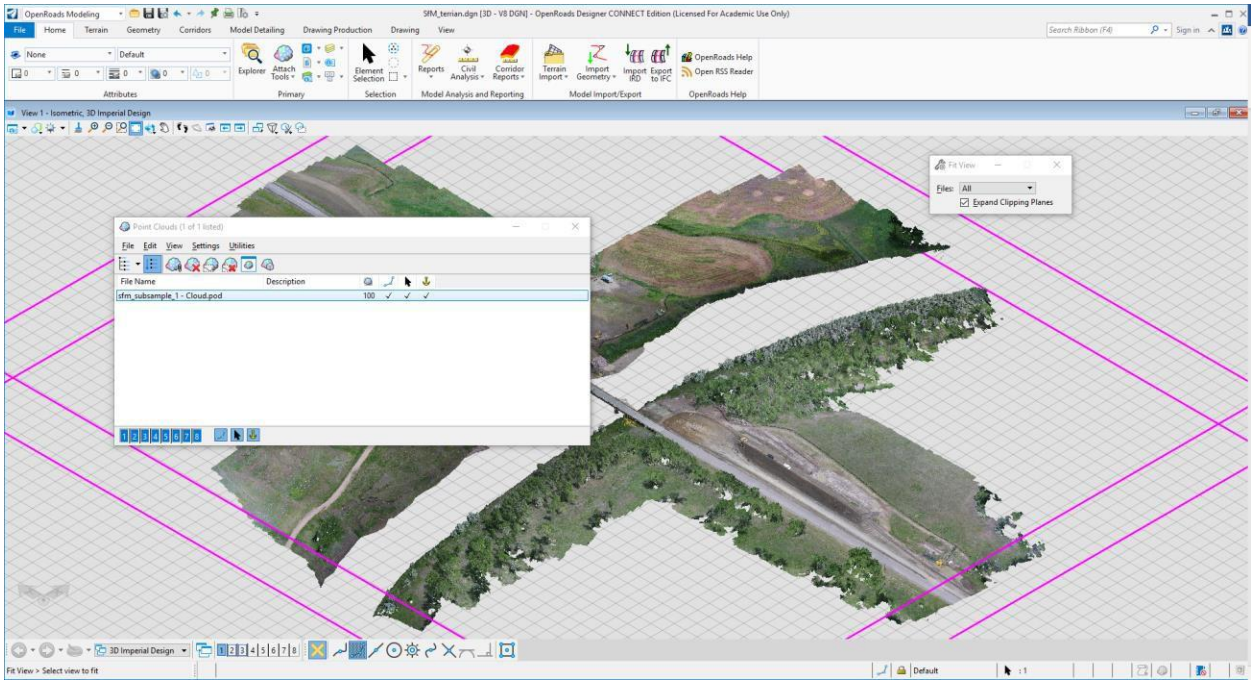

Figure 46. Attached point cloud.

General point cloud processing functions including view setups, classification, fit plane, clip, colorize, etc., as shown in Figure 47. To extract the roadway breaklines, the same function “3D Line Following”

was applied as done within InRoads. The function is selected under the “point cloud edit” tab as illustrated in Figure 47. The roadway breaklines can be identified and manually extracted using the function. The extracted roadway breaklines are shown in Figure 48 and Figure 49.

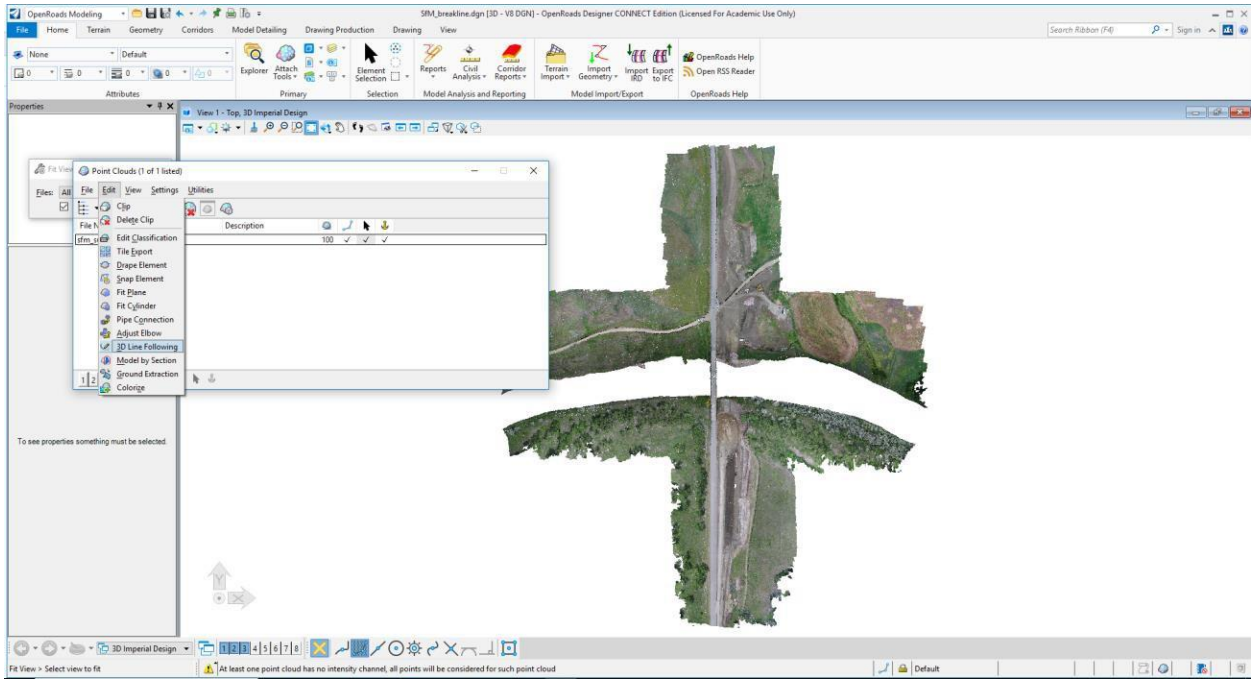

Figure 47. Select 3D Line Following to create breaklines.

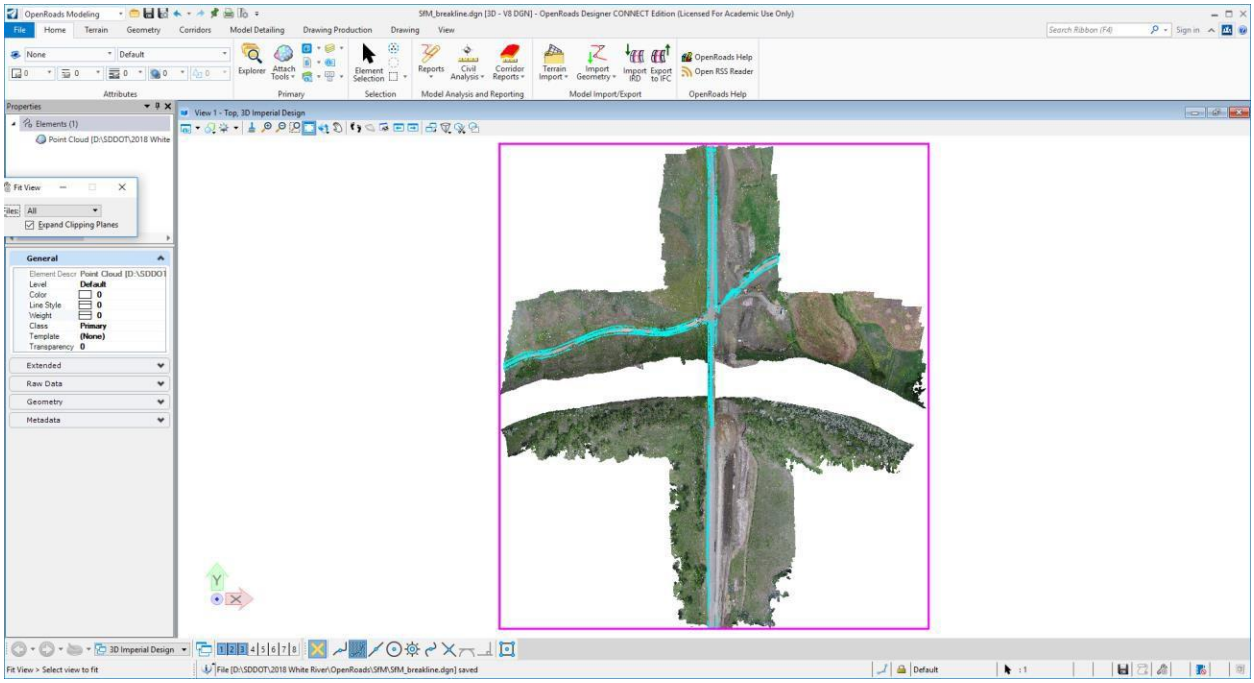

Figure 48. SfM point cloud extracted roadway breaklines.

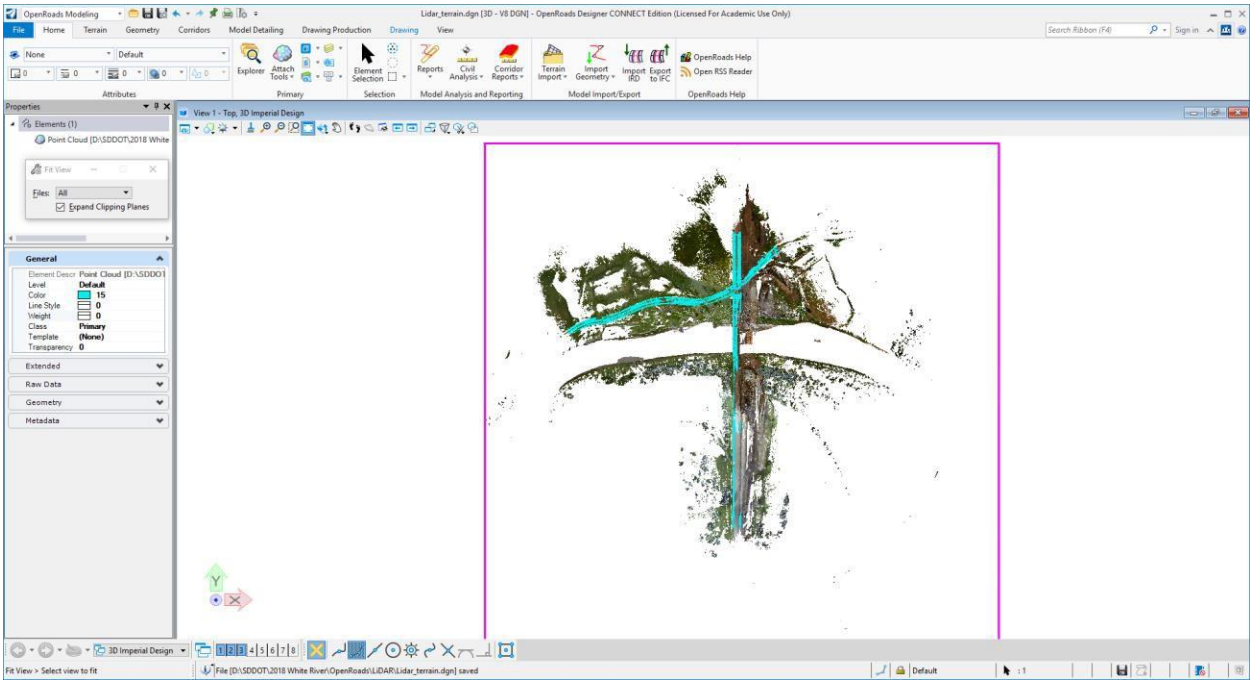

Figure 49. LiDAR point cloud extracted roadway breaklines.

In OpenRoads, the terrain can be generated from existing point cloud datasets. In Figure 50, under the terrain tab, there is an additional method to create the terrain, select “Create From Point Cloud”. The first step prior to terrain creation is to select a global option, as demonstrated in Figure 51. Under “Projection Target”, the projection is to be selected as the desired coordinate system. In this case, it is selected as “NAD 83/ South Dakota (US Survey Foot)” for SPC. As for file options, a filter is not needed since the point cloud is initially processed. The created SfM point cloud terrain triangulation is displayed in Figure 52.

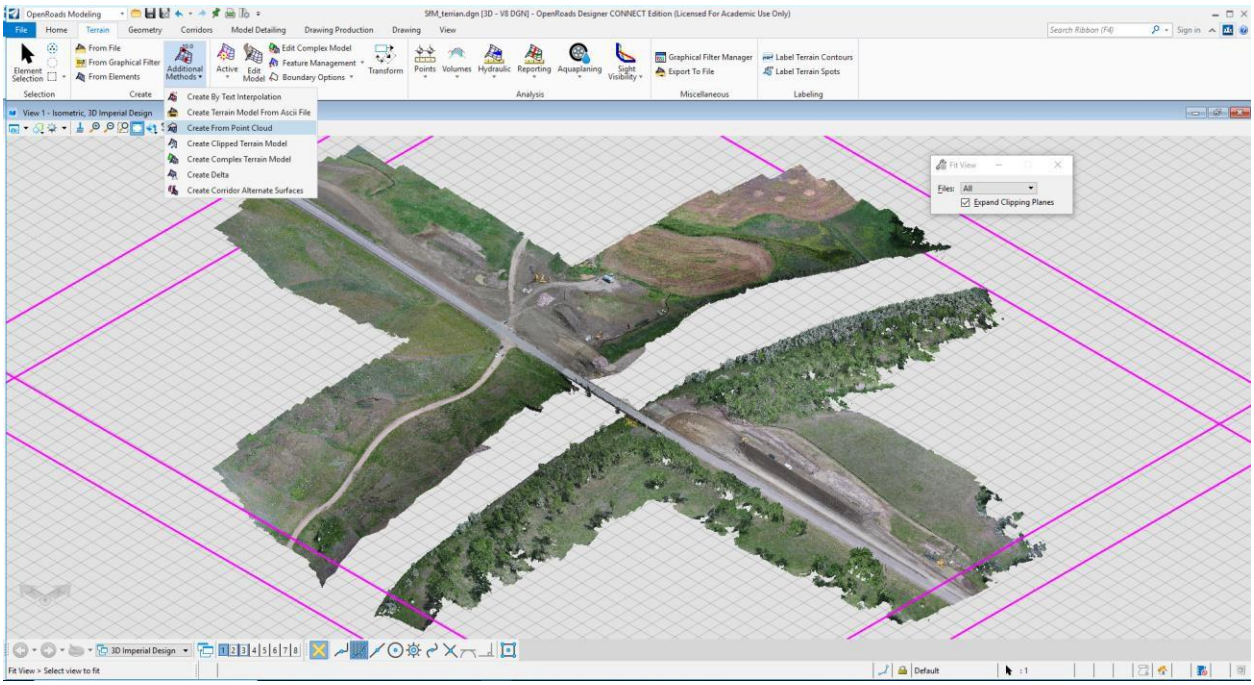

Figure 50. Create terrain from point cloud.

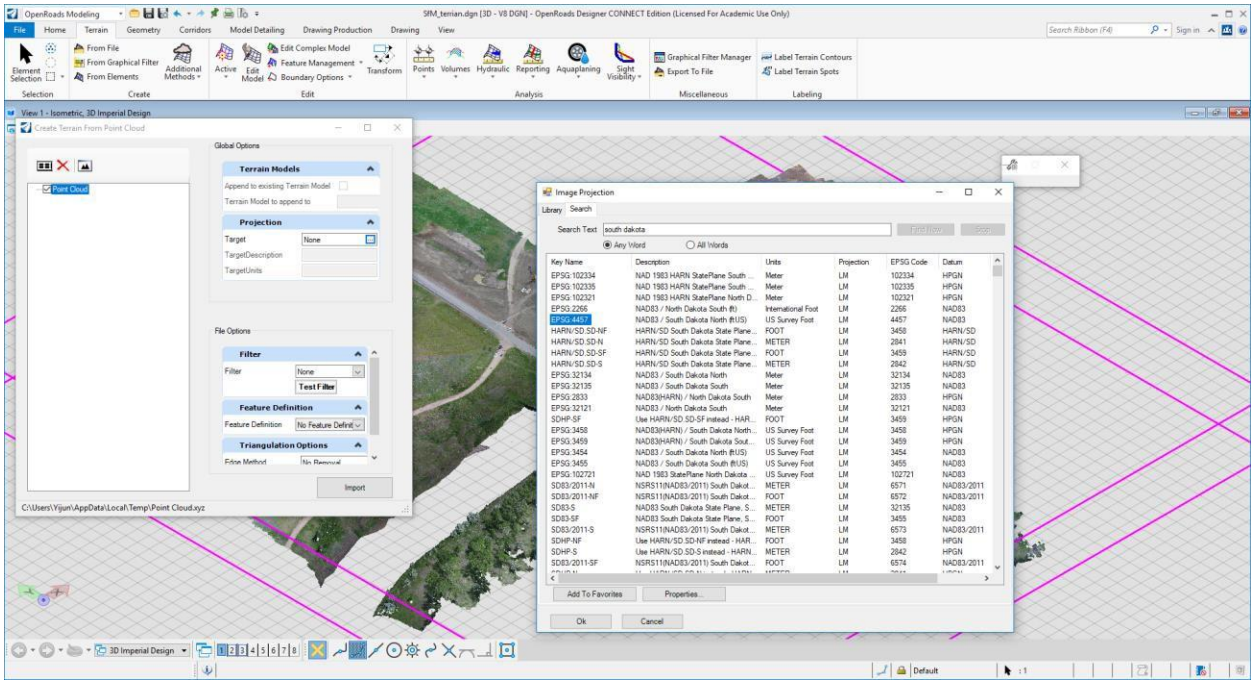

Figure 51. Select coordinates system.

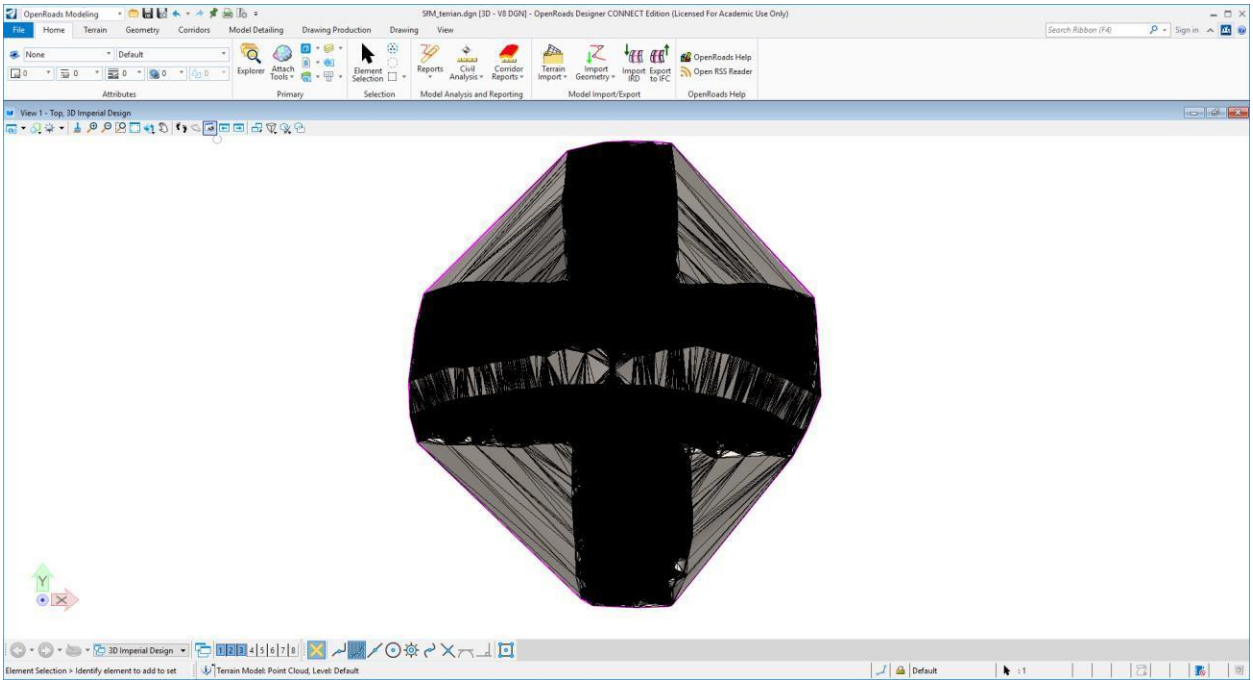

Figure 52. Created terrain triangulation.

To adjust terrain properties, the options will appear if the terrain object is selected as in Figure 53. The triangulation can be turned off, for ease of visualization, and contour results are selected for as shown in Figure 54. The SfM point cloud contour is demonstrated in Figure 55. The same step applied to the LiDAR point cloud creates the terrain and contour results shown in Figure 56 and Figure 57. In addition, the created terrain models can be exported in various formats for some specific software. In Figure 58, under “export tab”, file-formats including InRoads DTM, GEOPAK TIN, LandXML, etc.

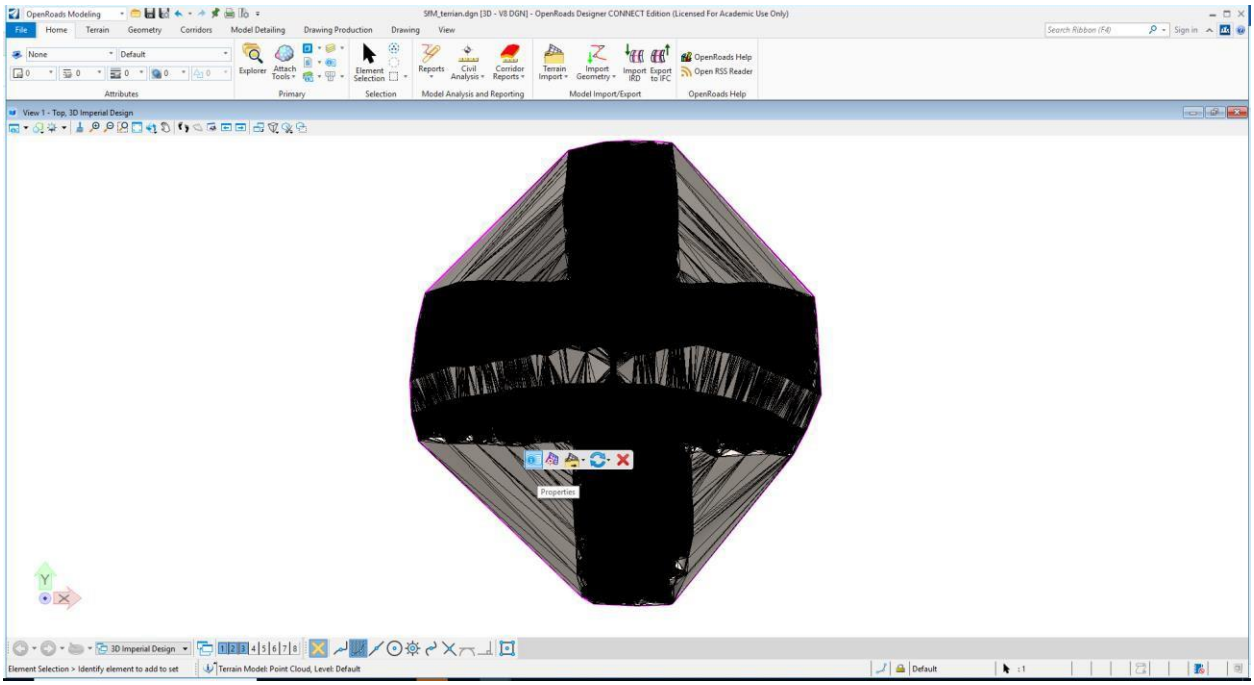

Figure 53. Adjust terrain properties.

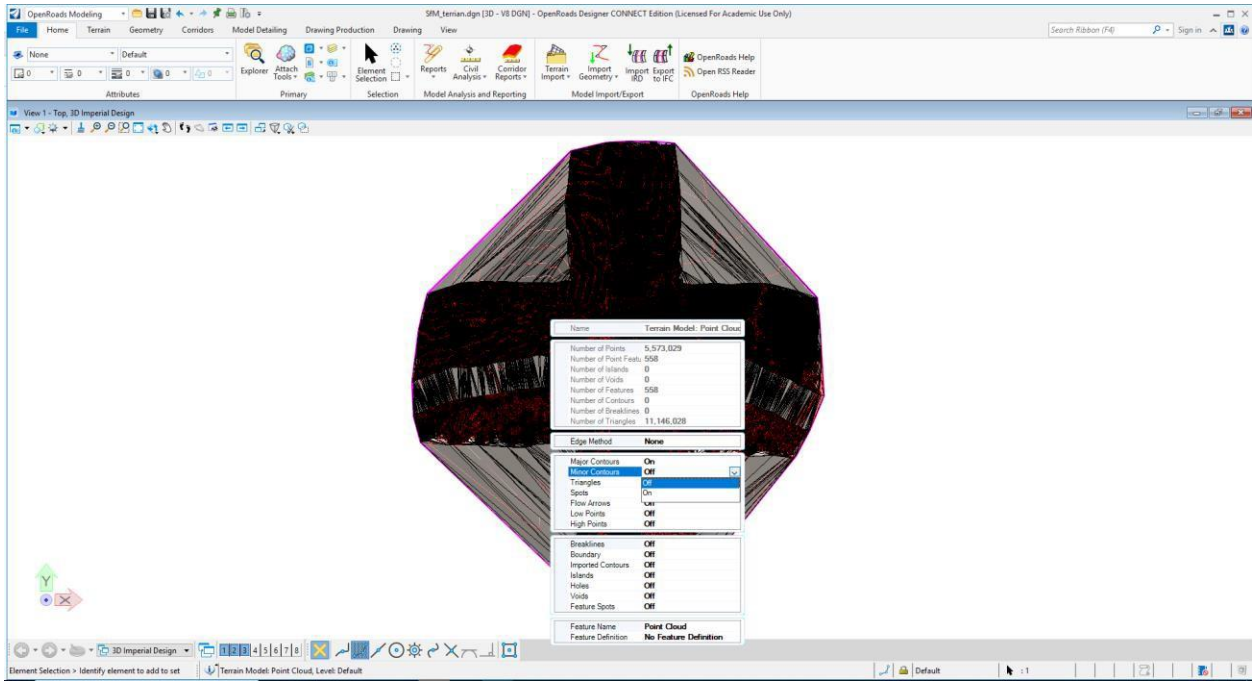

Figure 54. Show contour results.

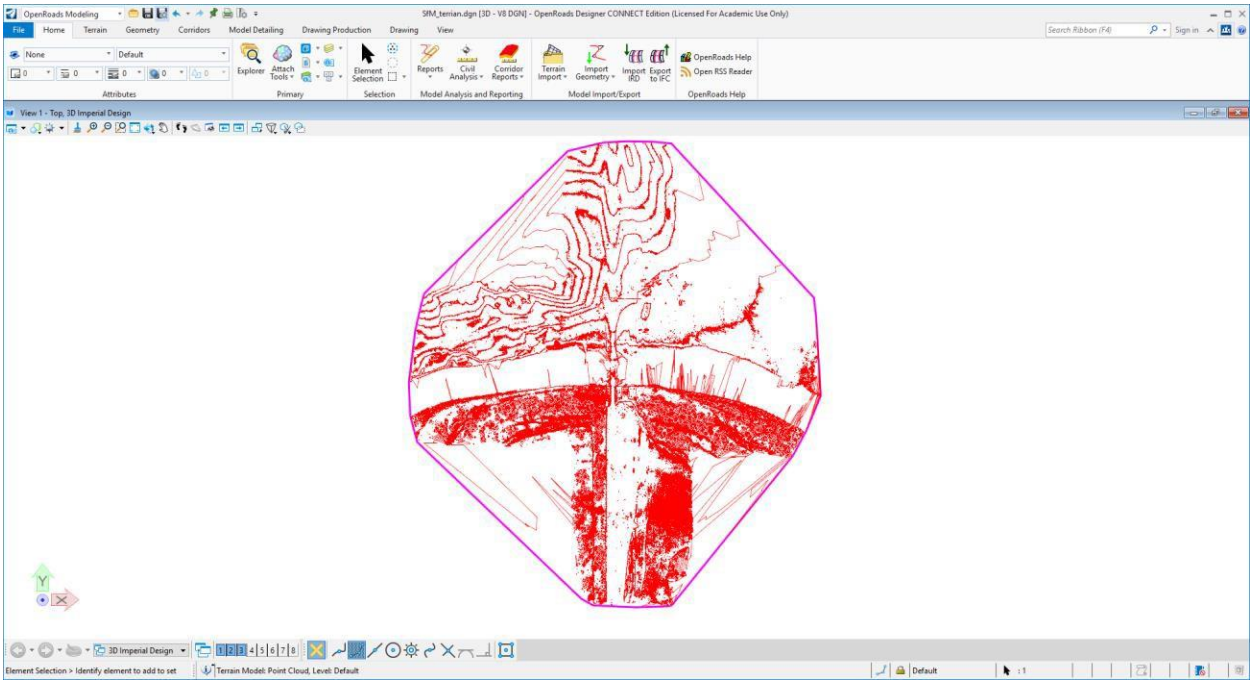

Figure 55. SfM point cloud contour.

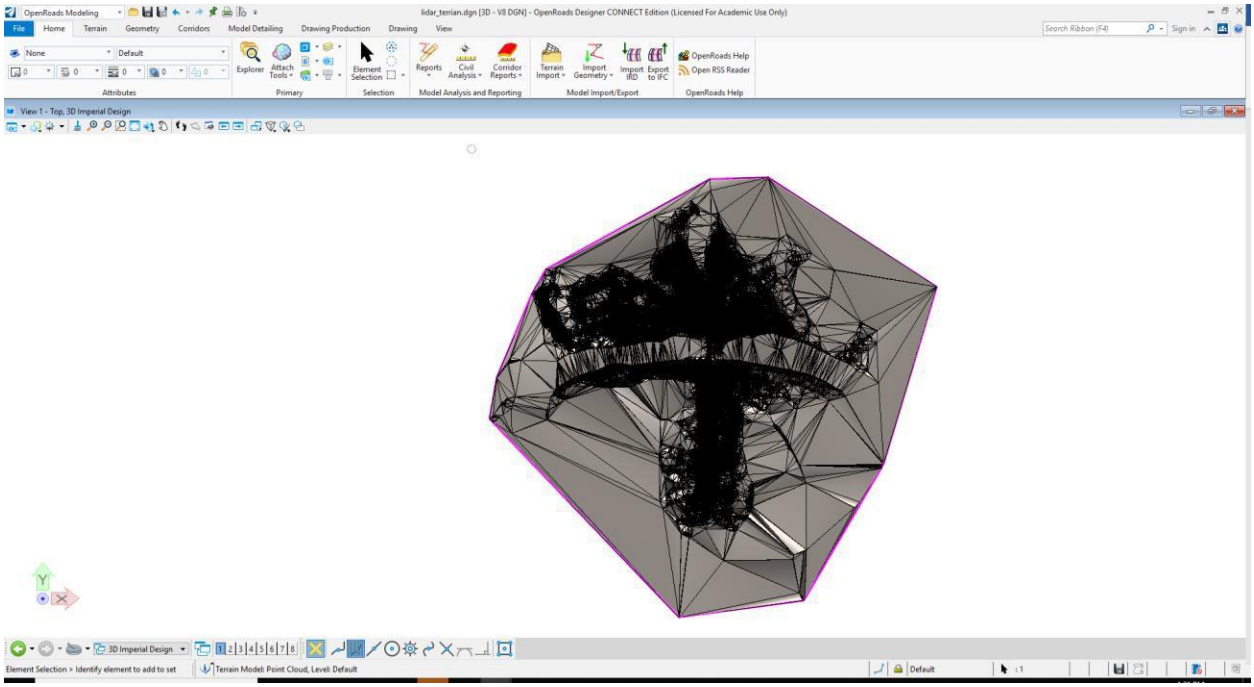

Figure 56. LiDAR point cloud terrain triangulation.

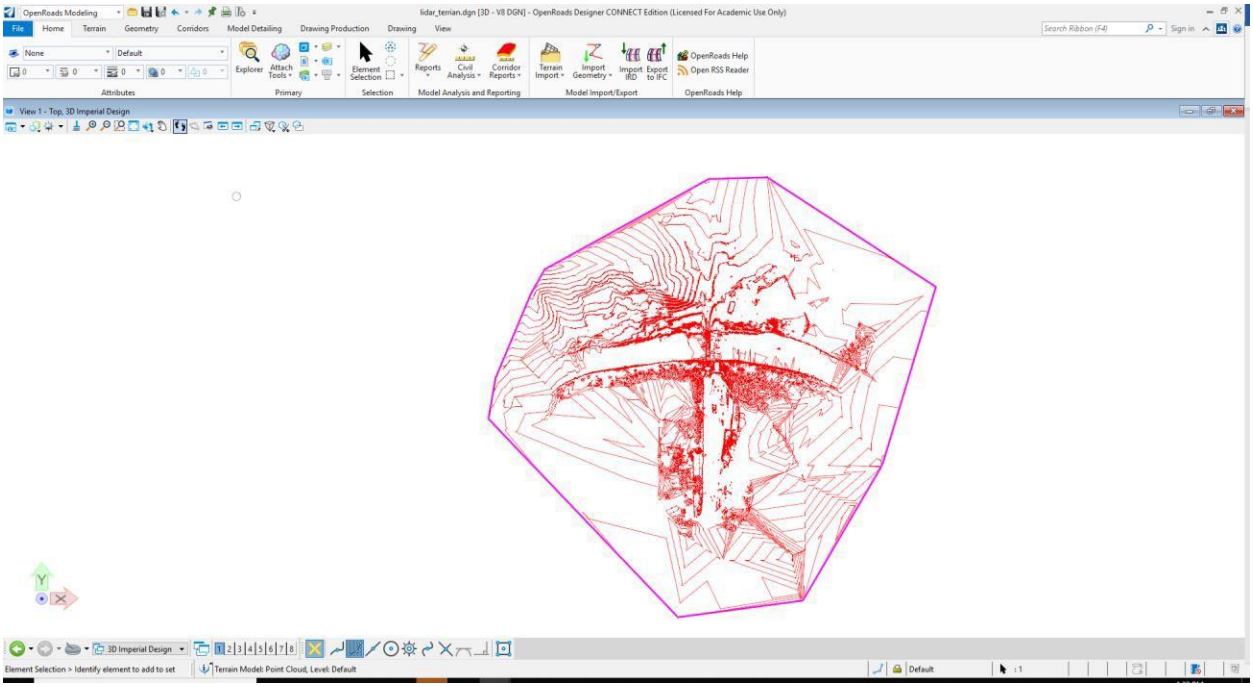

Figure 57. LiDAR point cloud contour.

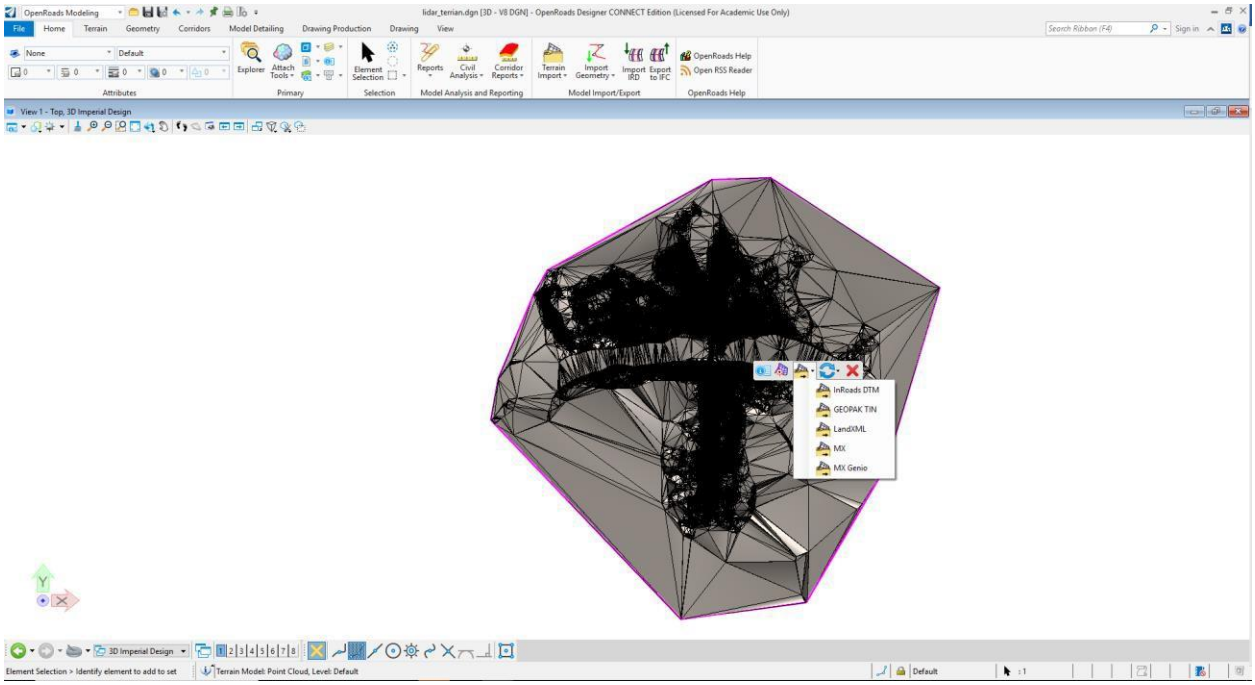

Figure 58. Export terrain model to other MicroStation software.

7.6 ContextCapture Processing

SfM point cloud was processed in both Pix4D and ContextCapture for a consistency comparison. This comparison was added to the scope because ContextCapture is an SfM software platform within the Bentley software suite. The detailed processing steps within ContextCapture is shown as flowchart in Figure 59. The ContextCapture created a terrain from point clouds within 40 hours using a computer that is equipped with two Xeon 16-core CPUs, 256 GB of RAM, two GPUs with a total global memory of 24 GB, and an SSD. In this processing, eleven well-distributed GCPs were selected as shown in Figure 60. Note this is a reduced number of GCP from the earlier processing, but this at the recommendation of Bentley support. The processed SfM clouds from each platform are displayed in Figure 61 and Figure 62 with consistent GCP selection. To quantify the errors and any discrepancies between the software platforms, the two SfM point clouds were processed to determine the cloud-to-cloud distance function in CloudCompare, where Figure 63 illustrates this comparison. Larger differences are detected at vegetation edges primarily due to the slightly different coverage and the corresponding areas of limited number of overlapping images. However, most of the interior areas have errors of 0.2 – 0.5 ft in comparison to the Pix4D file, which is not negligible and exceeds the error found in Pix4D.

To better estimate the SfM processing software in terms of accuracy, four CPs are selected representing each direction, shown as white points in Figure 63. While ContextCapture does not directly compute the CP errors like within the Pix4D environment, the 4 CP errors are exported from Pix4D as reference for accuracy estimation as summarized in Table 10. The cloud-to-cloud (C2C) distance at the selected CPs are also measured in the vicinity of the CP and reported in Table 10. It can be observed that the C2C distance for the 4 CPs is significantly higher than errors in Pix4D, up to a maximum of 0.62 feet (7.44 inches or 18.9 cm). Note this value exceeds the error drastically in comparison in the RTK survey. Therefore, in conclusion, the ContextCapture processed point cloud has larger errors than Pix4D. While this may be acceptable on a given project, specific to the deliverables and desired accuracy, care should be taken if this is the chosen software platform.

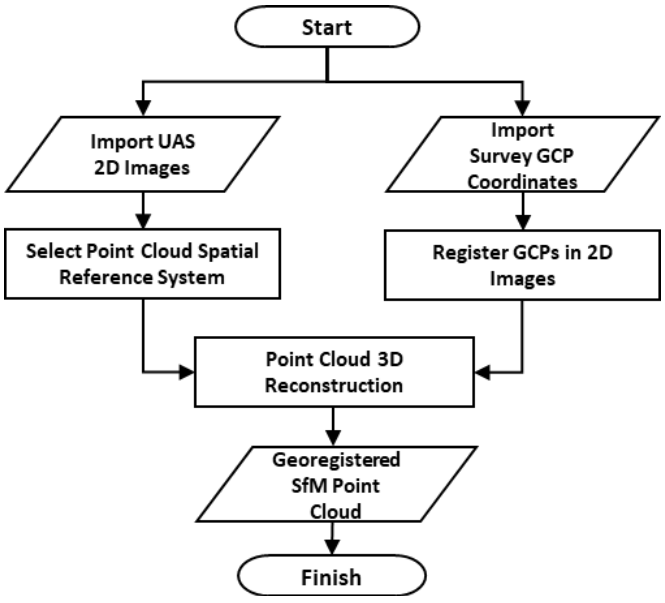

Figure 59. Flowchart of ContextCapture processing.

Figure 60. GCP locations.

Figure 61. Pix4D SfM point cloud (with 11 GCP).

Figure 62. ContextCapture SfM point cloud (with 11 GCP).

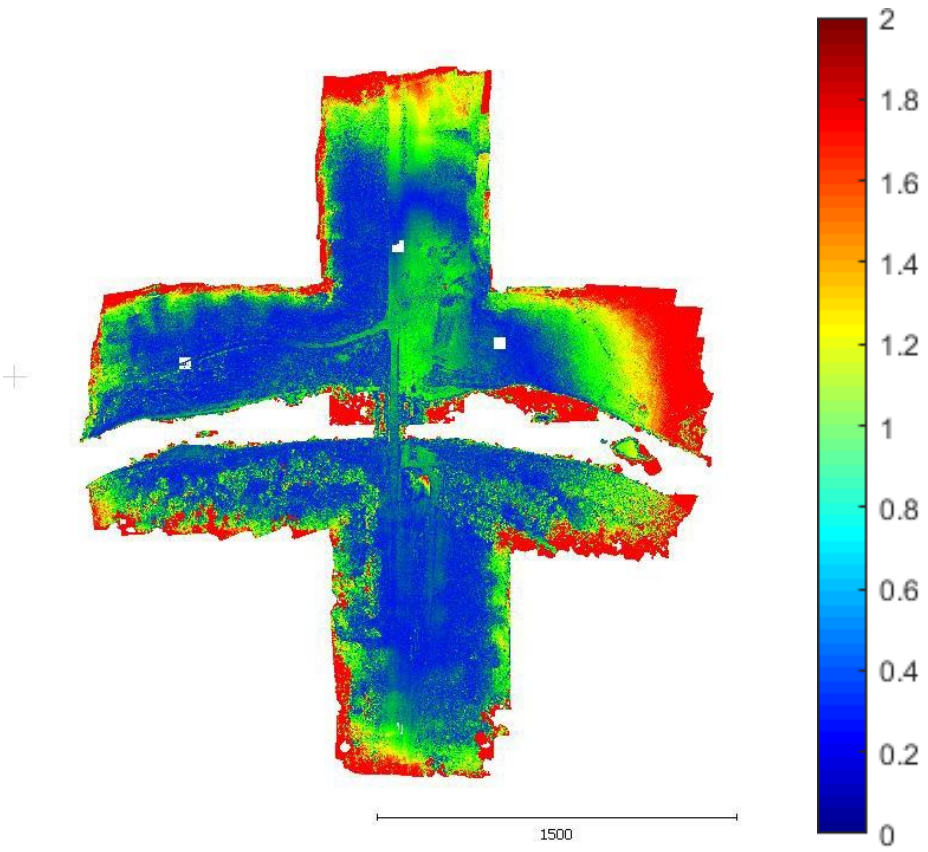

Figure 63. Cloud-to-cloud comparison. Distance is in feet.

Table 10: CP errors and C2C distance at the four selected points.

CP	Pix4D Results			C2C distance (ft)
	Error X (ft)	Error Y (ft)	Error Z (ft)	
3	-0.0107	0.0005	0.0751	0.3070
102	0.0461	0.0381	0.0330	0.0986
314	-0.0423	-0.0787	0.1916	0.2112
5016	0	0	0	0.6208

7.7 Data File Curation

The data as collected and processed is available for the project participants on the box folder. This includes the raw LiDAR files (*.fls), images from the UAS platform (*.jpg), and the RTK ground control survey. Processed files are also provided, where the point clouds are provided in two formats (*.e57 and *.las). Note the *.e57 files are approximately half the size of the *.las files due to the compression algorithm. Further processed and interpreted files are provided from the MicroStation, InRoads, and OpenRoads platforms (*.dgn).

8.0 Lidar Surveying and Mapping Specifications

8.1 Overview and Introduction

In this section, the LiDAR Surveying and Mapping Specifications for SDDOT are outlined. This summarizes the resolution, accuracy, platform selection, data storage, data quality, software, and hardware specifications. At its conclusion, the minimum acceptable standards for various applications and data collection methods are summarized. This section utilizes guidance from NCHRP 748 (Olsen et al. 2013a) and the literature review outlined previously.

8.2 Resolution and Accuracy

Resolution can be defined in many ways indicating the smallest level of details required. This can include density (points that occupy a given space, e.g., 10 pts/ft^3) or as often specified for aerial platforms, the GSD which represents more of a point-to-point spacing. *The suggested levels of detail will vary for a variety of transportation projects and the desired applications. This directly relates to the resolution provided by the various platforms and how the platforms collect data (in terms of settings, speed, number of passes, distance to the object, etc.).*

Consequently, for resolution or density, three levels are defined in Table 11. Coupled with the resolution is accuracy, which can be defined as both local and global. Local is defined as the value that represents the uncertainty in the coordinates relative to its adjacent points, and global defines the value that represents the uncertainty in the geodetic datum or SPC. Accuracy in the table below represents a combination of the local and global, but the contract or project planning should state if a specific local and global accuracy threshold is required. A platform is selected based on project accuracy and resolution requirements as well as the project layout. Depending on the project scope, the recommended accuracy and resolution can be tabulated from Table 11. Once the accuracy and resolutions are determined, a platform that delivers the requirements based on the project size and covered area can be selected based on Table 6.

Table 11: Resolution and accuracy summary.

Resolution (inch)	**Density (pts/ft^3)**	**Accuracy (inch)**		
		High	**Medium**	**Low**
		< 0.5	<5	<10
High (<1)	High (>144)	Bridge assessment	Bridge survey, Tunnel assessment, Scour assessment	Roadway survey, Tunnel assessment, Scour assessment
Medium (1-4)	Medium (4 – 144)	Roadway design	Roadway design, Roadway construction, Asset management, Hydraulic/drainage	Hydraulic/drainage, Earthwork, Slope analysis, Roadway construction
Low (>4)	Low (<4)	Terrain mapping	Terrain mapping	-

8.3 Platform Selection

Platform selection is at the discretion of the contractor or project planner given that all other requirements of the project are met. In general, GBL scanners will typically provide denser and more accurate point clouds, which are suitable for high resolution and high accuracy surveys of interest. However, ground-based LiDAR is often the slowest method for data collection. MLS will produce a medium level density and accuracy, in general. Aerial LiDAR scanning or UAS-SfM will provide various scan qualities depending on the platform, mounted instrument, and AGL altitude. When conducting point cloud surveys, CPs should be obtained to validate the survey. LiDAR is a line-of-sight technology, and occlusion will exist due to natural and manmade objects that may be static or dynamic in nature. The former includes bridge structures, guide rails, and vegetation (e.g., trees, grasses), but vehicular traffic and pedestrians may also result in occlusions. Occlusions or voids in the data should be minimized by collecting additional data at a different temporal state or alternative location/viewpoint.

Most of the commercial surveying platforms (e.g., LiDAR scanners) are accompanied by their proprietary pre-processing software packages that deliver the aligned dataset and further perform a series of post-processing (e.g., mesh reconstruction capability of Faro Scene software). Currently, the minimum software requirements for these programs are 64-bit operating systems, including 64-bit Windows server, 7, 8, and 10 and graphics processing unit (GPU) supporting an OpenGL version of 4.1 or higher. More detail regarding software and hardware specifications are provided in sections 6.2, 8.6, and 8.7.

Regarding equipment acquisition, the key ideas to consider are the current and future projects as well as the corresponding accuracy requirements, which determine the platform type. In general, the equipment specifications that need to be considered to compare various platforms are the scanning range (both minimum and maximum ranges), data collection speed, accuracy and resolution, weather rating, battery life, transferability of the equipment, and the ability of the equipment to accommodate other sensors (e.g, thermal camera or GNSS receivers). As for the software, important parameters to consider are the processing software capability, software support, whether training is offered for the software and equipment, licensing costs, its adaptability to the current software used in the office, and compatibility with available computer hardware should be considered. At the time of this report, the basic minimum suggested is a 6-core CPU, 32 GB of RAM, GPU with 4 GB of global memory, and 1.5 TB SSD. While this is the minimum, no upper bound limit can be specified as it likely budget constrained. The recommended minimum will be able to manipulate point clouds with the Bentley software suite, but if photogrammetry or structure-from-motion workstations should have higher computational and graphical resources.

8.4 Data Storage

Collected LiDAR data can be cumbersome due to its large file size, which may range from several gigabytes to even terabytes. *The file size is a function of the project size and the desired density.* For example, MLS may vary from anywhere between 1-2 GB/mile for the raw collected data and may expand to a total of 8-10 GB/mile depending on processing. Data collected should follow a traceable and documented process, since early processing and filtering steps may influence the final products. Given their size, the physical location and network connectivity are vital steps for the data implementation into existing workflows. *For this reason, it is recommended to manage and store data using online or cloud storage services.* Using a cloud storage service provides easy accessing and sharing to multiple users. Users are reminded of data degradation, and consequently, redundant storage arrays

are highly recommended. Physical backup tapes may be a cost-effective solution for cold storage. Physical backup can be accommodated using large Hard Disk Drives (HDD) in lieu of Solid-State Drives (SSD) as a cost-effective solution. The SSDs are faster in storing and retrieving data, and therefore, are better suited for data processing applications. However, in comparison to the HDDs of identical volume, SSDs are significantly more expensive.

File conversions can be handled through various options. Most of the proprietary software, but not all, are able to import and process popular file formats (e.g., XYZ, E57, LAS, etc.), and therefore convert one file format to other formats. Similarly, open-source software solutions such as CloudCompare, MeshLab, or Blender are able to import, process, and create different file formats. An exception can be made in regard to some of the software such as MicroStation where the input files for the MicroStation platform are POD, which will require a modest conversion procedure that can be accommodated through Bentley PODcreator. PODcreator is currently available for download without charge since it merely facilitates file conversion. Note that converting from one file format to other formats requires attention as the data accuracy or content can be lost as different file formats handle data structure through different methods. Among all 3D data formats, one of the most flexible and compressed standardized filetype is E57; however, LAS tends to be more popular but is typically much larger. In addition, LAS files have a hard file size limit (only can store 4.2 billion points) while e57 files do not have size limits. It is however advised to store files in segments of less than 1 GB for efficient storing and transferring proposes.

8.5 Data Quality

Data quality can be described in its perceived uncertainty and noise. Uncertainty and noise will arise in the point cloud products as a result of equipment limitations, scan strategy/alignments, environmental effects, and occlusion. The most common way to report this is by using an RSME estimate at the 95% confidence interval for control points. However, a mean or median value may be reported but should not be considered as reliable given a sizeable potential variation in accuracy. The number of control points will vary depending on the size of the project, but in general for high accuracy they are spaced at 500-1000 feet, medium accuracy at 1,000 – 2,500 feet, and for low accuracy at 2,500 – 5,000 feet. The SDDOT Surveying Manual quantifies the acceptable accuracy level.

In line with recent NCHRP guidelines, when 20 control points are used, the following should be reported (Federal Geographic Data Committee (FGDC) 1998):

Tested at X.XX feet vertical (or horizontal) accuracy at the 95% confidence level.

When the data is not thoroughly tested and the accuracy is estimated, the following statement should be used:

Compiled to meet X.XX feet vertical (or horizontal) accuracy at the 95% confidence level.

The RSME values at the 95% confidence level can be estimated using the assumption that the errors are normally distributed in nature (Hoffman 2008). Estimations correspond to the use of the following equations for 3D, horizontal, and vertical equivalents:

Three-dimensional: $3D_{95\%\ confidence} = RMSE_{3D} x\ 1.6166$

Horizontal: $2D_{95\%\ confidence} = RMSE_{2D} x\ 1.7308$

Vertical: $1D_{95\%\ confidence} = RMSE_{3D} x\ 1.9600$

8.6 Software

The selected software platforms will be a function of the equipment deployed. Most LiDAR equipment depends on proprietary processing algorithms to assemble or register LiDAR data. Specifically, each software platform has two sets of requirements, namely minimum and recommended specifications. The general minimum software requirements for these programs are 64-bit operating systems, including 64-bit Windows server, 7, 8, and 10 or Mac Operating Systems using Boot Camp and availability of a graphics processing unit (GPU) supporting OpenGL 4.1 or higher. As for the recommended specifications for each software platform, if these specifications are met, it can result in the reduction of processing time, in particular for large datasets. However, the recommended requirements usually pertain to the hardware side of the machine.

As for the various software packages, currently, most of the available programs can take advantage of available hardware potentials (e.g., use all CPU cores and GPU to decrease processing time). For UAS platforms, various SfM software platforms are also available for use including Visual SfM (opensource) as well as proprietary software (e.g., Pix4D). In addition, various point cloud functionalities exist in CloudCompare, an open-source software, that can also be used to pre and post-process datasets. Specific applications and deliverables may rely on processing and interpretation using the Bentley MicroStation and InRoads software platforms.

8.7 Hardware Specifications

Three types of hardware are recommended for various implementations: GBL, MLS, and Aerial platforms. Typically, they will vary in price, resultant features, and output accuracy. Users are reminded to select such platforms to achieve the minimum specified density and accuracy over the area of interest, which will vary by application. Most systems require calibration to correct for manufacturing errors and are typically performed by the supplier or the manufacturer directly. The system calibration accounts for a set of parameters to optimize the scan quality for high accuracies and minimal noise. Systems are generally outlined with specific calibration schedules due to internal and external vibration and general usage.

Acceptable Standards

The acceptance criteria for determining whether the deliverables can be utilized for specific applications will vary by the application. *The user should report the accuracy of the collected data in accordance with FGDC standards, which correspond to the RMSE at the 95% confidence level. QA/QC of the project should be demonstrated through an independent survey using total stations, levels, and GPS equipment such as (RTK or PPK (post-processing kinematic) modes).* Density or resolution recommendations are provided for guidance in line with best practices and previous work.

8.8 Implementation Strategy

Point clouds, as collected from either LiDAR or SfM platforms, require various considerations that are specific to the project scope and its deliverables. This is anticipated to vary depending on the current and potential future projects, available equipment, time constraints, budgeting, personnel, site condition, and processing resources. While the acquisition of equipment may be a more cost-effective strategy, this also typically requires regular equipment maintenance plans (equipment and software), equipment and deployment insurance, and calibration according to the manufacturer's recommendation. In general, the following implementation is recommended for each type of data collection platform. Refer to Tables 1 to 6 for identified usages and implementation by equipment platform.

1. ***Ground-based LiDAR (GBL)***

   GBL has the lowest cost of equipment acquisition, maintenance, and deployment costs. While cost alone is not the governing factor, typically this equipment is user-friendly and the size of data produced is the most compact. For this reason, GBL is recommended for equipment acquisition, with a platform that can be integrated into the existing workflows. If planned usage warrants this investment, a couple of GBL platforms and a few dedicated workstations would enable efficient and effective processing of the point clouds. If the scanners are loaned between various districts, a centralized processing station or computer can be used for converting the data into the desired deliverables. The off-site computational resources could be managed via an enterprise and state-approved remote desktop software platform.

   GBL platforms are optimal to collect data from a small to moderate size projects (e.g., a bridge structure). Data collection using GBL needs to be planned to identify the optimal locations of the scanner based on the accuracy and resolution required by the project. The planning or scan strategy is equipment dependent. However, following parameters should be considered in the planning, included: consecutive instrument setups to ensure reasonable overlap between adjacent scans (e.g., 25% to 50% overlapped area). Moreover, the scan strategy should create a closed circuit or loop (i.e., first and last scans have a reasonable overlap). Lastly, if targets are used to assist the alignment process, the targets should not occlude the areas of interest and distribute evenly throughout the scanning areas.

2. ***Mobile LiDAR (MLS)***

   MLS has a moderate cost of equipment acquisition, maintenance, and deployment costs. While this cost may be manageable, particularly for larger states or projects, the equipment is much less user-friendly with a substantial size of data produced. Moreover, accuracy (locally and globally) within MLS may be a concern, particularly in areas with limited sky views, and care should be applied in these situations. For this reason, MLS is recommended for a specific project subcontract, as needed. MLS platforms are comprised of different sensors and, therefore, can collect a variety of data. As a result, when planning data collection based on an MLS platform, it is necessary to consider current and future needs (e.g., road surface assessment when planning to collect data for asset inventory). MLS platforms are most efficient when used to scan a roadway corridor (or other similar geometry). The final deliverables

produced should include processed point clouds in a convenient file format for SDDOT workflows with a statement regarding the accuracy of the data as per Federal Geographic Data Committee requirements.

3. ***Aerial LiDAR or Unmanned Aerial System-based Structure-from-Motion (Aerial)***

Aerial LiDAR is often the most expensive cost of equipment acquisition, maintenance, and deployment costs to obtain geospatial point clouds. These costs are often exceeding acceptable budgets, except for a few large-scale projects where this may make financial sense. For this reason, Aerial LiDAR is only recommended to be subcontracted as needed. Aerial platforms are most efficient when a wide area or hard to reach regions are needed to be surveyed.

Aerial point clouds, as derived from Unmanned Aerial Systems or drones via the structure-from-motion algorithm (SfM, or photogrammetry), may be an acceptable replacement for Aerial LiDAR and other LiDAR platforms for specific projects. An aerial point cloud may include the same point cloud features as an MLS dataset, but this is anticipated to vary in areas of canopy cover and tunnels. The accuracy and density of UAS-based SfM may meet or exceed MLS and Aerial LiDAR, but care must be taken in the use of ground control points to serve as reference measurements and other check points to verify the quality and accuracy of the dataset. These surveys are best performed when access can be provided to the site/project of interest to conduct the supplemental ground survey. Newer technology has outlined deployments of RTK-based UAS platforms for limited ground control. However, even with an RTK-based UAS, ground control points are highly recommended to verify and validate the data for engineering applications.

Consequently, the recommendation for UAS-based SfM point clouds is for both in-house processing (equipment acquisition and processing) and subcontracting. UAS-based point clouds are generally easy to construct in an autonomous approach (flight path and point cloud formulation), and supplemental surveying equipment (for the ground surveys) is generally already available for use. The recommendation for subcontracting is also suggested given the sensitivity and risk of UAS deployments. The remote pilot in charge is completely responsible for the mission safety and adherence to federal aviation administration (FAA) regulations. For that reason, in the event of an incident, the state employee and the state itself may be liable and insurance may or may not be reasonable for particular projects or deployments. Any UAS deployed flights must be conducted in accordance with FAA airspace regulations and any local or state regulations regarding site or right-of-way access for commercial UAS flights.

9.0 Recommendations and Research Benefits

9.1 Overall Project Conclusions

This project aims to identify the current and potential application of commonly used remote sensing technologies (with a focus on LiDAR technology) for Surveying and Mapping within the scope and framework of SDDOT in terms of resolution and accuracy required, platform selection, data collection, cost estimate analysis, planning and procedures, data storage and quality, and software and hardware specifications. The identified applications included a preliminary survey for new road design or current improvements, clearance surveys of bridges and tunnels, roadway geometry survey for safety analysis, slope stability analysis, excavation and cut fills during construction, asset and inventory management of road signs, light poles, etc. For each identified application, the optimal surveying platform options were studied and summarized with respect to their required resolutions, possible data collection, analysis, handling methods, and processing software and hardware. An example of field data collection using two commonly used surveying platforms and preprocessing as well as postprocessing is described in detail from a selected construction site at Presho, SD. The goal of the data collection and processing demo is to demonstrate various steps described in the document in practice. The steps that are demonstrated in the demo included data collection planning, data preprocessing (i.e., registration), and deliverables of each remote sensing platform. At its conclusion, the minimum acceptable standards for various applications and data collection methods are summarized. This section utilizes guidance from NCHRP 748 (Olsen et al. 2013a) and the literature review outlined previously.

9.2 Recommendations

This project provides a guide to identify the optimal platform and implementation of commonly used remote sensing platforms within SDDOT workflows. This section utilizes guidance from NCHRP 748 (Olsen et al. 2013a) and the literature review presented previously. The list below provides the steps to identify the optimal platform and implementation for a selected project:

1- To best implement the use of LiDAR and point clouds within SDDOT workflows, careful evaluation of the selected platform and processing steps should be performed in regard to achieve the project deliverables in terms of resolution/density and accuracy. Keep in mind that data sizes will increase exponentially as the density or resolution increases.

2- To speed up the implementation of LiDAR platforms into current workflows, a task force can be created to identify potential applications of LiDAR data and optimize the current workflows, where guidance is provided in Table 1 (applications), Table 3 (software), and Table 6 (workflow).

3- The deciding factor between equipment acquisition, rental, or contract (Tables 4 and 5) can be further determined through the evaluation of current and future project needs and layouts (Table 1), accuracy and resolution requirements (Table 2 or Table 11), data processing training, software licensing costs, and equipment usage costs where maintenance and calibration is performed as needed per the manufacturer's schedule or when data quality degradation occurs.

9.3 Research Benefits

This project is expected to illustrate the benefits of LiDAR and point cloud data projects over traditional surveying techniques. Such benefits include being less labor-intensive and time-consuming, more accurate measurement results, the minimization of worker exposure to live traffic, and general datasets that have multiple applications. The time and labor benefits will be directly demonstrated through the example LiDAR project in Task 7 in terms of data capture effort (Chapter 7). LiDAR applications are being used for current projects, and its future use is anticipated to increase. Due to its upcoming implementations, the necessity to develop LiDAR specifications to guide its use for quality data exists. A draft of these specifications is provided in Chapter 8, which includes unmanned aerial system derived point clouds (via photogrammetry).

10.0 References

Akgul, M., Yurtseven, H., Akburak, S., Demir, M., Cigizoglu, H. K., Ozturk, T., and Akay, A. O. (2017). "Short term monitoring of forest road pavement degradation using terrestrial laser scanning." *Measurement*, 103, 283-293.

Autodesk. (2016). "ReCap 360 general discussion.", *Autodesk forums,* http://forums.autodesk.com/t5/-recap-360-general-discussion/recap-user-s-guide/td-p/4328036, (Aug. 9, 2016).

Bendaanane, M., Eddahmani, K., and Sebari, I. (2015). "Urban objects extraction from 3D laser point clouds acquired by a static laser scanner and a mobile mapping system." *Int. J. Remote Sens.*, 5, 33-44.

California Department of Transportation. (2016). *Caltrans surveys manual*, http://www.dot.ca.gov/ hq/row/ landsurveys/SurveysManual/Manual_TOC.html, (Aug. 8, 2017).

CloudCompare (version 2.7). (2016). *Re*trieved from <http://www.cloudcompare.org> (Aug. 8, 2016)

Colorado Department of Transportation. (2015). *Survey manual*, https://www.codot.gov/ business/manuals/survey, (Apr. 27, 2017).

Dobson, R. J., Brooks, C. N., Roussi, C., Shuchman, R. A., Ahlborn, T. M., and Dean, D. (2013). "Development and application of three-dimensional optical bridge deck evaluation system." *Proc. Transportation Research Board Annual Meeting,* TRB, Washington, D.C., No. 13-4451.

Dunham, L., Wartman, J., Olsen, M. J., O'Banion, M., and Cunningham, K. (2017). "Rockfall activity index (RAI): a lidar-derived, morphology-based method for hazard assessment." *Eng. Geol.,* 221(1), 184-192.

Eker, R., Aydın, A., and Hübl, J. (2018). "Unmanned aerial vehicle (UAV)-based monitoring of a landslide: Gallenzerkogel landslide (Ybbs-Lower Austria) case study." Environ Monit Assess, 190(1), 28.

Ellis, S. A. (2017). "Using mobile lidar to deliver survey accurate data." *Proc. Transportation Research Board 96th Annual Meeting,* TRB, Washington, D.C., 17-00597.

Federal Highway Administration (FHWA). (2016). *Guide for efficient geospatial data acquisition using lidar surveying technology.* Rep. No. FHWA-HIF-16-010. Washington, D.C.

Federal Aviation Administration (FAA). (2011). *Standards for using remote sensing technologies in airport surveys.* AC 150/5300-17C, Washington, D.C.

FARO. (2011). *FARO laser scanner focus 3D: features, benefits & technical specifications.* FARO Technologies, Lake Mary, FL.

FARO. (2015). "Faro helps tri-tech bridge the gap on laser scanning." *Application in Industries,* http://www.faro.com/measurement-solutions/industries/bridge/2015/01/07/faro-helps-tri-tech-'bridge-the-gap-on-laser-scanning, (Aug. 9, 2016).

Federal Geographic Data Committee (FGDC) (1998). *Geospatial Positioning Accuracy Standards Part 3: National Standard for Spatial Data Accuracy.* Report No. FGDC-STD-007.3-1998, USGS, Reston, Virginia.

Gargoum, S., El-Basyouny, K., Sabbagh, J., and Froese, K. (2017). "Automated highway sign extraction using lidar data." *Transp. Res. Rec.*, (2643), 1-8.

Guo, F. (2016). *Civil integrated management and the implementation of CIM-related technologies in the transportation industry*. Ph.D. Dissertation, Department of Civil Engineering, Iowa State University. 15923.

Gurganus, C. F., Gharaibeh, N. G., and Scullion, T. (2017). "A case study on the use of mobile LiDAR to produce a preliminary drainage design." *Proc. Transportation Research Board 96th Annual Meeting,* TRB, Washington, D.C., 17-03657.

Harris, D. K., Brooks, C. N., and Ahlborn, T. T. M. (2016). "Synthesis of field performance of remote sensing strategies for condition assessment of in-service bridges in Michigan". *J. Perform. Constr. Fac.*, 30(5), 04016027.

He, Y., Song, Z., and Liu, Z. (2017). "Updating highway asset inventory using airborne LiDAR." *Measurement*, 104(1), 132-141.

Hoensheid, R. C. (2012). *Evaluation of surface defect detection in reinforced concrete bridge decks using terrestrial LiDAR.* Master's thesis, Michigan Technological University, Houghton, MI.

Huber, D. (2011). "The ASTM E57 file format for 3D imaging data exchange." *Proc. in Three-Dimensional Imaging, Interaction, and Measurement*, International Society for Optics and Photonics, vol. 7864, p. 78640A.

Jet Propulsion Laboratory (JPL). (2012). "ALHAT helicopter campaign." *Autonomous Landing Hazard Avoidance Technology*, http://alhat.jpl.nasa.gov/image.php?galleryID=11, (Aug. 8, 2016).

Johnson, S. D., Bethel, J. S., Supunyachotsakul, C., and Peterson, S. (2016). *Laser mobile mapping standards and applications in transportation*, Joint Transportation Research Program Publication No. FHWA/IN/JTRP-2016/01, Purdue University, West Lafayette, IN, 10.5703 /1288284316164.

Kentucky Transportation Cabinet (KYTC). (2013). *Working with LiDAR in MicroStation.* Division of Highway Design, http://transportation.ky.gov/highwaydesign/documents/, (Apr. 27, 2017).

Kong, Z., Liu T., Balasundaram, B., Emerson, R. and Ley, T. (2013) *Acquisition of a LiDAR laser scanner for bridge inspection*. Report No. OTCES10.2-05-F, Oklahoma Transportation Center, Midwest City, OK.

Liu, Q., Wang, T., and Souleyrette, R. R. (2017). "A 3D evaluation method for rail–highway hump crossings." *Comput-Aided Civ. Infrastruct. Eng.*, 32(2), 124-137.

Martí Carrillo, F. (2015). *Monitoring and managing interaction patterns in human-robot interaction.* Master Thesis, Lund University, LU-CS-EX 2015-37, Lund, Sweden.

Miller, N., Brain, S., Nicholson, K. (2012). A comparison of mobile scanning to a total station survey at the I-35 and IA 92 interchange in Warren County, Iowa. Report No. RB22-0111, Iowa Department of Transportation, Ames, IA.

Miyamoto, M. (2016). *Tips and tricks for creating civil 3D surfaces from lidar data.*, Ideate Inc., https://bundycad.files.wordpress.com/2010/06/lidar-tips-tricks.pdf, (Apr. 27, 2017).

Passe, P. D. (2000). *Mechanically stabilized earth wall inspector's handbook*. Florida Department of Transportation. Tallahassee, FL .

Olsen, M. J., Roe, G. V., Glennie, C., Persi, F., Reedy, M., Hurwitz, D., Williams, K., Tuss, H., Squellati, A., and Knodler, M. (2013). "Guidelines for the use of mobile LiDAR in transportation applications" *TRB NCHRP Final Report 748,* Transportation Research Board, Washington, D.C., USA.

Oskouie, P., Becerik-Gerber, B., and Soibelman, L. (2016). "Automated measurement of highway retaining wall displacements using terrestrial laser scanners." Automat Constr, 65, 86-101.

RoadScanners Inc. (2017). "Road detector survey van." https://www.roadscanners.com, (Jan. 23, 2018)

Surveying Solutions Incorporation (SSI). (2016). "SSI expansion." *Mobile Lidar and Mobile Mapping*, https://mobilelidarblog.com, (Aug. 8, 2016).

Swanston, T., Yen, K., Donecker, S., Ravani, B., and Lasky, T. (2016). *Research and support for MTLS data management and visualization.* Report No. 10.5703 /1288284316164, California Department of Transportation, Sacramento, CA.

Vincent, R. and Ecker, M. (2010). *Light detection and ranging (LiDAR) technology evaluation.* Rep. No. OR11-007, Missouri Department of Transportation (MoDOT), Jefferson City, MO.

Yang, B., Dong, Z., Liu, Y., Liang, F., and Wang, Y. (2017). "Computing multiple aggregation levels and contextual features for road facilities recognition using mobile laser scanning data." *ISPRS J. Photogramm. Remote Sens.*, 126(1), 180-194.2.

Yu, H., Mohammed, M. A., Mohammadi, M. E., Moaveni, B., Barbosa, A. R., Stavridis, A., and Wood, R. L. (2017). "Structural identification of an 18-story RC building in Nepal using post-earthquake ambient vibration and lidar data." *Front. in Built Environ.*, 3, 11.

Zheng, H., Wang, R., and Xu, S. (2017). "Recognizing street lighting poles from mobile lidar data." *IEEE Trans. Geosci. Remote Sens.*, 55(1), 407-420.